Hamburg University of Applied Sciences

Faculty of Life Sciences

Potential analysis of the integration of flexibly operated Direct Air Capture (DAC) plants in the heat and power system using the example of Hamburg

Master thesis

in the study program

M. Sc. Renewable Energy Systems – Environmental and Process Engineering

submitted by

Moritz Peter Rickert

[redacted]

Hamburg

On 21. July 2023

1st reviewer: Prof. Dr. Carsten Frank (HAW Hamburg)

2nd reviewer: M. Sc. Hendrik Zachariassen (CC4E / HAW Hamburg)

The thesis was supervised and prepared in cooperation with the Competence Centre für Erneuerbare Energien und EnergieEffizienz (CC4E)

Title of the Master Thesis

Potential analysis of the integration of flexibly operated Direct Air Capture (DAC) plants in the heat and power system using the example of Hamburg

Keywords

Climate neutrality 2045, greenhouse gas emissions, direct air capture, flexible operation, surplus heat utilization, district heating system, economic feasibility, scenario development, mixed-integer linear programming optimization

Abstract

For climate neutrality by 2045, Germany must compensate unavoidable residual greenhouse gas emissions by negative emission technologies such as direct air capture (DAC) technology. This study explores the technical feasibility and economic viability of implementing flexibly operated DAC plants in Hamburg's district heating system in 2045. Literature about DAC technology requests high full-load operation hours (FLOH) to achieve the economic feasibility of DAC plants. In this work, scenarios of different DAC plant scales on both flat rooftops and open fields are developed considering a range of demand-related costs and various district heating (DH) system designs with deviating short-term and seasonal thermal energy storage capacities. Construction sites for DAC plants are identified on open spaces and rooftops near the DH grid. Unused heat generation capacities in the DH system are identified. The DAC application, along with heat pumps, shall operate during periods of negative residual loads in the power system. Results of a mixed-integer linear programming optimization indicate that DAC plants on rooftops and open fields are technically feasible for different DH system designs. The proposed carbon dioxide removal rate for Hamburg in 2045 is achievable in a flexible operation mode. The DAC application can efficiently utilize surplus heat and unused heat pump capacities from the DH system. Economically, large-scale DAC plants on open fields prove more feasible than on rooftops, with levelized costs of CO_2 removal below 100 €/tCO_2, dependent on the DH system design and demand-related costs. A flexibly driven DAC plant with lower FLOHs on an open field has an achievable economic break-even point if the demand-related costs can be partially compensated through e.g., political incentives such as industrial DR or dynamic electricity pricing. The findings suggest that economically viable DAC plants in Hamburg's DH system depend mostly on the specific investment costs rather than the final DH system design.

Content

List of Figures V
List of Tables VII
List of Equations VIII
List of Abbreviations IX
List of Symbols XI
1 Introduction 1
1.1 Research Subject 2
2 Theoretical Background 4
2.1 Sector Coupling 4
2.2 Power System 5
2.2.1 Residual Loads 5
2.2.2 Electricity Sector and Market Regulations 5
2.2.3 Merit Order Effect 5
2.2.4 Flexibility Services 6
2.2.5 Baseline Scenario: Power System in Germany 7
2.3 Heating Sector – District Heating 9
2.3.1 Baseline Scenario: District Heating in Hamburg 10
2.4 State of the Art: Direct Air Capture 12
2.4.1 Sorbent-Based DAC Process 12
2.4.2 Alternative DAC Technologies 15
2.4.3 Companies and Projects 15
2.4.4 Excursus: DAC Business Cases and Their Environmental Impact 16
2.5 Optimizations 17
2.5.1 Components of an Optimization 17
2.5.2 Real-World Optimization Problems 18
2.5.3 Optimization Programming Environment 18
2.6 Calculation of Economic Efficiency 19
3 Materials and Methods 20
3.1 Definition of Scenarios 21
3.2 Deriving Negative CO_2 Emissions Demand by DAC-Technology in Hamburg 23
3.2.1 Gross Negative CO_2 Emission Demand 24
3.3 Electricity Supply 25
3.3.1 Electricity Costs 26
3.4 Heat Supply by District Heating System 27

3.4.1 Heat Generator Capacities 27
3.4.2 Thermal Energy Storage Scenarios 30
3.5 Techno-Economics of LT DAC Plants 31
3.5.1 Dimensions 31
3.5.2 Economic Aspects 32
3.5.3 Technical Aspects 35
3.6 Spatial Analysis for DAC Plants in Hamburg 38
3.6.1 Open Fields 38
3.6.2 Flat Rooftops 39
3.7 Scenario Optimization Modeling 41
3.7.1 System and Model Requirements 42
3.7.2 Decision Variables 43
3.7.3 Scenario Constraints 45
3.7.4 Objective: Minimum $LCoCO_2$ 48
3.7.5 Summary of Inputs and Expected Outputs of the Scenarios 50
4 Results 51
4.1 Energy Consumption and CO_2 Isolation of DAC Plants 52
4.2 Demand-Related Costs and Their Impact 53
4.2.1 Electricity and Heat Prices 53
4.2.2 Compensation Fee 54
4.3 Energy Flows and Composition of the Heat Supply for DAC Plants 56
4.3.1 1-Hour Short-Term TES Capacity Scenario 57
4.3.2 12-Hour Short-Term TES Capacity Scenario without Seasonal TES 58
4.3.3 12-Hour Short-Term TES Capacity Scenario with Seasonal TES 59
4.4 DAC Plants' Dimensions and Costs 60
4.4.1 Power Capacity and Full-Load Operation Hours 60
4.4.2 Capital-Related Costs 61
4.4.3 Spatial Requirements 62
4.5 Spatial Analysis 63
4.5.1 Open Fields 63
4.5.2 Flat Rooftops 64
4.6 Minimum $LCoCO_2$ Objective 65
4.6.1 1-Hour Short-Term TES Capacity Scenario 66
4.6.2 12-Hour Short-Term TES Capacity Scenario without Seasonal TES 66
4.6.3 12-Hour Short-Term TES Capacity Scenario with Seasonal TES 67

4.6.4 Impact of Specific Investment Costs 69
5 Discussion 70
5.1 General Limitations of this Work 71
5.2 Data Basis and Assumptions 72
5.2.1 DH System of Hamburg 72
5.2.2 Power System of Germany 75
5.3 Literature Research and Assumptions 77
5.3.1 Negative CO_2 Emission Demand in Germany 77
5.3.2 Techno-Economic Parameters of DAC Plants 78
5.4 Optimization Modeling 80
5.4.1 Assumptions for the Objective Modeling 80
5.4.2 Evaluation of Optimization Tool 81
5.5 Spatial Analysis in Hamburg 82
5.5.1 DAC Plants on Open Fields 82
5.5.2 DAC Plants on Flat Rooftops 82
5.6 Evaluation of Scenario Results 84
5.6.1 Energy Flows of the Power and Heat System 84
5.6.2 Full-Load Operation Hours of Heat Pumps 85
5.6.3 Demand-Related Costs 86
5.6.4 DAC Plants on Open Spaces vs. Flat Rooftops 87
5.6.5 Economic Feasibility 87
6 Conclusion 89
6.1 Outlook 91
References XIII
A Appendix ..... A
A.1 1st TES Scenario with a 1-hour Short-Term TES Capacity of the DH System + Heat Pumps ..... B
A.2 2nd TES scenario with a 12-hour short-term TES capacity of the DH system + heat pumps C
A.3 3rd TES scenario with a 12-hour short-term TES and seasonal TES + heat pumps ..... D
A.4 Workflow Diagram of Spatial Analysis ..... E
A.5 Time Series of *OF-stTES1h-wo/SeasTES-elUpper* ..... F
A.6 Time Series of *OF-stTES12h-wo/SeasTES-elOptimum* and *OF-stTES12h-wo/SeasTES-elUpper* ..... G
A.7 Time Series of *OF-stTES12h-w/SeasTES-elUpper* ..... H
A.8 Time Series of *FR-stTES1h-wo/SeasTES-elOptimum* I
A.9 Time Series of *FR-stTES12h-wo/SeasTES-elOptimum* ..... J

A.10 Scenario-Specific In- and Outputs of All 1-Hour Short-Term TES Capacity Scenarios ..... K

A.11 Scenario-Specific In- and Outputs of All 12-Hour Short-Term TES Capacity Scenarios L

A.12 Scenario-Specific In- and Outputs of All 12-Hour Short-Term + Seasonal TES Capacity Scenarios ..... M

B Digital Appendix ..... N

B.1 Flexible_DAC_plant_operation_optimization_model.py ..... N

B.2 Input_time_series_MILP - Parameter - Additional_calculations.xlsx ..... N

B.3 Collection of scenarios and their time series (inputs, variables, and other outputs).xlsx ..... N

B.4 Figures of the scenarios' time series ..... N

Statutory Declaration XX

List of Figures

Figure 1: Schematic of the methodological concept of this thesis. (Own illustration)..... 3
Figure 2: Residual load in Germany's power system in 2045 predicted by the optimization model REMod. The data contains only inflexible electricity producers and inflexible consumers of the reference scenario. (Own illustration based on (Kaiser, 2022; Sterchele et al., 2021)) 8
Figure 3: Sustainable heat generation-mix and demand profile of Hamburg's district heating grid in 2045 with an hourly resolution by (Kicherer et al., 2021) 10
Figure 4: Merit order of the heat generators for the DH concept of Hamburg in 2045. (Kicherer et al., 2021)..... 11
Figure 5: A simplified representation of a sorbent-based DAC process with its energetic inputs and outputs. In the adsorption phase, ambient air flows into the DAC plant using electrical fans. CO_2-poor air leaves the DAC contactor after CO_2 is bound to the filter inside the plant. Afterward follows the desorption phase when residual air is evacuated by an electrical plant and the contactor is heated up to detach the CO_2 of the filter. Steam can be used to increase the desorption efficiency. Concentrated CO_2 can be processed for further transportation or storage. (Own illustration)..... 13
Figure 6: A process flow diagram of a TVSA DAC plant that includes the adsorption and the desorption phase. The blue line determines a liquid flow. The green lines illustrate gaseous flows and the dashed green line connects the contactor with the vacuum pump to illustrate the removal of remaining air from the contactor which is necessary before starting the desorption phase. (McQueen et al., 2021)..... 14
Figure 7: Diagram with the specific investment costs in €/(tCO_2/a) with a logarithmic dependency on the plant size. The blue points represent the data basis of the specific investment costs for pre-determined plant sizes in 2020. The orange dots are the data basis of the projected specific investment costs for pre-determined plant sizes in 2040. The dotted lines represent the logarithmic extrapolation trend lines that are built on the available data points. (Own illustration)..... 33
Figure 8: Potential for solar thermal systems on open fields in Hamburg and the district heating system of Hamburg. The blue lines show the DH grid of Hamburg. Brown areas would be open fields that would fit solar thermal systems. Suitable locations with a possible DH system connection are marked with red cycles. (Modified after (Kicherer, 2020)) 39
Figure 9: An exemplary tile with filtered buildings according to a flat roof structure that fits one DAC plant container module. The light grey forms are buildings with another roof structure. The forms in the darker grey color are flat roofs with a size smaller than 60 m². Black-colored buildings are equal to or larger than 60 m², however, they do not fit a polygon of the dimension of a common container. Red-colored buildings fit the necessary dimensions. (Trosdorff, 2023) 40
Figure 10: Overview of the optimization tool's procedure including inputs and outputs. Inputs are either constant values, time series containing hourly data for the year 2045, or properties of the model itself. The scenarios must be translated into an algebraic model. A defined objective and the model are handed over to a solver that solves the optimization problem. Output data of the optimization tool are constant values or time series of decision variables, the objective, and other computational results which are of interest for the follow-up processing. (Own illustration) 41
Figure 11: Exemplary time series of CO_2 isolation dispatch of the DAC plants using the 1-hour short-term TES (top), 12-hour short-term TES (middle), and 12-hour short-term and seasonal TES (bottom) of the DH system. The CO_2 isolation dispatch schedules of the 1- and 12-hour short-term scenarios vary significantly in April 2045 (purple circle). Differences between the 12-hour short-term TES and the 12-hour short-term with a seasonal TES can be seen on 1st June (red circle). (Own illustration).. 52

Figure 12: Overview of the compensation fee to limit the FLOH of the sewage water heat pump. The values are affected by the overall needed heat supply by the HPs, the costs for electricity for the HPs, and the surplus heat of the DH system in the scenarios. (Own illustration)..... 55
Figure 13: Heat supply for DAC plants in the specific scenarios distinguished by surplus heat of the DH system and heat pumps and their respective full-load operation hours. (Own illustration)..... 56
Figure 14: Used share of electricity of the total available negative residual load in the power system that is scaled down to the size of Hamburg in each scenario. Further, the used share of the DH system's surplus heat is depicted in grey per scenario. The maximum usage of surplus heat is limited to 66.995 and 66.359 % in the scenarios considering 1- and 12-hour short-term TES capacity due to the constraint of having electricity available at the same time for the DAC plants. (Own illustration) 57
Figure 15: Optimized DAC plant capacity in tCO_2/a and the corresponding full-load operation hours in h/a of the DAC plants in the respective scenarios. (Own illustration) 61
Figure 16: Investment costs of the DAC plants in the respective scenarios. In the considered cases, the specific investment costs have a more significant impact on the investment costs than the DH systems' designs that influence the plant's capacity. The specific investment costs depend on the position and scale of the DAC plant which is either on an open field or a flat rooftop. (Own illustration) 62
Figure 17: Potential for solar thermal systems on open fields in Hamburg and the district heating system of Hamburg. The blue lines show the DH grid of Hamburg. Brown areas would be open fields that would fit solar thermal systems. Suitable locations with a possible DH system connection are marked with red cycles. (Modified after (Kicherer, 2020)) 63
Figure 18: Tiles of the 3D building map which intersect with the DH system of Hamburg (Trosdorff, 2023)..... 64

List of Tables

Table 1: Examined scenarios for the implementation of DAC plants in Hamburg with a fixed carbon dioxide removal rate. Different thermal energy storage capacities of the DH system are considered. It is further distinguished by the position and scale of the DAC modules which correlate with different specific investment costs and space demands. A range of levelized costs of electricity is also investigated and an optimum levelized cost of heat is reflected in specific cases. Each scenario receives a specific name code. (Own illustration) 22
Table 2: Net and gross negative emission goals in 2045 for Germany and Hamburg based on the per-capita ratio between Hamburg and Germany. (Own illustration) 24
Table 3: Range of wholesale electricity prices to be investigated on the scenarios. (Own illustration based on assumptions* and (Fraunhofer IEE et al., 2021)) 26
Table 4: Technical characteristics of the river water and sewage water heat pumps of the DH system. Two time series are considered regarding different thermal energy storage (TES) capacities. The time series are modified so that the HPs cannot contribute to the heat supply of DAC plants when their operation is prohibited by temperature restrictions of the river or when the HPs are already operating at full load. (Own illustration based on (Kicherer, 2020; Kicherer et al., 2021)) 29
Table 5: Characteristics of the DH system in Hamburg for the heat supply for DAC plants in 2045. (Own illustration based on (Kicherer, 2020; Kicherer et al., 2021) and own assumptions*) 30
Table 6: Specific space demand values in dependency on the scale of the plant capacity. (Own illustration based on (Beuttler et al., 2019; Deutz and Bardow, 2021a, 2021b) and own assumption*) 31
Table 7: Specific investment costs in €/(tCO_2/a) for differently scaled DAC plants in the years 2020 and 2040. (Own illustration based on data by (Fasihi et al., 2019; Roestenberg, 2015) and own calculations*) 34
Table 8: Overview of economic parameters of DAC plants that are used in the optimization model. (Own illustration based on (Beuttler et al., 2019; Fasihi et al., 2019; Lackner and Azarabadi, 2021; Ozkan et al., 2022)) 35
Table 9: Electricity and heat demand development of LT DAC plants until 2050. The energy demands in 2045 are calculated by linear interpolation and are used in this thesis. (Own illustration based on (Fasihi et al., 2019) and own calculation*) 36
Table 10: Overview of economic parameters of DAC plants that are used in the optimization model. (Own illustration based on (Beuttler et al., 2019; Fasihi et al., 2019; Lackner and Azarabadi, 2021; Ozkan et al., 2022)) 37
Table 11: Overview of the input time series for the scenarios and model. (Own illustration) 43
Table 12: Modelling properties of the decision variables defined in the model. (Own illustration) 44
Table 13: Uniform parameter inputs and assumptions for all scenarios. (Own illustration) 50
Table 14: Optimum LCoE and LCoH of the scenarios to operate DAC plants at $LCoCO_2$ below 100 €/tCO_2. (Own illustration) 53
Table 15: Optimized levelized costs of CO_2 isolation in each scenario. $LCoCO_2$ highlighted in blue are below 100 €/tCO_2 and are achieved within the range of assumed energy costs. $LCoCO_2$ highlighted in orange are also below the proposed 100 €/tCO_2, however, they are only achieved by applying negative energy prices in the optimization model. $LCoCO_2$ highlighted in red are achieved within the range of assumed energy costs but resulted in CDR costs above 100 €/tCO_2. (Own illustration) 65
Table 16: Comparison of the $LCoCO_2$ differences between the DH system designs at the same LCoEs and DAC plant properties. (Own illustration) 68

Table 17: Comparison of the $LCoCO_2$ differences of the DAC plants installed on flat rooftops and open spaces in the individual DH system designs. The DAC plant capacity and the respective FLOHs influence the difference between the $LCoCO_2$ values. (Own illustration) 69

List of Equations

(1) 18
(2) 19
(3) 19
(4) 19
(5) 28
(6) 45
(7) 45
(8) 45
(9) 45
(10) 45
(11) 45
(12) 46
(13) 46
(14) 46
(15) 46
(16) 47
(17) 47
(18) 47
(19) 48
(20) 48
(21) 48
(22) 49
(23) 49

List of Abbreviations

Abbreviation	Meaning
AF	Annuity factor
AR	Afforestation and reforestation
BECCS	Bioenergy carbon capture and storage
BG	Balancing group
CAPEX	Capital expenditure
CCS	Carbon capture and storage
CCU	Carbon capture and utilization
CDR	Carbon Dioxide Removal
CHP	Combined heat and power
CityGML	City Geography Markup Language
COP	Coefficient of performance of a heat pump
DAC	Direct air capture
DACCS	Direct air carbon capture and storage
DACCU	Direct air carbon capture and utilization
DH	District Heating
DSI	Demand side integration
DSM	Demand side management
DR	Demand response
FLOH	Full-load operation hours in h/a
GHG	Greenhouse gas
HT	High Temperature (process)
HP	Heat pump
$LCoCO_2$	Levelized costs of CO_2 removal/isolation
LCoE	Levelized costs of electricity – in this thesis: generic term for electricity costs
LCoH	Levelized costs of heat – in this thesis: generic term for heat costs
LFC area	Load frequency control area
LP	Linear programming
LT	Low Temperature (process)
MILP	Mixed-integers linear programming
MINLP	Mixed-integers non-linear programming
NET	Negative emission technology
NLP	Non-linear programming
NNI	Non-negative integer
NNR	Non-negative real
OPEX	Operational expenditure
Pyomo	Python Optimization Modeling Objects
RE	Renewable Energy
REMod	Regenerative Energy Model
SC	Sector coupling
SCS	Soil carbon sequestration
TES	Thermal energy storage
TRL	Technology readiness level

Abbreviation	Meaning
TRY	Test reference year of the Deutscher Wetterdienst
TSO	Transmission service operator
TVSA	Temperature Vacuum Swing Adsorption
UNFCCC	United Nations Framework Convention on Climate Change

List of Symbols

Symbol name	Meaning	Unit
CO_2e	Carbon dioxide equivalence	-
Comp_fee	Compensation fee for additional FLOH of the sewage water HP	€/MWh
DAC_CO2_cap	Necessary DAC plant power capacity in 2045	tCO_2/h or tCO_2/a
DAC_CO2_out	CO_2 removal rate in 2045	tCO_2/h
DAC_cost_el	Specific electricity costs per removed ton of CO_2	€/tCO_2
DAC_el_consumption	Variable of electric energy consumption of DAC plants	MWh/timestep
DAC_el_demand_per_tCO2	Electricity demand of DAC plant to remove 1 ton of CO_2	kWh/tCO_2
DAC_heat_demand_per_tCO2	Heat demand of the DAC plant to remove 1 ton of CO_2	kWh/tCO_2
DAC_module_size	Established capacity of a DAC plant module	tCO_2/a
DAC_number_of_plants	Number of DAC plant modules with a specific power capacity	-
DAC_th_consumption	Variable of thermal energy consumption of DAC plants	MWh/timestep
DH_cost_th	Demand-related heat costs of the DAC plant received from the DH system	€/tCO_2
DH_system_th_supply	Variable of thermal energy supply of the DH system for the DAC application	MWh/timestep
DH_TES_cap_Xh	Input time series of the district heating residual load curve with X hours of short-term thermal energy storage capacity	MWh/timestep
electricity_hh	Input time series of the residual load curve of Germany scaled to the size of Hamburg	MWh/timestep
gross_cdr_hh	Gross negative emission demand scaled down to the size of Hamburg in 2045	tCO_2/a
HP_cop	Coefficient of performance of the heat pumps considered in the optimization model	-
HP_river_dr_cost	Specific demand-related costs of the river HP per ton of CO_2	€/tCO_2
HP_river_el_consumption	Electricity consumption of the river heat pump for heat supply of DAC plants in 2045	MWh/timestep
HP_river_th_availability_Xh	Theoretically available thermal energy supply of the river heat pump	MWh/timestep
HP_river_th_supply	Heat production of the river heat pump for the DAC plants in 2045	MWh/timestep
HP_sewage_dr_cost	Demand-related costs of the sewage water HP per ton of CO_2	€/tCO_2

Symbol name	Meaning	Unit
HP_sewage_el_consumption	Electricity consumption of the sewage water heat pump for the heat supply of DAC plants in 2045	MWh/timestep
HP_sewage_th_availability_Xh	Theoretically available thermal energy supply of the sewage water heat pump	MWh/timestep
HP_sewage_th_supply	Heat production of the sewage water heat pump for DAC plants in 2045	MWh/timestep
i	Index of time series equal to 1 hour per timestep	h/timestep
net_cdr_hh	Annual mass of net CO_2 removal	tCO_2
r_{int}	Interest rate on the investment costs	%
T_{max}	Maximum temperature of the district heating system's design	°C
T_{min}	Minimum temperature of the district heating system's design	°C
$t_{project}$	Lifetime of the DAC plant and the project	a

1 Introduction

Through anthropogenic global warming, irreversible and uncontrollable tipping points in the Earth's climate system are about to be triggered, endangering the livelihoods of many ecosystems and the world's future human population. (IPCC, 2022a) Therefore, members of the United Nations Framework Convention on Climate Change (UNFCCC) established the *Paris Agreement* in 2015. In the *Paris Agreement*, the goal was set to keep global warming well below 2 °C and preferably at 1.5 °C above pre-industrial temperature levels (*ADOPTION OF THE PARIS AGREEMENT - Paris Agreement text English.* UNFCCC, 2015) As of 1st January 2020, a global CO_2 equivalent (CO_2e) emissions contingent of 400 Gt or 1,150 Gt remains to stay within the 1.5 °C or 2.0 °C global warming limitation with 67 % probability. (IPCC, 2021)

According to the *Intergovernmental Panel on Climate Change* (IPCC), a reduction of greenhouse gas (GHG) emissions must be achieved to stay within the respective limits of global warming. Therefore, the expansion and integration of renewable energies (RE) and other sustainable resources into all energy-consuming processes are required. In addition, atmospheric carbon dioxide removal (CDR) will play an important role in accomplishing GHG neutrality. (IPCC, 2022b)

Even after decarbonization, sectors such as agriculture or waste management will continue to emit CO_2e due to inherent processes that cannot entirely eliminate GHG emissions. Therefore, negative emissions technologies (NET) can be used. NET is a superordinate term for various technologies that have a negative CO_2e emission balance in common. (Erans et al., 2022)

Direct air carbon capture and storage (DACCS) is recognized to be a promising NET for CDR. The *International Energy Agency* projects global negative emissions of 980 $MtCO_2/a$ by DACCS in its net-zero emissions scenario for 2050. (IEA, International Energy Agency, 2022) In addition, the IPCC assumes capture rates to be between 0 and 1.74 Gt CO_2/a by DACCS in 2050. (IPCC, 2022b)

Among other countries, Germany has agreed to become GHG neutral in 2045 and to achieve overall net negative GHG emissions by 2050 in its *Federal Climate Change Act* § 3. (*Federal Climate Change Act.* Federal Ministry of Justice, 2021) Research groups that examine pathways towards a GHG-neutral Germany also consider DACCS as part of the solution. (DENA, 2021b; Prognos et al., 2021)

Despite its potential, Direct Air Capture (DAC) technology encounters substantial challenges. Its current scale of devices in operational use is very low compared to the capacity that is proposed in the future. As of 2022, all globally installed DAC plants have a capture rate of only 0.01 $MtCO_2/a$. (Ozkan et al., 2022) The current low-scale deployment is correlated with the high investment costs of the technology. In addition, its operation resources are heat and electricity which are also cost-intense. (Lackner and Azarabadi, 2021) Concerning economics, current literature suggests that high full-load operation hours (FLOH) should be targeted to compensate for the high cost of DAC technology and promote technical development through increased use. (Block, 2022; Fasihi et al., 2019)

However, power and heat systems must be restructured as well as other sectors for the electrification of the whole energy sector to enable sector coupling (SC). (Ramsebner et al., 2021) In the case of coupling the heat and power sectors, some adjustments are essential. Due to fluctuating RE and the seasonal differences in the heat demand, there is a need to install larger RE plant capacities as well as short-term and seasonal thermal energy storages (TES) to be able to serve consumption peaks and to use peak generation of RE. Overall, more flexibility is needed. In the heating sector, technologies have already been identified to be flexible consumers such as power-to-heat plants. (Wietschel, 2019)

1.1 Research Subject

In this thesis, the potential of a flexible operation mode of DAC plants is investigated as sector coupling is progressing. The potential analysis of this thesis is conducted for the example of Hamburg in 2045. It shall be determined whether flexibly operated DAC plants in Hamburg can contribute a significant share of the negative GHG emissions to the goals of Germany. The service of CO_2 isolation should be provided at viable costs and help to stabilize the heat and power system of Hamburg. Further clarification is needed to determine whether the FLOHs of DAC plants in Hamburg can reach sufficiently high levels to remain economically viable under the condition of utilizing surplus heat and negative residual loads in the power system while minimizing demand-related costs.

Studies considering Hamburg's district heating (DH) designs in 2045 are the basis of this thesis. For the research subject, unused surplus heat, and heat generator capacities within the DH system of Hamburg are identified. For the electricity supply of the DAC plants, a study about the power system of Germany containing a forecast of negative residual loads in 2045 is used and modified in a per-capita approach to the size of Hamburg. In literature research, a proposed CDR rate of Hamburg in 2045 is derived. Parameters concerning the techno-economics of DAC plants are also retrieved by literature research and further assumptions.

Scenarios are developed to consider three different DH system designs. Further, space requirements for DAC plants and the space availability in Hamburg for a physical integration are also analyzed. Therefore, two design options for DAC plants are considered with different investment costs and space demands. The first one deals with a large-scale DAC plant located on an open field and the second option examines several small-scale plants positioned on buildings that have flat rooftops.

Different demand-related costs are considered to take uncertainties of future developments into account that could affect the potential of a flexible operation. An optimization model is programmed and used to solve the developed scenarios. The design options are solved to find the minimum levelized costs for the CO_2 isolation of the DAC plants.

The results of the optimized scenarios are also reconciled with the spatial analysis of Hamburg. The objective of this thesis is to make a statement about whether flexibly operated DAC plants in Hamburg could be implemented in a physically, technologically, and economically feasible way. Therefore, the DAC plant capacity, space demand, and minimum costs for CO_2 removal are determined next to the compatibility of the DAC plants with the used heat and power system. An overview of the logical concept of the methodology of this thesis is illustrated in Figure 1.

In this thesis, only the DAC plant's process until the point of CO_2 isolation is addressed. The post-processing steps consisting of the transport and storage of CO_2 are not part of this thesis. Further, the thesis' results only consider the economic viability in 2045 as a snapshot. A larger period is not considered, and the profitability of this operation mode can change throughout the lifetime of the DAC plant's project. The parameters and data that are used within this thesis are obtained by literature research and do not consist of measured data of a real-world application. A distinction is not made whether the power system or the DH system is served more by this operation mode. Additionally, this thesis does not address the issue of public acceptance regarding the actual implementation of DAC plants within the city of Hamburg. Further limitations and uncertainties occurring due to assumptions and simplifications in this thesis are presented in Chapter 5.1.

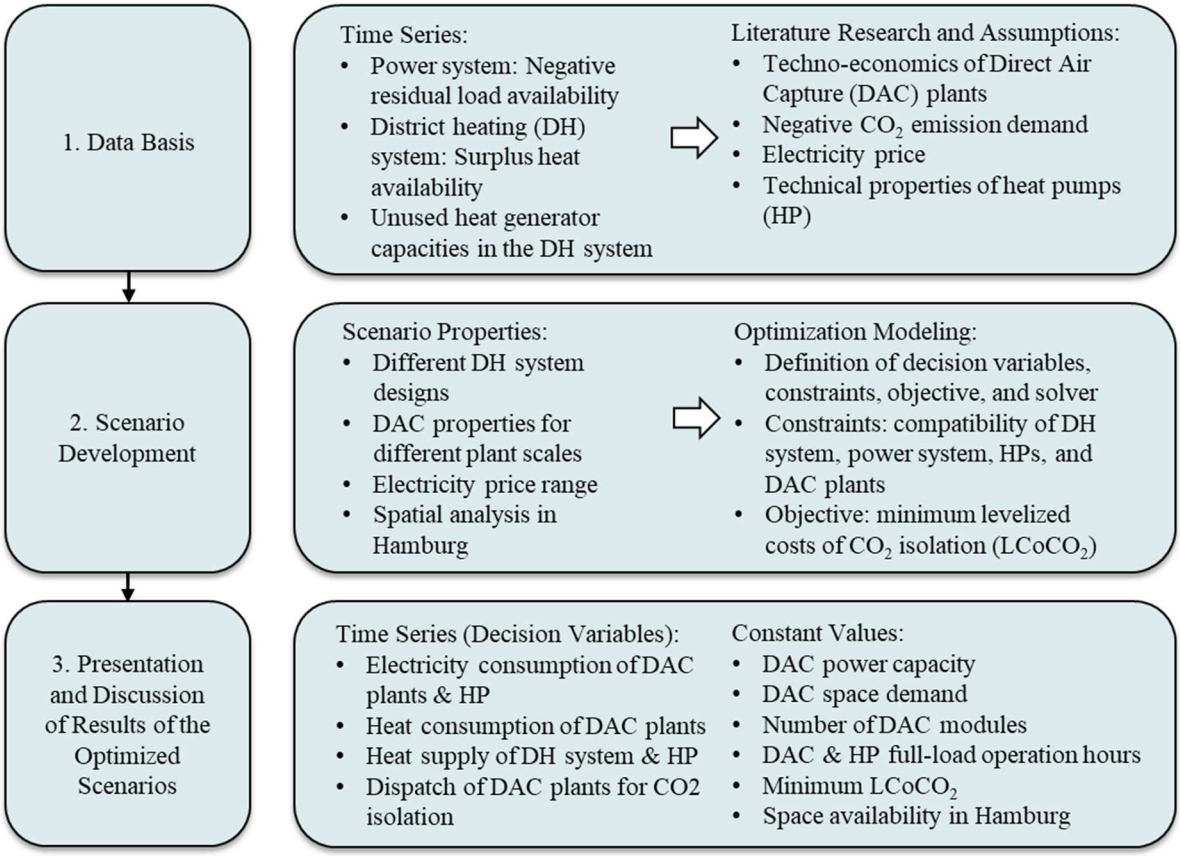

Figure 1: Schematic of the methodological concept of this thesis. (Own illustration)

2 Theoretical Background

In the theory section, a common background of knowledge is formed for understanding this thesis. It starts with the overall goal of sector coupling in Germany in Chapter 2.1 as the research subject investigates synergies between the heat and power sectors by integrating flexibly operated DAC plants in Hamburg. Therefore, the basics of the German power system and district heating systems are mentioned in Chapters 2.2 and 2.3, respectively. The baseline scenarios of both sectors for this thesis are introduced. Afterward, the state of the art in direct air capture technology with a focus on low-temperature processes is described in Chapter 2.4. This is done with the help of the latest literature considering mainly the timeframe from 2018 until March 2023. Further, the framework of optimization modeling is explained in Chapter 2.5 to get familiar with the used methodology. At last, the basics of the calculation of economic efficiency concerning DAC plants are given in Chapter 2.6.

2.1 Sector Coupling

In the future, the energy sector is expected to be mainly based on electricity as the primary energy source provided by RE. Therefore, most of the energy-demanding processes need to be electrified and thus transformations in all sectors are necessary. However, most REs such as wind energy and photovoltaics are non-dispatchable generation plants because of their dependency on changing weather conditions during the day and throughout the year. Their inflexibility can cause bottlenecks in the electricity grid and therefore in the entire energy system. (Ramsebner et al., 2021)

Sector coupling (SC) deals with the plan of linking the sectors of electricity, heat, and transport. Further, industrial processes and their infrastructures, communication grids as well as street grids can be integrated into a comprehensive view of SC. Useful synergies across the sectors and grids are developed to improve the overall stability and flexibility of the energy system. In case certain processes are not capable to operate directly with electricity, the required energy form needs to be provided indirectly by electricity or by another sector's energy form with the beneficial energy type. Concepts for energy storage capacities are also included in SC to smooth the intermittent feed-in of RE and to fulfill the required energy balances. The measures of SC shall lead to increased flexibility in energy demand and supply for the total energy system. (Fridgen et al., 2020)

The research subject of this thesis concentrates on the potential of DAC plants which should be operated as flexible consumers in the power and heat sector of Hamburg. The following sections contain basic information about the sectors that is required in the context of this work.

2.2 Power System

The electrical power system is very sensitive and needs to maintain equilibrium in terms of the physical and regulative balance of demand and supply at every point in time. In theory, Germany's power system uses an alternating current with a frequency of 50 Hz. However, fluctuating RE sources with uncertain weather conditions, deviations in the forecast, unpredicted plant failures, and grid contingencies cause imbalances in the power system and therefore lead to deviations of the frequency which could lead up to a blackout in the worst case. (Gorjão et al., 2022) In the past, the balance was accomplished by regulating conventional power plants in demand-driven power production. However, a paradigm change is necessary for the integration of non-dispatchable RE. Flexibility has to be provided by producers and consumers in future power systems. (Kondziella and Bruckner, 2016) The frequency of the power system is an important indicator of the stability of the power system and is always monitored to restore the balance. (Gorjão et al., 2022)

2.2.1 Residual Loads

Imbalances in the power system are also called residual loads. Residual loads can be either negative or positive. Negative residual loads appear if the energy generation is higher than the energy consumption. This affects an increase in the frequency. Positive residual loads appear if the demand is higher than the energy supply and this results in a decrease of the frequency. (Gorjão et al., 2020; Kohlhepp et al., 2019)

2.2.2 Electricity Sector and Market Regulations

In Germany, the federal law *Energiewirtschaftsgesetz* establishes the framework for the electricity sector and market among other things. Several mechanisms such as the balancing group management are set in place. The balancing group management aims to balance the demand and power generation every 15 minutes throughout the day within a balancing group (BG). Each BG has a balance responsible party that is in charge to match the energy balance. On a higher level, several BGs are integrated into load frequency control areas (LFC area). The remaining deviations of the BGs within a LFC area must be leveled out by the Transmission System Operators (TSO). (*Energiewirtschaftsgesetz.* Federal Ministry for Economic Affairs and Climate Action, 2005)

2.2.3 Merit Order Effect

For the following paragraph, it is recommended to be familiar with the terms *spot market*, *merit order*, and *clearing price* in the context of the electricity market. The massive implementation of RE in the electricity sector reduces electricity prices at the spot market. As RE has marginal costs close to zero, the clearing price for a fixed electricity demand within a trading period is shifted towards lower prices when more RE is fed in. More cost-intense power plants are forced out of the market. This is the merit order effect. In the past, the clearing price could reach negative values at times of negative residual loads. This is due to the inflexibility of conventional base-load power plants whose operators are willing to offer negative prices to avoid a total shutdown of their facilities. However, the current electricity market pricing model is criticized as not being suitable for a 100 % RE power system as the profits for electricity become smaller due to lowered clearing prices. New electricity market designs are necessary to maintain an economic business case for the integration of RE. (Kolb et al., 2020)

A research group consisting of members of the *Fraunhofer IEE*, *Fraunhofer ISE*, and *Becker Büttner Held* examined a framework of an electricity market model that is attractive for further RE integration until 2045 and 2050. They developed the study during the revision of the *Federal Climate Action Act*. They stated that in 2050 and 2045 negative electricity prices are likely to occur for 300 to 400 hours per year at negative residual loads. However, they outline that negative prices must be avoided with modifications in political regulations. They assume that periods of negative electricity prices can be met with cascading RE offers in the market for 0 €/MWh in the future. (Fraunhofer IEE et al., 2021)

2.2.4 Flexibility Services

Flexibility services are implemented on a medium- to low-voltage level next to the high-voltage level balancing services. (Eid et al., 2016) Flexibility within the system can be initiated on both the production and demand sides. Applications and methods such as energy storage, curtailment of RE surplus production, demand side management, grid extension, and the integration of virtual power plants become more relevant. (Kondziella and Bruckner, 2016)

2.2.4.1 Balancing Services

For the balance on the level of the LFC areas, balancing services are used. Therefore, the TSOs arrange auctions to contract and pay for positive or negative balancing services depending on the type of balancing service. (*Energiewirtschaftsgesetz.* Federal Ministry for Economic Affairs and Climate Action, 2005) The balancing services can be distinguished in their activation time and operating time until and how long they have to provide the contracted full power. (Eid et al., 2016)

The balancing services can be either negative, positive, or symmetric. Negative balancing services are realized by lowering the energy production or increasing the energy consumption while positive balancing services provide higher energy production or take energy consumers off the grid. Symmetric reserves can do both, provide or consume power. (Boldrini et al., 2022)

2.2.4.2 Demand Side Integration

The term demand side integration (DSI) is used generically for methods that deal with the flexibilization on the demand side. DSI includes demand-side management (DSM) and demand response (DR). DSM is used to directly influence and actively control energy consumers. (Stötzer et al., 2015) DR is used to manipulate the end user's behavior indirectly. Incentives such as dynamic prices over time or compensation payments are provided depending on the upcoming residual load. The load shift aims to reduce peak demands and fill valleys within the power system. (Chen et al., 2021)

Recent literature considers industrial DR to be promising. The industrial sector strives for maximizing its profits. Since most processes will be based on electricity in the future, electricity price-based DR and other incentives become more important and could be of advantage for effective load shifting. (Chen et al., 2021; Yan et al., 2018) Further information about DR and DSM can be retrieved from the following textbook. (Mohammad and Mishra, 2019)

2.2.5 Baseline Scenario: Power System in Germany

At *Fraunhofer Institute for Solar Energy System ISE,* the energy system model *REMod* (*Regenerative Energy Model*) has been developed and is used to minimize the costs of different SC scenarios in Germany. A CO_2 emission budget is defined, and the model must adhere to several CO_2 reduction targets for specific years. In the optimization model, energy suppliers, consumers, converters, and storage applications in different sectors are considered and implemented. All energy flows are balanced out in an hourly resolution throughout every year within the timeframe of the simulation to ensure a secure and robust energy system. (Bürger et al., 2019) *REMod* is based on non-linear optimization programming. (Fraunhofer Institute for Solar Energy Systems ISE, 2023)

In 2020, *Sterchele et al.* used *REMod* to model different possible scenarios for Germany starting in 2020 up to its way to net-zero GHG emissions in 2050. (Sterchele et al., 2020) The *Federal Climate Action Act* constituted that the objective has to be already achieved by 2045. (*Federal Climate Change Act.* Federal Ministry of Justice, 2021) Therefore, the research group has updated their study and investigated stricter scenarios. The study and the simulation of *REMod* take the SC of heating, power, buildings, industry, and mobility into account. The weather conditions in the model are based on time series of the years 2011 to 2015 (Sterchele et al., 2021)

However, the integration of flexible energy producers and flexible consumers into the newly described simulation of *REMod* is very complex. Therefore, the model has so far only been able to compute a residual load containing inflexible demands subtracted by inflexible power production. Inflexible production would be supplied by fluctuating RE and inflexible feed-ins by district heating, industry, and residentials that might use combined heat and power (CHP) plants or fuel cells. Shares of inflexible power demands can occur in processes that are also considered flexible. For example, hydrogen production needs to cover the minimal hydrogen supply of other processes but in times of surplus energy, hydrogen production can be increased to store hydrogen. The inflexible and flexible parts of processes are split up in *REMod*. Other inflexible power consumers are residentials and industries that consume electricity for light, space, or process heating and information communication technology. Further, inflexible demand shares of battery electric vehicles, power-to-X, and district heating are considered. However, no information is provided about the specific share of power generators in the total electricity supply. (Kaiser, 2022) The residual load of the reference scenario in 2045 is illustrated in Figure 2.

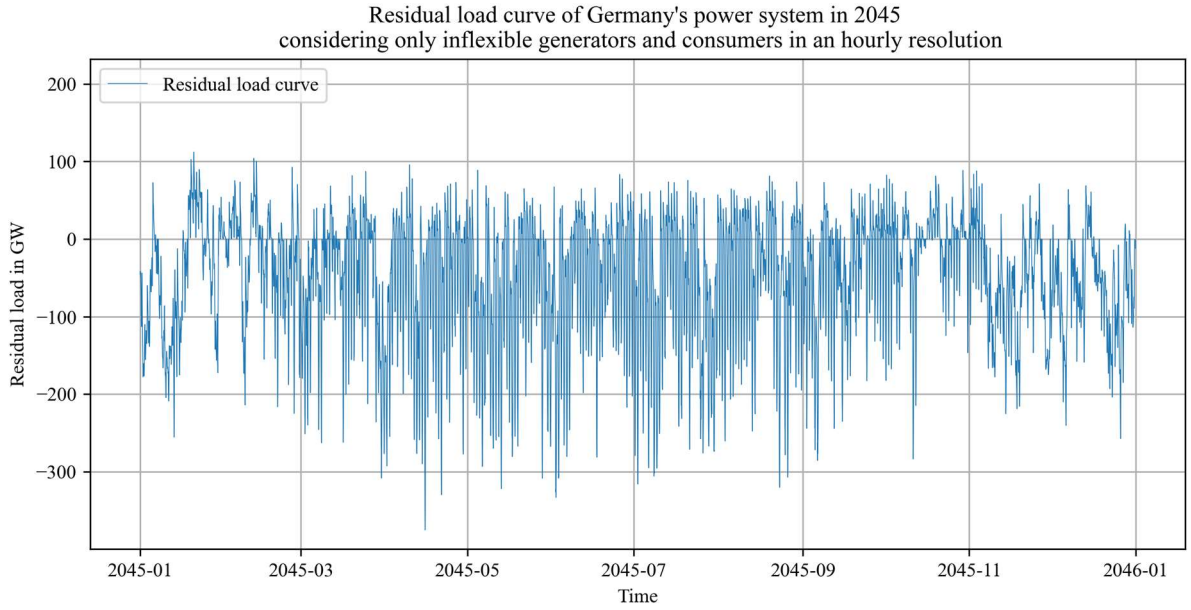

Figure 2: Residual load in Germany's power system in 2045 predicted by the optimization model REMod. The data contains only inflexible electricity producers and inflexible consumers of the reference scenario. (Own illustration based on (Kaiser, 2022; Sterchele et al., 2021))

2.3 Heating Sector – District Heating

In 2022, Germany's heating sector reached a renewable share of 17.4 % in its final energy consumption. (German Environment Agency, 2023) The heating system must become more sustainable and aim for a complete supply of RE and other sustainable heat resources. The transformation of current DH systems is necessary to achieve an overall climate-neutral energy system. (Lund et al., 2014) For a further understanding of the integration of DAC plants in a DH system, a baseline of knowledge about DH systems must be formed.

DHs are isolated networks that are each owned and operated by single companies. The DH systems are distinct and fulfill different purposes and have different dimensions that are needed in the specific local network. Because DH systems are isolated, they cannot sell surplus heat to another DH system operator but only to the consumers within their network. (Triebs et al., 2021) DHs are mainly used if a high heat demand density is in place to operate feasibly although the heat distribution infrastructure costs are high. (Lund et al., 2014)

Most of Germany's current heat grids are based on the 3rd generation of DH. Those systems operate with temperatures regularly below 100 °C. The 3rd generation of DH was introduced in the 1970s after the two oil crises. Local fuels such as coal, gas, waste, biomass, and renewable heat sources should be enabled as heat sources and increased energy efficiency was also achieved by the reduction of the temperature level compared to the 1st and 2nd generations of DH. (Lund et al., 2014)

In the latest literature, research focuses on the implementation of the 4th and 5th generations of DH. (Gudmundsson et al., 2021) However, the name of the 5th generation is misleading, because it is not meant to be the consecutive improvement of the 4th generation DH system but it is rather a parallel design approach. (Lund et al., 2021) The 5th generation of DH would be more drastic in lowering the temperature level to ambient temperature for heat pumps (HP). (Buffa et al., 2019; Gudmundsson et al., 2021) The characteristics and transformation steps of a 4th generation of DH are explained, because some DAC plants can operate with temperatures below 100 °C (see Chapter 2.4.1). (McQueen et al., 2021)

Li & Nord researched on technical issues and challenges of the transition towards 4th generation DH and suggested that the transformation should be planned and performed thoroughly and stepwise. (Li and Nord, 2018) According to *Triebs et al*., most of Germany's municipalities have planned a strategy to decarbonize their DH system. However, accurate data are often not publicly available, because there are no disclosure obligations in the heating sector as there are in the electricity sector. In their literature review, it is stated that the publicly available strategies do not announce specific measures that would have to be taken to achieve the goals but rather mention general proposals and potentials. (Triebs et al., 2021)

In general, heat grids to the 4th generation of DH shall enable the further integration of sustainable and renewable heat sources and thermal energy storages (TES) that are locally available. The most important measure is the further reduction of the temperature level within the heat grid compared to the 3rd generation of DH. This is a requirement to integrate large-scale solar thermal and geothermal systems, as well as industrial and urban waste in a DH system. These heat generators are not suitable for a decentralized heat supply in rural areas among other things. (Li and Nord, 2018) Additional integration of power-to-heat systems and HPs enhances the sector coupling between the heat and electricity sectors. (Lund et al., 2014) The latest measuring equipment shall ensure a more flexible, robust, and smarter heat system. (Li and Nord, 2018)

2.3.1 Baseline Scenario: District Heating in Hamburg

Kicherer et al. design a detailed transformation roadmap for a large-scale DH system of Hamburg until 2050. They identify local renewable heat resources and lay them out to fulfill the expected heat demand in 2050. (Kicherer et al., 2021) Their paper is based on the master thesis by *Kicherer* which includes more detailed information and explanations about the DH system. (Kicherer, 2020) In the following, technical characteristics of the DH system design approach are given.

The temperature level of Hamburg's DH system is higher than usual due to its scale. The DH system's design by *Kicherer et al.* includes a temperature level reduction from its current maximum of up to 130 °C down to below 100 °C. The model is expected to achieve a maximum temperature of about 94 °C by an assumed mix of the heat generators. The total heat demand in 2050 is generated by a standard load profile generator which is based on the test reference year (TRY) 2045 due to availability restrictions. As a result, the heat generation mix is modeled as a time series for 2050 in an hourly resolution considering the TRY 2045. (Kicherer et al., 2021)

The time series of the heat demand of the consumers and the heat supply by different heat sources is shown in Figure 3. Between May and September 2045, timeslots with surplus heat are available. However, from January until April as well as November and December the energy demand is higher than the production of renewable and sustainable heat sources can cover.

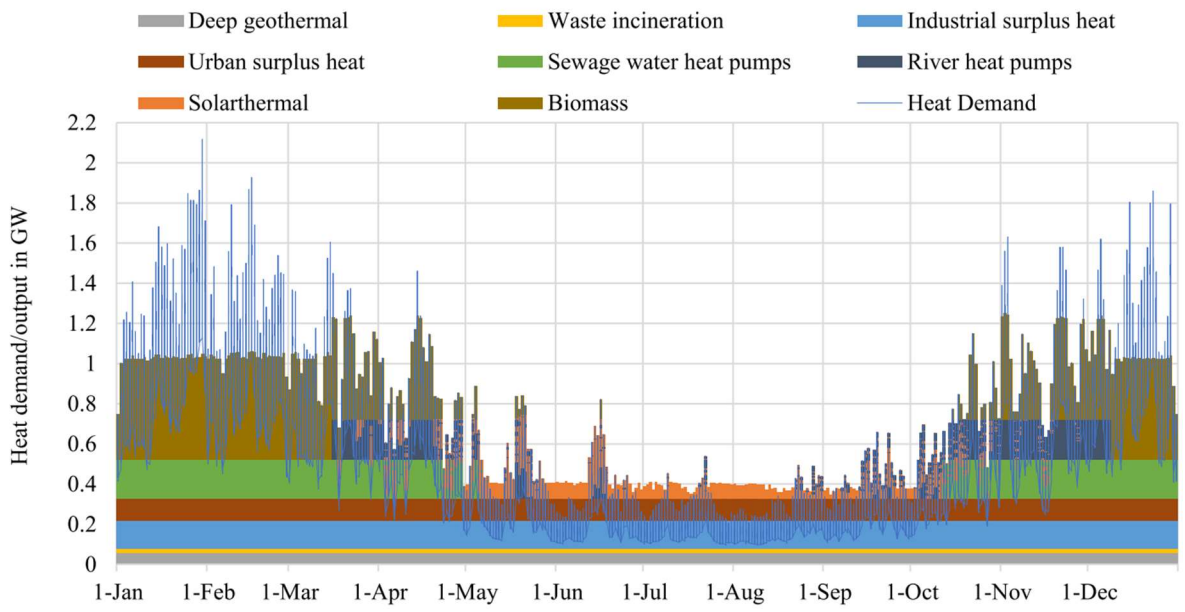

Figure 3: Sustainable heat generation-mix and demand profile of Hamburg's district heating grid in 2045 with an hourly resolution by (Kicherer et al., 2021)

Kicherer et al. consider short-term TES for smoothing the residual load peaks up to 6 hours while the master thesis of *Kicherer* also considers 2 and 12 hours of storage capacity. (Kicherer, 2020) In addition, seasonal TES could be used to shift surplus heat of the amount of 416 GWh that is produced during summertime into the wintertime when 326 GWh heat demand is not covered, yet. Consideration of seasonal TES is not made in detail. (Kicherer et al., 2021)

In addition, the research group *Kicherer et al.* developed a merit order for the prioritization of heat source utilization. The merit order is designed to integrate the must-run generators at first. These are deep geothermal energy, waste incineration, industrial and urban surplus heat, as well as solar thermal energy. (Kicherer et al., 2021) The merit order is depicted in Figure 4.

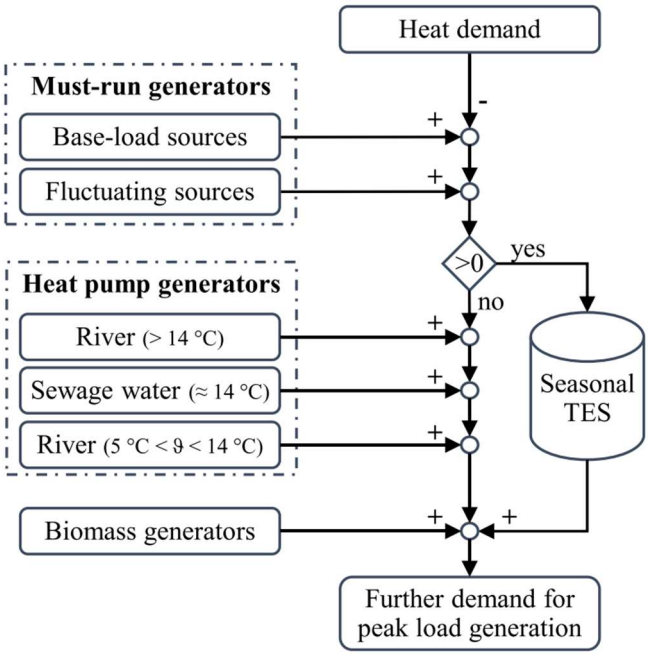

Figure 4: Merit order of the heat generators for the DH concept of Hamburg in 2045. (Kicherer et al., 2021)

In case the heat supply cannot be covered by the must-run generators HPs' power is added. There are two different kinds of HP implemented in the DH system. One HP uses sewage water, while the other HP is designed to utilize water sourced from the Elbe River. The river HP is only allowed to operate if the temperature of the Elbe is higher than 5 °C to avoid internal damage to the HP due to freezing water. The temperature of the Elbe varies throughout the year while the sewage water temperature is thought to be constant. The respective HP with the higher inflow water temperature is selected first if additional heat is needed to ensure a cost-efficient heat supply by the more efficient HP. In case the firstly chosen HP is operating at its maximum power capacity and further heat supply is needed, the second HP is added. (Kicherer et al., 2021)

After the HP usage, biomass incineration would be applied. In addition to biomass incineration, heat would be supplied by a seasonal TES. As a last resort, more expensive peak load generators such as electric boilers are scheduled. (Kicherer et al., 2021)

2.4 State of the Art: Direct Air Capture

DAC has the potential of isolating emitted CO_2 by mobile and nonpoint sources reliably and predicably as well as saving resources in terms of land use and water. Further, it can enable long-term geological storage in DACCS applications. They are flexible in their choice of location as they can operate near energy production sites or next to the respective storage or utilization site. However, the DAC technology has a lower technology readiness level (TRL) and higher levelized costs of CDR compared to afforestation and reforestation (AR), bioenergy carbon capture and storage (BECCS), or soil carbon sequestration (SCS). (Erans et al., 2022)

Currently, DAC technology faces several challenges. Different materials, chemicals, and methods are available within the DAC market with different technical readiness levels. Despite this, the most prominent and mature DAC methods according to literature and in current operations applied are based on sorbents. (Low et al., 2023; Ozkan et al., 2022) Sorbent-based DAC plants have a TRL of 6 to 7 which means that there are demonstration plants in place. However, a wide range of values for investment costs, energy demand, and levelized costs of CO_2 removal is stated in the literature for different sorbent-based DAC approaches. (Erans et al., 2022)

A rapid expansion and deployment of DACCS applications are needed considering the globally existing DAC capture rate in 2022 of about 0.01 $MtCO_2/a$ and the projected capture rates of up to 1.74 $GtCO_2/a$ in 2050 by *IPCC*. (IPCC, 2022b; Ozkan et al., 2022) This can be achieved by implementing political incentives. Current political funding in an international context on DAC technology is also described in the following papers. (Erans et al., 2022; Ozkan et al., 2022)

In the following, the principle of a sorbent-based DAC process is described. The solid sorbent-based process is applied in this thesis. Therefore, more details on the process, its current energy demands, and costs are given below. Alternative approaches are only mentioned shortly and afterward, DAC actors and projects are presented. There is also an excursus to business cases and their impact on the net CO_2 emissions.

2.4.1 Sorbent-Based DAC Process

The process of sorbent-based DAC is including the following simplified steps. The ambient air is drawn into the system towards the sorbent. The inflow can be either natural or speeded up by fans. In the next step, the air flows over a sorbent. In this step, CO_2 molecules are bound to the sorbent. The CO_2 concentration in the outgoing air stream is reduced. After the filter is saturated with CO_2, the separation of the CO_2 from the sorbent takes place. For this purpose, thermal or electrical energy is added in the desorption phase. Once the regeneration phase is completed, the sorbent can be recharged again in the next CO_2 capture cycle. (Viebahn et al., 2019) A schematic of the most important energy flows of the process is illustrated in Figure 5.

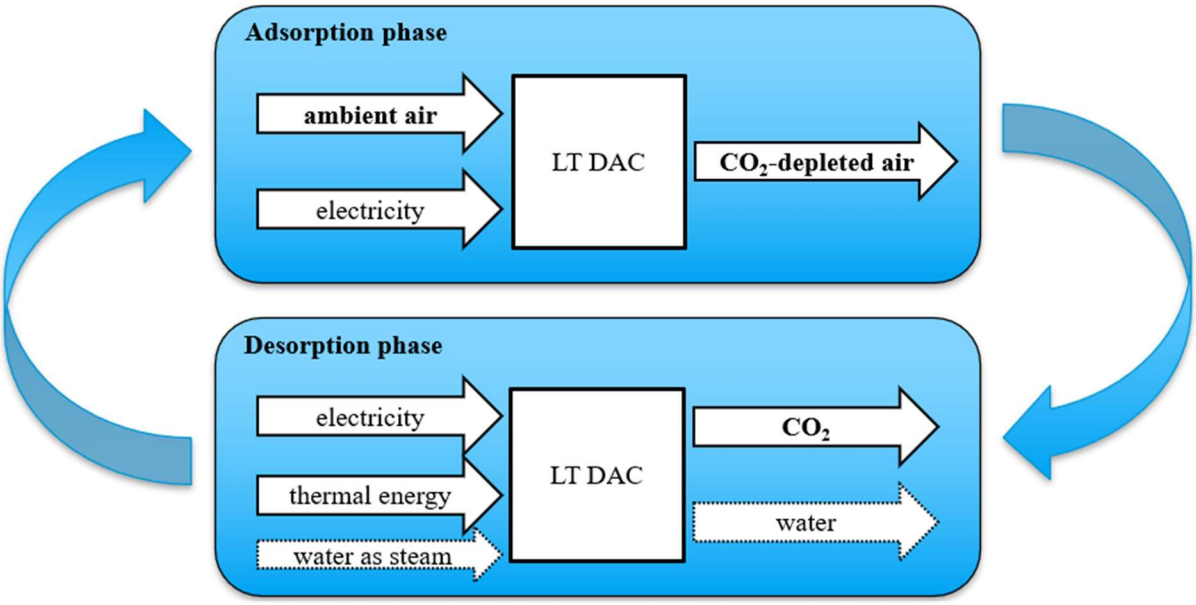

Figure 5: A simplified representation of a sorbent-based DAC process with its energetic inputs and outputs. In the adsorption phase, ambient air flows into the DAC plant using electrical fans. CO_2-poor air leaves the DAC contactor after CO_2 is bound to the filter inside the plant. Afterward follows the desorption phase when residual air is evacuated by an electrical plant and the contactor is heated up to detach the CO_2 of the filter. Steam can be used to increase the desorption efficiency. Concentrated CO_2 can be processed for further transportation or storage. (Own illustration)

In literature, the sorbent-based DAC processes can be distinguished by their sorbent material. DAC plants can operate with solid adsorbers or liquid absorbers. In the case of the liquid sorbent-based process, absorption and desorption can operate in parallel. Solid sorbent-based DAC must however first perform the adsorption and afterwards the desorption of the CO_2. (Fasihi et al., 2019) Further, liquid sorbent-based DAC processes consume water. Solid sorbent-based DAC can also use water, however, water can be gained as a byproduct and has a positive water balance. In both cases, the heat demand is about 80 % of the total energy demand and the electricity demand is up to 20 %. However, they require different temperature levels for the sorbent's regeneration. Liquid absorbers require temperatures of up to 900 °C while solid adsorbers manage to operate within a temperature range of about 80 and 120 °C. (McQueen et al., 2021) Solid adsorbers and liquid absorbers are therefore often called Low-Temperature (LT) DAC and High-Temperature (HT) DAC, respectively. (Beuttler et al., 2019; Fasihi et al., 2019) For a detailed description of the HT process, it is referred to (Sabatino et al., 2021). The LT DAC process is revisited in the next chapter.

2.4.1.1 Low-Temperature DAC Process

In the LT DAC market, temperature vacuum swing adsorption (TVSA) and moisture swing adsorption (MSA) are prominent. (Fasihi et al., 2019) The TVSA procedure is explained in detail in this subsection.

LT DAC plants can be constructed in a modular design to save spatial resources. (Beuttler et al., 2019) In the TVSA approach, the charging and discharging phases of the sorbent alternate. The adsorption and desorption phases do not operate in parallel. Both phases of the process take place in the same contactor chamber. (Fasihi et al., 2019) In the adsorption phase, the ambient air is directed toward the solid adsorbent by fans. The fans consume electricity and can control the air mass flow. CO_2 is adsorbed

chemically at the sorbent. (Stampi-Bombelli et al., 2020) Different solid sorbents such as carbonates, silica-supported sorbents, and amine-based or metal-organic frameworks can be used. Those have different durability and timeframes for saturation as well as regeneration. (Azarabadi and Lackner, 2019)

The filtered air stream leaves the DAC plant in the atmosphere. The blowdown step is initiated when the sorbent is saturated by CO_2. In this quick step, the further inflow of air into the contactor is blocked where the sorbent is positioned in. The blowdown step includes the evacuation of the contactor to lower pressure by a vacuum pump which consumes electricity. Afterwards, the contactor is preheated to the desorption temperature which is about 100 °C. By the combination of low pressure and heat supply, CO_2 is detached from the sorbent material. Some TVSA processes include a steam purge of the sorbent to increase the output of CO_2 in the desorption phase. The main energy resource used in the TVSA is thermal energy. (Stampi-Bombelli et al., 2020)

Next to CO_2, pure water can be gained as a byproduct in the TVSA process due to the moisture in the inflowing air stream and the steam purge in the desorption phase. In the case of steam purge, the steam is mixed with the CO_2 and then condensed as a byproduct at the condenser. Afterward, the CO_2 can be compressed to transport it to a storage site or another utilization site. (McQueen et al., 2021) The process and the most important components of the TVSA plant are illustrated in Figure 6.

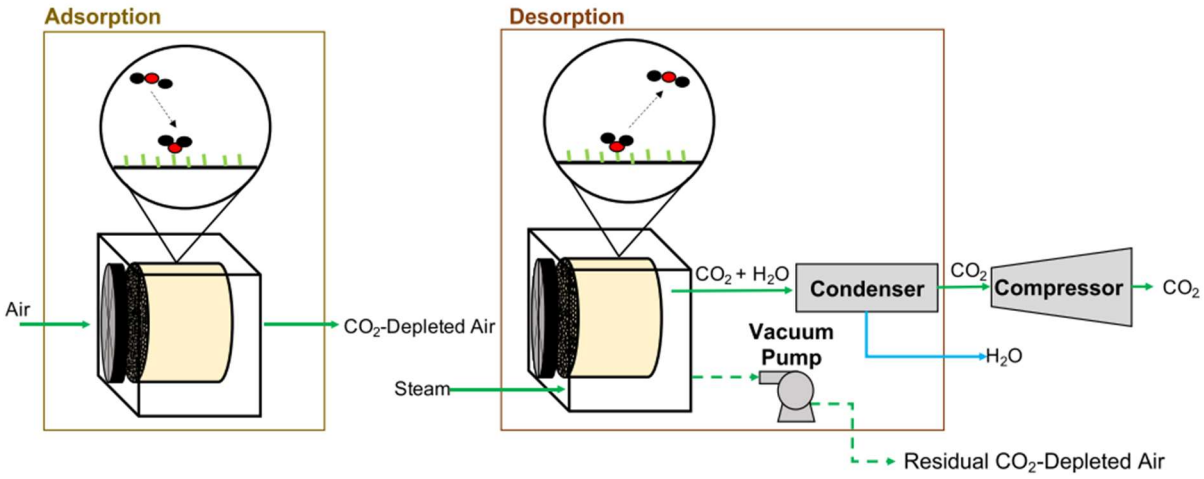

Figure 6: A process flow diagram of a TVSA DAC plant that includes the adsorption and the desorption phase. The blue line determines a liquid flow. The green lines illustrate gaseous flows and the dashed green line connects the contactor with the vacuum pump to illustrate the removal of remaining air from the contactor which is necessary before starting the desorption phase. (McQueen et al., 2021)

The heat and electricity demand for the operation of DAC plants using TSVA procedures are given in a wide range in the literature. They are often related to the specific energy consumption to remove one ton of CO_2. *Beuttler et al.* state for large-scale DAC plants the goal of reaching a total of 2,000 kWh/tCO_2 in 2025 with an electricity share of 400 kWh and 1,600 kWh thermal energy consumption. (Beuttler et al., 2019) *Fasihi et al.* scanned the literature for energy demands and investment costs. They assume a range between 200 to 300 kWh for electricity and 1,500 to 2,000 kWh for the LT DAC plant's heat demand. (Fasihi et al., 2019) *Hanna et al.* assume a minimum electricity demand of 286 kWh paired with a 944 kWh heat demand. (Hanna et al., 2021) *Deutz & Bardow* calculated a heat consumption of 3,306 kWh and an electricity demand of 700 kWh. (Deutz and Bardow, 2021b)

Further information about technical and financial data concerning LT DAC plants is given in the methodology as the research of those data is necessary for the parameter setting for the optimization problem of this thesis (see Chapters 3.5.2 and 3.5.3).

2.4.2 Alternative DAC Technologies

Next to the sorbent-based DAC, there are alternative methods for DAC in research. Those are mentioned briefly to underline the open research field on DAC technology.

Developments in energy-efficient polymeric membranes with ultra-high CO_2 permeance and high CO_2/N_2 selectivity increase the potential for a business case of membranes in carbon capture of ambient air. (Fujikawa et al., 2021) However, the method needs higher CO_2 concentrations to work efficiently. (Castro-Muñoz et al., 2022) Further, membrane-based DAC faces economic challenges and is on a low TRL of 2 to 3. (Castro-Muñoz et al., 2022; Erans et al., 2022)

Other DAC methods such as cryogenic gas separation or electro-swing adsorption are also on a lower TRL between 2 and 4. More alternative methods and their TRLs are shown in the paper of *Erans et al.*. They review the techno-economic and socio-political challenges of different DAC technologies. (Erans et al., 2022)

2.4.3 Companies and Projects

As mentioned before, the most promising DAC technologies are based on solid or liquid sorbents. Those technologies have been tested in demonstration plants. As of 2022, all globally installed DAC plants have a capture rate of 0.01 $MtCO_2/a$. (Ozkan et al., 2022) The three commercial DAC market actors and some of their projects are introduced here.

The largest commercial plant currently in operation has been realized in the project *Orca* by *Climeworks AG* in Iceland in 2021. It has a capture rate of 4 $ktCO_2/a$. It is based on the TVSA process. Heat for the DAC is provided by a geothermal plant. In this project, CO_2 is captured by a solid sorbent and is geologically stored. Their partner for the carbon capture and storage (CCS) application is *Carbfix*. (Erans et al., 2022) For storage, CO_2 is mixed with water to mineralize naturally in deep geological layers as it has been tested in 2017 with a smaller prototype. Also in 2017, *Climeworks AG* commissioned their first commercial DAC plant with a 900 tCO_2/a capacity. It was built in Hinwil in Switzerland. Here, the business case was based on a carbon capture and utilization (CCU) application. The captured CO_2 was used in greenhouses for agriculture. (Gutknecht et al., 2018) However, the operation of the plant has been phased-out in October 2022, because *Climeworks AG* wants to focus on CCS applications. (Climeworks AG, 2022b) They also announced in June 2022 the start of another DACCS application construction with a capacity of 36,000 tCO_2/a in the project called *Mammoth*. It shall be located in Iceland as well. (Climeworks AG, 2022a)

Other established companies in the DAC project development field are *Carbon Engineering* and *Global Thermostat* who are both relying on sorbent-based DAC technology, too. *Global Thermostat* works on LT DAC plants while *Carbon Engineering* develops HT DAC plants. (Ozkan et al., 2022) However, both mainly focus on CCU applications such as enhanced oil recovery in joint ventures promoted by *ExxonMobil* or *Occidental Petroleum*, respectively. (Erans et al., 2022)

The largest project in development to date is being planned by *Carbon Engineering* in Texas and is expected to be operational by the mid-2020s. It shall operate with a net capture rate of 1 $MtCO_2e/a$. The basis for this plant development is given by the up-scaling and improvement of their current pilot plant with a net capture rate of 365 tCO_2/a which is in operation since 2015 in Canada. In both projects, *Carbon Engineering* uses or plans on using natural gas (NG) for the thermal energy supply of about 900 °C. The CO_2e emissions of the NG combustion result in a decrease in carbon capture efficiency.

Therefore, the carbon footprint of the energy sources has to be taken into account. In the case of the targeted 1 $MtCO_2/a$ net capture rate, a higher gross capture rate of approximately 1.5 $MtCO_2/a$ is installed to compensate for the carbon footprint of NG. (Keith et al., 2018)

Next to the three introduced DAC market players from above, more companies and joint ventures started entering the market lately. For an overview of other actors and their technologies, it is referred to (Fasihi et al., 2019). In addition, a list of companies and their current and planned projects can also be retrieved from the following papers. (Erans et al., 2022; Ozkan et al., 2022)

2.4.4 Excursus: DAC Business Cases and Their Environmental Impact

The two business cases for the DAC technology are DACCS and direct air carbon capture and utilization (DACCU). However, the DACCS and DACCU strategies should be considered complementary as they aim for different objectives. (Zhang et al., 2020) The DAC technology itself is only capable to isolate the CO_2 from the ambient air. However, the further processing of CO_2 determines the impact and contribution to the climate change mitigation goals. (Gutknecht et al., 2018)

The demand for CO_2 as a raw material for successful decarbonization is increasing in various sectors. CO_2 can be used or embedded in new products, such as low-GHG synthetic fuels, polymers, or the food industry in beverages. DAC technology can be used to enable a circular CO_2 economy and which increases the economic value of CO_2. (Ozkan et al., 2022) A low number of existing plants correlates with high investment costs. In addition, the high energy demands and prices for electricity and heat make the fast deployment of DAC plants difficult. That is the reason why most DAC plant operators currently sell the captured CO_2 as feedstock to the industry to reduce the net cost per ton of CO_2. (Erans et al., 2022; Ozkan et al., 2022)

DACCS applications aim for the permanent removal of CO_2 from the atmosphere. Long-term removal can be achieved by injecting CO_2 into geological sites. One approach is to mix water and CO_2. The mixture then has a higher density than the reservoir fluid in the geological layers due to the CO_2 content and is not prone to rise back to the surface. Once injected, the CO_2 reacts with metals in the surrounding and creates solid and robust carbonate minerals. (Gutknecht et al., 2018) DACCS projects are often funded by governments. (Erans et al., 2022)

As of April 2023, the German government has not allowed CCS applications to operate in Germany. Mostly because of the lack of acceptance in society in the past. (Vögele et al., 2018) However, the government is expected to propose a carbon management strategy in 2023 taking the latest technical improvements and developments of the CCS business case into account. (Federal Ministry for Economic Affairs and Climate Action, 2023)

CO_2e emissions of DAC plants as well as the processes that follow the CO_2 isolation can be net negative or net positive. It depends on the carbon footprint of the electricity mix and heat source. Net negative emissions can be achieved using DACCS applications if the share of fossil fuels in the electricity mixture is low. (Terlouw et al., 2021) However, DACCU applications cannot reach net zero emissions even in the case of electricity supply by RE and the utilization of waste heat. The DACCU applications achieve net positive emissions as the captured CO_2 is not permanently removed from the atmosphere. It is recycled into products for a time that is too short to be relevant for a positive climate impact. (Hepburn et al., 2019)

2.5 Optimizations

In general, optimizations are used to search for the best solution to a mathematical problem. Several solution sets can exist for a problem. Depending on the objective, the most favorable one can be found at the minimum value. Maximization problems can be solved by a mathematical transformation to a minimization problem. Optimization problems can involve one or multiple objectives. (Gunantara, 2018)

An objective is formulated by several variables that are influenced by constraints. Depending on the constraints, the solution of the optimization can be feasible or infeasible. If two constraints contradict a shared value of a variable, the overall solution to the problem does not exist. Therefore, all constraints for the variables must be fulfilled to get a solution for the objective at all. Global optimization algorithms can be distinguished as being stochastic or deterministic. (Snyman and Wilke, 2018)

2.5.1 Components of an Optimization

The most important components of an optimization model are parameters, variables, constraints, and one or more objectives.

The parameters are the input data. They are represented as constants that are necessary for the overall framework of the model. Together with the variables they are used to define the objective and the constraints. (Hart et al., 2011)

The variables are also called decision variables and their values are unknown at the beginning of the optimization. They are part of the optimization output of the program. However, they must be defined to be non-negative reals (NNR) or non-negative integers (NNI) before the program is started. (Hart et al., 2011) If both types of variables are defined within the program, the optimization becomes a mixed-integer optimization. However, optimizations that use NNI or MI optimizations result in a higher computation time. (Gurobi Optimization LLC., 2022; Hart et al., 2017)

Constraints are used to influence the variables. Variables are forced to be equal or unequal to another value that is based on given parameters. By integrating more constraints, variables are further restricted and become dependent on each other. Constraints and variables can be vectorized which is also called indexed. (Hart et al., 2011) This can be helpful for optimizations including time series when each timestep creates a new variable value that must be in line with the constraints.

An objective is a function based on a mathematically formulated equation. It takes the parameters as well as the variables that are influenced by the constraints into account. The objective is minimized concerning the optimum by the solving algorithm. (Snyman and Wilke, 2018) Different objectives can be pursued in parallel by various methods if the complexity of the considered system increases. (Pereira et al., 2022)

A solver is needed to solve the optimization model. There are more solvers available which are capable to solve a variety of optimization models such as linear programming (LP), non-linear programming (NLP), mixed-integer linear programming (MILP) as well as mixed-integer non-linear programming (MINLP). However, a list of solvers and their detailed mathematical solving processes is not part of this thesis. Information can be retrieved from literature e.g., (Hart et al., 2017; Snyman and Wilke, 2018)

An example of an optimization model can be depicted by equations containing the constraints, variables, and objectives. An example is given in Equation (1).

$$\begin{aligned} \text{minimize} \quad & f(x,y) = x + y \\ \text{such that} \quad & C1: y \leq 4 \cdot x \\ & C2: y \geq 3 \cdot x \\ & x, y \in \text{NNR} \; or \; x, y \in \text{NNI} \end{aligned} \tag{1}$$

With: f (x, y) = objective function
x, y = variables
3, 4 = parameters
C1, C2 = constraints

2.5.2 Real-World Optimization Problems

Different techniques can be used to solve deterministic optimization problems depending on the level of complexity and the scope of the application. In science, engineering, and for commercial and financial interests, mathematical optimizations of real-world problems are mostly based on nonlinear optimizations. NLP is more sophisticated because the variables are in a nonlinear relationship within the objectives and constraints. (Snyman and Wilke, 2018) LP is a special case of optimizations. The constraints and the objective involved contain only linear relationships of the variables. (Snyman and Wilke, 2018) Therefore, it is less complex than NLP, resulting in lower demand for computation resources. (Hart et al., 2017)

Complex multi-energy systems in the context of SC are approached by different mathematical optimizations. The SC scenario by *Sterchele et al.* is based on a nonlinear optimization model called *REMod*. (Fraunhofer Institute for Solar Energy Systems ISE, 2023; Sterchele et al., 2021) The methodology of *REMod* and the results of a model considering the power and heat system of Germany are described in the papers of *Henning & Palzer*. (Henning and Palzer, 2014; Palzer and Henning, 2014) An example of a real-world problem optimization with LP is given by *Kurucz et al.* who reduced system peak loads by modeling customer load control programs in Florida. (Kurucz et al., 1996)

2.5.3 Optimization Programming Environment

An optimization problem can be modeled with the help of the open-source software package called *Python Optimization Modeling Objects* (Pyomo). It is embedded in the high-level programming language *Python*. In their paper, *Hart et al.* state the origin of *Pyomo* and explain code syntax, its flexibility, and further advantages compared to other algebraic modeling languages. It can be used to model LP, NLP, MILP, and MINLP problems. (Hart et al., 2011) More details on the *Pyomo* software package are given in the respective textbook. (Hart et al., 2017)

2.6 Calculation of Economic Efficiency

For the economic efficiency review of a building installation, the *VDI 2067* policy is in place. It includes the annuity method which can be applied to the costs of a DAC plant. The annuity method uses an annuity factor (AF) which is later multiplied by the capital-related costs of the plant. The AF includes the interest rate r_{int} on the investment costs and the project's lifetime $t_{project}$ in years. The calculation of the AF is given in Equation (2). The costs of a plant are capital-related, operation-related, and demand-related next to others. (Verein Deutscher Ingenieure e.V., 2012)

$$AF = \frac{r_{int}^{t_{project}} \cdot (r_{int} - 1)}{r_{int}^{t_{project}} - 1} \quad [-] \tag{2}$$

Capital-related costs are stated as capital expenditures (CAPEX) in the form of investment costs. They can be determined by the multiplication of the specific investment costs and the power capacity of the plant. This is shown in Equation (3). (Fasihi et al., 2019; Verein Deutscher Ingenieure e.V., 2012)

$$CAPEX = Specific\ Inv.Costs \cdot Capacity_{plant} \quad [€] \tag{3}$$

With: CAPEX = investment costs [€]
Specific Inv. Costs = specific investment costs per power unit [€/(tCO_2/a)]
$Capacity_{plant}$ = power capacity of DAC plant [tCO_2/a]

The economics of DAC plants are usually indicated by the levelized costs of CO_2 isolation ($LCoCO_2$) in €/tCO_2 or \$/tCO_2. (Fasihi et al., 2019; Sinha and Realff, 2019) In literature related to LT DAC, the $LCoCO_2$ is calculated according to Equation (4). The CAPEX is multiplied by the annuity factor to break the investment costs down to an annual cost rate. Operation-related costs are given as annual operational expenditures (OPEX). The annual OPEX and CAPEX are divided by the net amount of CO_2 that is removed within a year. Demand-related costs are given by the specific consumption of electricity heat per ton of CO_2 multiplied by the levelized costs of electricity (LCoE) and heat (LCoH), respectively. (Fasihi et al., 2019) In the further course of this thesis, the abbreviations LCoE and LCoH are adopted as a generic term for electricity costs and heat costs for reasons of simplicity, regardless of the incorrect description of the content. In Equation (4), the specific energy demand of electricity and heat are called *DAC_el_demand_per_tCO2* and *DAC_heat_demand_per_tCO2*, respectively.

$$LCoCO_2 = \frac{CAPEX \cdot AF + OPEX}{Output_{CO2}} + DAC\_el\_demand\_per\_tCO2 \cdot LCoE + DAC\_heat\_demand\_per\_tCO2 \cdot LCoH \quad \left[\frac{€}{tCO_2}\right] \tag{4}$$

With: CAPEX = investment costs [€]
AF = annuity factor [-]
OPEX = annual operational expenditures [€]
$Output_{CO2}$ = annual mass of net CO_2 removal [tCO_2]
DAC_el_demand_per_tCO2 = electric energy demand per ton of CO_2 [kWh/tCO_2]
DAC_heat_demand_per_tCO2 = thermal energy demand per ton of CO_2 [kWh/tCO_2]
LCoE = levelized costs of electricity [€/kWh]
LCoH = levelized costs of heat [€/kWh]

3 Materials and Methods

To analyze the potential of flexibly operated DAC plants in Hamburg in 2045, several criteria and boundary conditions must be met. The DAC technology shall be used in the context of DACCS. Only the implementation of the actual DAC plants is addressed in this thesis. The implementation challenges, costs, and sites for the CCS process are not considered in the scope of this work. Simplifications and assumptions must be made in advance to investigate the research subject. The resulting uncertainties and limiting effects on the potential analysis that emerge due to the assumptions and simplifications are discussed in Chapter 5.

Different scenarios are created and investigated in terms of technical suitability and economics of the implementation of DAC plants in the heating and power system of Hamburg in 2045. An economic objective is developed and taken as the basis for the consideration of the feasibility of the scenarios. The outcome of these scenarios shall be obtained by a MILP optimization model.

Parameters about DAC plants, heat and power systems, and other necessary data for the model are retrieved by literature research and are further based on assumptions. The data and assumptions are used to develop the constraints and boundary conditions of the model and to identify the decision variables. The focus is on literature published between 2018 and 2023.

Chapter 3.1 explains the considered scenarios in short. The necessary parameters, assumptions, and system requirements for the optimization problem of integrating DAC plants in Hamburg are outlined in Chapters 3.2 to 3.7. First, the negative emission goal of Hamburg is determined in Chapter 3.2. The optimization model is built upon design approaches for the power and heat systems of Germany and Hamburg in 2045 introduced in Chapters 2.3.1 and 2.4.1. Those have to be further examined on requirements and modifications for the implementation of DAC plants. This is performed in Chapters 3.3 and 3.4. Afterward, parameters concerning the techno-economic aspects of DAC plants are worked out and determined for the optimization model in Chapter 3.5. Next to the investigation of the economic feasibility of the DAC plants, a spatial analysis is performed. Open fields as well as flat rooftops are considered in the city of Hamburg. The necessary DAC plant capacity shall be installed near the DH grid. The used methodologies are introduced in Chapter 3.6. Once the input data and parameters for the optimization model are determined, the development of the optimization model is addressed. Decision variables and constraints are established in Chapter 3.7.

3.1 Definition of Scenarios

Different scenarios with TES capacities between 1 and 12 hours are worked out in the master thesis of *Kicherer* (see Chapter 2.3.1). To take different DH system designs into account, three different scenarios of varying TES capacities in the DH system of Hamburg in 2045 are investigated. The impact of TES on the necessary power capacity of the DAC plants and the overall operation of flexibly driven DAC plants shall be addressed. The DAC application shall operate flexibly and serve both, the heat and power systems. The operation times of the DAC plants are therefore limited to timesteps when negative residual loads occur in both systems. A distinction of which system is served more by this operation mode is not made.

The first two main scenarios examine the minimum and maximum short-term TES capacities of 1 and 12 hours. In addition, the potential implementation of seasonal storage in the DH system is considered in a third main scenario. Seasonal TES would prohibit the utilization of surplus heat for DAC plants as the surplus heat would be stored in the seasonal TES instead. In this scenario, heat supply has to be provided only by unused heat generator capacities within the DH system. Further details of the TES capacity scenarios are described in Chapter 3.4.2. Sketches of the three main thermal energy storage capacity scenarios can be found in Appendix 1 to Appendix 3.

In the literature review on the techno-economics of DAC technology, it was found that specific investment costs and specific space demand of a LT DAC plant can be affected by its scale (see Chapters 3.5.2.3 and 3.5.1). Therefore, the implementation of flexibly operated DAC plants of different scales is investigated. The spatial availability in Hamburg and costs for differently scaled DAC plants shall be considered. Two sub-scenarios for each TES capacity scenario are examined in this thesis.

The first sub-scenario concentrates on the integration of a large-scale DAC plant in Hamburg. In this case, the DAC plant shall be placed on an open field. In the other sub-scenario, the implementation of multiple DAC plants of smaller scales is analyzed. Those are expected to be distributed on flat rooftops within the range of the heat grid of Hamburg.

Costs for the construction, the connection to the power and DH grid, the installation of a CO_2 transport infrastructure, and the following CCS process are not considered in the scope of this thesis. Further, the acceptance of Hamburg's citizens for the actual implementation of DAC plants within the city is not addressed here.

On a lower scenario level, a range of electricity prices is considered due to uncertainties in the price prediction until 2045. In this context, suitable electricity prices for the power consumption of the DAC plants and the HPs for the heat supply are additionally determined for economically feasible levelized costs of CO_2 isolation. In case the levelized costs of CO_2 isolation are higher compared to the reference value stated in Chapter 3.5.2.4 and the LCoE is at the lower boundary price range (see Chapter 3.3.1), negative LCoEs and LCoHs are determined for the DAC application. An overview of the investigated scenarios is given in Table 1.

The corresponding characteristics of the power grid and the LCoE are explained in Chapter 3.3. Further information about the interaction of the DAC plants with the heat and power system is given in the optimization model and its constraints in Chapter 3.7.

Table 1: Examined scenarios for the implementation of DAC plants in Hamburg with a fixed carbon dioxide removal rate. Different thermal energy storage capacities of the DH system are considered. It is further distinguished by the position and scale of the DAC modules which correlate with different specific investment costs and space demands. A range of levelized costs of electricity is also investigated and an optimum levelized cost of heat is reflected in specific cases. Each scenario receives a specific name code. (Own illustration)

Thermal energy storage (TES) capacity in the district heating system of Hamburg	**Position and scale of DAC plants**	**Energy prices (LCoE for DAC & HP // LCoH for DAC)**	**Name code of the scenario**
1-hour short-term TES	Open field (Large-scaled plant)	LCoE Lower limit	OF-stTES1h-wo/SeasTES-elLower
		LCoE Optimum	OF-stTES1h-wo/SeasTES-elOptimum
		LCoE Upper limit	OF-stTES1h-wo/SeasTES-elUpper
	Flat rooftop (Small-scaled plants)	LCoE Lower limit	FR-stTES1h-wo/SeasTES-elLower
		LCoE Optimum	FR-stTES1h-wo/SeasTES-elOptimum
		LCoH Optimum	FR-stTES1h-wo/SeasTES-thOptimum
		LCoE Upper limit	FR-stTES1h-wo/SeasTES-elUpper
12-hour short-term TES	Open field (Large-scaled plant)	LCoE Lower limit	OF-stTES12h-wo/SeasTES-elLower
		LCoE Optimum	OF-stTES12h-wo/SeasTES-elOptimum
		LCoE Upper limit	OF-stTES12h-wo/SeasTES-elUpper
	Flat rooftop (Small-scaled plants)	LCoE Lower limit	FR-stTES12h-wo/SeasTES-elLower
		LCoE Optimum	FR-stTES12h-wo/SeasTES-elOptimum
		LCoH Optimum	FR-stTES12h-wo/SeasTES-thOptimum
		LCoE Upper limit	FR-stTES12h-wo/SeasTES-elUpper
12 hour short-term + seasonal TES (No surplus heat, only unused heat generator capacities)	Open field (Large-scaled plant)	LCoE Lower limit	OF-stTES12h-w/SeasTES-elLower
		LCoE Optimum	OF-stTES12h-w/SeasTES-elOptimum
		LCoE Upper limit	OF-stTES12h-w/SeasTES-elUpper
	Flat rooftop (Small-scaled plants)	LCoE Lower limit	FR-stTES12h-w/SeasTES-elLower
		LCoE Optimum	FR-stTES12h-w/SeasTES-elOptimum
		LCoE Upper limit	FR-stTES12h-w/SeasTES-elUpper

3.2 Deriving Negative CO_2 Emissions Demand by DAC-Technology in Hamburg

Several studies and reports propose pathways for a climate-neutral Germany with similar expectations of negative GHG emissions. However, the projected roles of technical CDR strategies and the share in natural CO_2 sinks vary. Three exemplary studies are examined in the following.

A study conducted by *Deutsche Energie-Agentur* (DENA) assumes unavoidable GHG emissions at the scale of 70 $MtCO_2$ in 2045. The members of the study do not trust natural sinks such as land use, land use change, and forestry measures (LULUCF) which includes AR and SCS measures due to environmental hazards like wildfire. They also have concerns about the technical approach of BECCS due to space scarcity. Therefore, they assume that the total GHG negative emissions must be covered by DACCS. (DENA, 2021b)

Additionally, DENA published another study in the same year. In their final report of their lead study about climate neutrality in Germany, they state a total GHG emission compensation budget of 70 $MtCO_2e$ in 2045 as well. However, they only assume a DACCS share of 16 $MtCO_2/a$ from the total negative emission goal, if the LULUCF measures are restricted. BECCS would be implemented with 3.6 $MtCO_2/a$ in 2045. (DENA, 2021a)

The scientific cluster consisting of *Prognos AG*, *Öko-Institut e.V.*, and *Wuppertal Institut für Klima, Umwelt, Energie gGmbH* state in their report about Germany's transition towards climate neutrality in 2045 that unavoidable emissions of 63 $MtCO_2e$ would be present after all sectors would have been decarbonized. 64 to 65 $MtCO_2$ are expected to be removed as compensation. However, they distribute the CDR rate on several NETs in their study. They assume a share of 37 $MtCO_2$ to be covered by BECCS and 7 $MtCO_2$ by green polymers. For DACCS, a share of 20 $MtCO_2e$ is expected in Germany in 2045. The authors assume a CDR share of 20 $MtCO_2e$ by DACCS. (Prognos et al., 2021)

Erans et al. also state that all NETs have advantages and disadvantages that should cooperate for the overall goal of mitigating climate change. (Erans et al., 2022) Relying only on DACCS to achieve negative CO_2e emissions as it is presented in (DENA, 2021b) is a radical approach. In case the projected DAC deployment stagnates, and the forecasted decline of investment cost does not appear as expected, it would be hard to recover from the setback and achieve the CDR goals in time. The three introduced studies have a similar negative GHG emission goal in common. The lead study of DENA and the scientific cluster of *Prognos et al.* also suggest a similar DACCS utilization between 16 and 20 $MtCO_2$ in 2045.

This thesis orientates on the more balanced allocation of negative GHG emission contributions across multiple NETs that is suggested in the study by *Prognos et al.*. (Prognos et al., 2021) The negative emission demand covered by DACCS in the study of *Prognos et al.* is therefore chosen as the net negative emission baseline. Since this thesis only focuses on Hamburg, the overall negative emission goal for Germany must be broken down to an appropriate share for Hamburg. Therefore, predicted population data of Hamburg and Germany for 2045 are used. Different variants are provided by the *Federal Statistical Office Germany.* The moderate development of the birth rate, life expectancy, and migration balance of variant 2 (G2-L2-W2) is used from the 15th coordinated population projection. (Federal Statistical Office Germany, 2019)

Prognos et al. assume a CDR rate of -2 $MtCO_2$ by DACCS applications in Germany in 2040. (Prognos et al., 2021) In this thesis, the contribution to the CDR rate goal of Germany by Hamburg is considered to start in 2045. As a prerequisite, it is assumed that the negative CO_2 emission goals of Germany would not shift despite the later DAC implementation in the city of Hamburg.

3.2.1 Gross Negative CO_2 Emission Demand

To realize the net negative emission goal, the gross CO_2 removal rate must be determined. Therefore, the capture efficiency and the carbon footprint of the DAC plant must be addressed. Details on CO_2e emissions that occur due to CO_2 transport and storage in Hamburg are left out of the scope of this thesis due to the lack of released CCS sites in Germany (see Chapter 2.4.4). For general information about the emissions of CO_2 transport and storage, it is referred to the following paper. (Terlouw et al., 2021) In this thesis, gross negative emissions are only determined for the DAC plant and the process of isolating CO_2.

The carbon footprint of the DAC is mainly based on the emissions from the energy requirement. Only surplus heat is used. The future power system is based on RE and only negative residual loads are used. At times of negative residual loads, the electricity consumption is assumed to be surplus energy as well. This assumption is made to simplify the CO_2e emissions of the DAC plants' energy requirements as no detailed information about the electricity mix is provided for the time series of the power system (see Chapter 2.2.5). The heat and electricity carbon footprints are assumed to be 0 gCO_2/kWh in case of surplus energy consumption which are in line with assumptions of other research groups. (Deutz and Bardow, 2021b)

However, the carbon capture efficiency will always be lower than 100 %. This is due to the construction and end-of-life deconstruction of the plant which consumes energy that is probably not provided by surplus energy. The production of adsorbent material also has a positive GHG emission impact. According to *Deutz & Bardow*, the overall capture efficiency of a surplus energy-driven DAC plant can reach 97.1 % at best. (Deutz and Bardow, 2021a) The net and gross negative emission demands for Germany and Hamburg are listed in Table 2.

Table 2: Net and gross negative emission goals in 2045 for Germany and Hamburg based on the per-capita ratio between Hamburg and Germany. (Own illustration)

Scope	**Population**	**Net negative emissions in $ktCO_2$ in 2045**	**Gross negative emissions in $ktCO_2$ in 2045**
Germany	84,509,300	20,000.00	20,618.56
Hamburg	1,990,900	471.17	485.74

3.3 Electricity Supply

To the knowledge of the author of this thesis, there is no study available that includes a time series for Hamburg in 2045 particularly. Hence, a time series provided by *Fraunhofer ISE* of the power system of Germany is used for the electricity supply in 2045 in the scenarios of this thesis. The time series was generated with the help of *REMod* for the study of *Sterchele et al.* which is built upon a sector coupling objective for a climate-neutral energy sector. (Sterchele et al., 2021) The time series of the residual load curve for Germany is depicted in Figure 2.

As the scope of the study by *Sterchele et al.* refers to the power system of Germany, the energy availability of the system must be reduced to the scale of Hamburg. A per-capita approach is used that is also performed in the derivation of the negative emission demand for Hamburg (see Chapter 3.2). The factor of the ratio of Hamburg's and Germany's population in 2045 is applied to the time series. The decreased residual load curve is assumed to be the share that Hamburg is allowed to use based on the number of citizens of Germany. An allocation of electricity shares based on the economic strength of federal states is not performed.

The time series only considers inflexible power producers and inflexible consumers. Since the time series only contains an hourly resolution, it is assumed that the power system of Germany has multiple battery energy storage systems with a total storage capacity of 1 hour. The DAC plants shall operate flexibly and serve the power system. Therefore, only timeslots of negative residual loads are shortlisted for the operation time. Competing flexible technologies that may also offer flexible operation during those timeslots and potentially prove to be more viable are not included in the scope of this research. The overall balance of the power system is also not further investigated. The residual load curve is given for the total power system in Germany. Localization of the power production and consumption sites is not performed. For simpler handling, further grid losses for the electricity supply to Hamburg are neglected. An additional assumption is made that curtailments in the transmission and distribution grid do not occur.

3.3.1 Electricity Costs

Some studies exist which consider new electricity market designs and price developments for Germany until the time of net zero GHG emissions. (Fraunhofer IEE et al., 2021; Lenz et al., 2018) However, they are based on already outdated regulatory frameworks such as the *Climate Action Act* which has been revised in 2021, and an older version of the *Renewable Energy Sources Act* (EEG).

In addition, the geo-political developments concerning the Russian invasion of Ukraine in 2022 result in a risen energy price which is not considered in any publicly available price development scenario projected until 2045. As electricity cost projections will always face high uncertainties, this shall be addressed by a range of prices. Data are retrieved from the study by *Fraunhofer IEE et al.* in 2021. However, the study of *Fraunhofer IEE et al.* has been published before the Russian invasion and thus no geo-political events are considered in the prices of their study.

Fraunhofer IEE et al. state that dynamic prices will occur in the future depending on the ratio of electricity supply and demand. Positive residual loads are assumed to correlate with higher electricity prices as they need to reduce peak loads, stimulate load shifts, and use expensive peak-load power plants. Negative residual loads can result in lower prices. Negative payments can also occur. Their study investigates two scenarios. One of them is the basic scenario that contains negative prices. The other one is the reform scenario which restricts wholesale electricity prices to a minimum of 0 €/MWh to prevent further economic losses for power plant operators. In the reform scenario, the average wholesale electricity price is mentioned to be 80.79 €/MWh. The basic scenario's wholesale electricity price is assumed to be 72,20 €/MWh. The reform scenario is more cost-intense due to the lack of periods with negative prices and the assumption of the increased electricity demand of sector coupling consumers. (Fraunhofer IEE et al., 2021)

An assignment of dynamic prices to the adapted residual load time series of the power system is not performed. To reduce electricity costs, only negative residual loads are used in this thesis research subject. Positive residual loads are therefore not considered. The utilization of positive residual loads would also not contribute to the power system stability which is one of the conditions of flexibly operated DAC plants. For this thesis, the calculated average wholesale electricity price in 2050 in the reform scenario of *Fraunhofer IEE et al.* is set as the maximum value of the considered price range. The upper limit is therefore set to 81 €/MWh. It is assumed that the price would also be valid for the reform scenario that is achieved in 2045 when the goal of GHG neutrality is brought forward 5 years.

Due to considerations of literature in industrial DR incentives, the electricity price span is extended to a lower boundary of 1 €/MWh. Optimum wholesale electricity prices for the scenarios of this thesis are investigated in the optimization. Negative electricity prices could be achieved by the implementation of DAC plants as a balancing service. However, the fulfillment of the requirements for the registration of DAC plants as a balancing service is not part of the scope of this thesis. Concerns and limitations for the range of LCoE are addressed in Chapter 5.2.2.1. The considered electricity prices in the scenarios are depicted in Table 3.

Table 3: Range of wholesale electricity prices to be investigated on the scenarios. (Own illustration based on assumptions and (Fraunhofer IEE et al., 2021))*

Sub-scenarios	**Wholesale electricity prices in €/MWh**
Lower limit	1*
Optimum value	To be tested iteratively in optimization*
Upper limit (average value of reform scenario)	81

3.4 Heat Supply by District Heating System

As the DH systems are isolated, they cannot sell surplus heat to another DH system operator but only to consumers within their network. In the future, surplus heat within large DH systems that is low in GHG emissions could be potentially used as a heat supply for DAC plants. This is considered in this work for the DH system of Hamburg in 2045.

The designs of a DH system by *Kicherer et al.* and *Kicherer* are used as a baseline. (Kicherer, 2020; Kicherer et al., 2021) The design approach and the merit order for different heat generators have been introduced in Chapter 2.3.1. However, key features, additional assumptions, and limitations are outlined in the following subchapters to determine the compatibility of the DH system and its components for powering flexibly operated DAC plants by surplus heat in the optimization model.

Kicherer designed four scenarios that involve short-term TES capacities of 1, 2, 6, and 12 hours for the DH system. Peak load generation by the heat generators can be reduced using larger short-term TES capacities. This results in more continuously driven heat generator feed-ins. This influences the feed-in time series of each heat generator unit in the respective scenarios. Next to the heat generation time series, a time series of the heat load profile of all consumers in the DH system is provided. Residual load curves are developed for the total DH system in each scenario. The heat generators and the heat demand profile are based on a TRY in 2045. (Kicherer, 2020)

The DH design of *Kicherer* and *Kicherer et al.* has been laid out for 2050 because the new target of the *Federal Climate Action Act* of becoming GHG neutral in 2045 has been claimed after the release of their publications. Since the weather conditions are based on the TRY in 2045, it is assumed that the DH design and the time series can be similarly realized in 2045. Thus, it can be applied to the research subject of this thesis.

Successful implementation of flexibly operated DAC plants and the coverage of the heat demand shall be achieved. Therefore, the available heat generators are examined to identify surplus heat suppliers and unused heat supply capacities that can be activated to provide additional heat. Scenarios are derived from the findings of the investigation of the unused heat supply capacities. Their characteristics are explained in Chapter 3.4.2.

3.4.1 Heat Generator Capacities

Due to the merit order in the DH system, flexible as well as inflexible heat generators can provide heat for the operation of DAC plants (see Chapter 2.3.1). The heat generators are both, necessary and useful, to cover the heat demand of the DAC plants for the proposed carbon dioxide removal rate in Hamburg. It is assumed that all heat generators would be installed independently of the DAC plant integration and that the heat suppliers' economic feasibility would not be dependent on the additional operation for the DAC plants. In this thesis, it is assumed that the DH system operators would be willing to provide their unused heat without an extra charge at times of surplus heat generation. For further simplification, it is assumed that additional heat generation capacities would only ask the DAC plant operators to compensate for their demand-related costs such as electricity or fuel. In case the levelized costs of CO_2 removal are higher than the reference value (see Chapter 3.5.2.4), the optimum negative LCoH for the DAC thermal energy consumption is determined.

3.4.1.1 Must-run Generators

The must-run generators operate continuously. In the short-term TES scenarios of the DH system, they cannot sell the accumulated heat to a seasonal TES (see Chapter 3.2). The heat load profile of the heat consumers is assumed to be comprehensive in 2045 except for the DAC plant implementation. Must-run generators would have to implement a cooling application themselves which would create additional costs for the operators. Therefore, it is assumed that the must-run generators of the DH system would be willing to provide their unused heat without an extra charge at times of surplus heat generation. A competitive customer for surplus heat is assumed in the scenario including a seasonal TES. In that case, it is assumed that all available surplus heat is stored in the seasonal TES. In the next step, the flexible heat generators are examined.

3.4.1.2 River and Sewage Heat Pumps

The river and sewage HPs start to operate after the must-run generators in the merit order. Therefore, it must be considered, that their full load operation hours are already high and that it should be avoided to take too much additional stress on the HP. The river and sewage HPs have a power capacity of 200 MW and approximately 194 MW, respectively. The HPs are not used continuously throughout the year. They are selected in dependency on the ambient inflow temperature of the sewage water and the river *Elbe*. In general, the FLOH of a plant is calculated according to Equation (5).

$$FLOH\_plant = \frac{\sum_{i=1}^{8760} output[i]}{power\ capacity \cdot 8760\ \mathrm{h/a}} \cdot 8760\ \mathrm{h/a} \quad \left[\frac{h}{a}\right] \tag{5}$$

With: FLOH_plant = full-load operation hour of a plant [h/a]
Output = achieved energy/product output in a year of the plant [MWh/a]
power capacity = maximum energy/product output per hour of the plant [MWh/h]

In theory, the sewage water HP could supply a maximum energy of 1,708 GWh/a at 8760 h/a. It provides thermal energy at the scale of 880 GWh in 2045. This results in a full-load hour rate of approximately 4,513 h/a. The river HP would be able to provide 1,752 GWh/a in theory if there would be no further restrictions for the operation with the minimum temperature above 5 °C for the river (see Chapter 2.3.1). The river HP provides 375 GWh in 2045 which leads to a full load hour rate of approximately 1,875 h/a. (Kicherer, 2020)

In 2019, plans for the DH system of Hamburg in 2025 intended a range between 3,300 and 5,300 h/a FLOHs for a sewage water HP. (Authority for Environment and Energy, 2019) It is assumed that 5,300 h/a are the maximum FLOHs on a technical level that can be reached for the sewage water HP and the river HP as well.

In a preliminary modification of the time series of the river HP by *Kicherer*, timeslots with temperature restrictions are crossed out. (Kicherer, 2020) In addition, timeslots at full load operation are also crossed out for the heat supply of the DAC plants. In the case of the partial load operation, the residual power to a full-load operation is available. This is performed twice for the time series in the 1- and 12-hours short-term TES scenarios (see Chapter 3.4.2). In the optimization model, the HPs should further only operate at negative residual loads in the power system (see Chapter 3.7.1.3).

As the sewage water HP runs at a higher full load operation rate than the river HP, a compensation fee is added. Thus, the full load operation hours of the river HP are increased, and the utilization of the sewage water HP is reduced. The impact of the compensation fee on the levelized costs of CO_2 isolation shall be limited to less than 0.01 €/tCO_2. A suitable value for the compensation fee has to be detected iteratively during the scenario modeling.

The inlet temperature of the HPs is anticipated to be at 80 °C as it is specified in *Kicherer*'s design approach. (Kicherer, 2020) *Kicherer et al.* assume an average coefficient of performance (COP) of 3.0 in a conservative consideration in 2050. (Kicherer et al., 2021) However, other research groups such as *Cames et al.* or *Fasihi et al.* use more optimistic COPs of 3.5 in their projections for the utilization of HPs for DAC plants. (Cames et al., 2021; Fasihi et al., 2019) For the projection of HP usage in this thesis, an average COP of 3.0 in 2045 is assumed to be in line with the research group of the DH system's design. A summary of the characteristics and data of the used HPs can be retrieved in Table 4.

Table 4: Technical characteristics of the river water and sewage water heat pumps of the DH system. Two time series are considered regarding different thermal energy storage (TES) capacities. The time series are modified so that the HPs cannot contribute to the heat supply of DAC plants when their operation is prohibited by temperature restrictions of the river or when the HPs are already operating at full load. (Own illustration based on (Kicherer, 2020; Kicherer et al., 2021))

Characteristics and restrictions of the heat pumps in the district heating system in 2045 for additional heat supply for DAC plants		**Data/value**
Temperature level of heat supply		80 °C
Coefficient of performance		3.0
River water heat pump	Maximum power	200 MW
	1 or 12 h short-term TES	Time series
	At a temperature of *Elbe* < 5 °C	No contribution
	At full load operation in the DH system	No contribution
	Approx. full-load operation hours in the DH system	1,875 h/a
Sewage water heat pump	Maximum power	194 MW
	1 or 12 h short-term TES	Time series
	At full load operation in the DH system	No contribution
	Approx. full-load operation hours in the DH system	4,513 h/a
	Compensation fee for high full-load operation hours	To be detected

3.4.1.3 Biomass incineration

If the heat demand within the DH system can be covered by the must-run heat generators and the HPs, biomass incineration would be available for the heat supply of DAC plants. At first glance, additional heat supply for DAC plants by biomass incineration would be possible for a long period in 2045 which can be derived from Figure 3. However, biomass incineration is not an ideal choice, due to additional costs for fuel and fuel transportation. Besides, an increased utilization of biomass in the mobility sector of Hamburg is expected which results in a scarcity of biomass for heating purposes. For this reason, biomass incineration is solely employed for flexible heat generation within the DH system during periods when HPs are unavailable, facing operational restrictions, or operating at maximum capacity. (Kicherer et al., 2021) Therefore, biomass incineration is not considered to be an option for additional heat supply in this thesis.

3.4.2 Thermal Energy Storage Scenarios

Three scenarios with different thermal energy storage capacities are applied to the optimization model. Two scenarios are based on only using short-term TES capacity. The considered scenarios of the DH system are chosen to have a 1- and 12-hour short-term TES capacity. They are examined to work out the maximum influence of short-term TES on the respective DAC plant capacity. The implementation costs of short-term TES are not considered. Further, the implementation and costs of peak load heating sources due to the lack of seasonal TES must be clarified outside the thesis.

However, *Kicherer* and *Kicherer et al.* recommended research on the implementation of a seasonal TES to be able to shift surplus heat of 416 GWh to timeslots of positive residual loads. Positive residual loads occur in the magnitude of 326 GWh. The compatibility and costs for the integration of one or several seasonal TES in the DH system of Hamburg have not been solved. (Kicherer, 2020; Kicherer et al., 2021)

While the primary objective of this thesis is not to optimize the DH system, the inclusion of a seasonal TES implementation could significantly influence the research focus of this thesis. Therefore, a seasonal TES is considered in the third scenario. 90 GWh of waste heat would be available if no storage losses would be assumed. The prediction of timeslots, when it is suitable to store or supply heat by a seasonal TES, cannot be answered within the scope of this thesis and is outsourced. The remaining negative residual heat loads are considered to be not available for the DAC application in this scenario. Therefore, solely unused heat generator capacities are assumed to be an option for heat supply.

For the temperature level, a maximum temperature of the DH system of 94 °C is presented depending on the heat generator mix. (Kicherer, 2020) Temperature level changes throughout the year are not examined within this thesis and are therefore not assigned to the time series. However, the minimum temperature level is assumed to be 80 °C because of the temperature level provided by the utilization of HPs in case the surplus heat of the DH system is not sufficient for the proposed CDR rate (see Chapter 3.4.1). Heat transport losses and heat storage losses are not further considered in this thesis. A temperature range between 80 and 94 °C is compatible with the regeneration phase of LT DAC plants (see Chapter 3.5.3.2). An overview of the most essential characteristics of the DH system and the considered scenarios are presented in

Table 5. The three scenarios are also illustrated in Appendix 1 to Appendix 3.

Table 5: Characteristics of the DH system in Hamburg for the heat supply for DAC plants in 2045. (Own illustration based on (Kicherer, 2020; Kicherer et al., 2021) and own assumptions)*

Characteristics	**Data/value**
Temperature level: T_{min}* to T_{max}	80* to 94 °C
DH system: residual load curve	416 GWh negative residual load in total
	1- and 12-hour short-term TES time series
Free heat generator capacities	Heat pumps (1- and 12-hour short-term TES time series)
1st scenario*	1-hour TES capacity: DH system & free capacities of HPs
2nd scenario*	12-hour TES capacity: DH system & free capacities of HPs
3rd scenario*	Seasonal TES + 12-hour TES capacity: free capacities of HPs

3.5 Techno-Economics of LT DAC Plants

This thesis concentrates on the use of the TVSA DAC technology. In this section, the techno-economic parameters of the LT DAC plants are compiled for the optimization model. Therefore, recent literature about DAC technology is scanned from 2018 to 2023.

Fasihi et al. researched available and published data and literature about DAC plants in 2019. In their paper, they assess financial and technical information. They examine different DAC plant capacities and different learning rates. The learning rates correlate with respective large-scale deployment rates of DAC technology up to 2050. (Fasihi et al., 2019) Their paper is considered a primary source for the techno-economics of DAC plants in this thesis. It is often referenced and well-established in current literature. In this context, especially information by the research groups of *Azarabadi & Lackner*, *Beuttler et al.*, *Deutz & Bardow*, *Erans et al.*, *McQueen et al.*, *Sabatino et al.* and *Sinha & Realff* are categorized as trustworthy as well.

3.5.1 Dimensions

There are different data in the literature available concerning the dimension of DAC plants. They take the DAC plant itself as well as the RE power plant capacities that would be needed for the energy supply into account. (Viebahn et al., 2019) The research subject focuses on using negative residual loads, surplus energy, and unused power capacities, thus solely considering the physical dimensions of the actual DAC plants.

Data about specific space demands of existing DAC plants can be retrieved from the literature. According to *Deutz & Bardow*, the specific spatial resources depend on the scale of the plant. The scale of the plant in the project *Orca* has a specific area demand of 0.261m² per tCO_2/a. The plant has a capacity of 4,000 tCO_2/a and one process unit. However, they assume that a large-scaled plant has a lower specific space demand because it would need only one large-scaled process unit for multiple DAC modules. A specific area demand of 0.078 $m^2/(tCO_2/a)$ is stated for a DAC plant capacity of 100,000 tCO_2/a. (Deutz and Bardow, 2021a, 2021b)

However, *Beuttler et al.* stated that their current TVSA-based DAC plant with a capacity of 300 tCO_2/a fits into a 40 feet container. This is approximately an area of 30 m² which results in a specific area consumption of 0.1 m² per tCO_2/a. They announce that they will work on a space reduction in the future but do not mention an objective. (Beuttler et al., 2019)

For this study, the specific space demand of a modular DAC plant in the size of a container after *Beuttler et al.* is considered for the implementation on buildings (see Chapter 3.6.2). The capacity of one module is set to 300 tCO_2/a. For open spaces, the specific space demand from *Deutz & Bardow* is used for a large-scale DAC plant (see Chapter 3.6.1). Since the specific space demand of large-scaled and small-scaled modular DAC plants are close to each other, it is assumed that a larger DAC plant would have a similar specific area demand to the large-scaled DAC plant identified by *Deutz & Bardow*. The chosen values for the optimization model are represented in Table 6.

Table 6: Specific space demand values in dependency on the scale of the plant capacity. (Own illustration based on (Beuttler et al., 2019; Deutz and Bardow, 2021a, 2021b) and own assumption)*

Scale of plant in tCO_2/a	**Specific space demand in $m^2/(tCO_2/a)$**
Small: 300	0.1
Large: 100,000 and beyond*	0.078

3.5.2 Economic Aspects

In this section, only economic data for the DAC technology itself are considered. Additional costs for constructing the CO_2 infrastructure, enabling CO_2 transport, and its storage are not examined in the scope of this thesis. Policies about CCS sites in Germany are left out. Inflation of the costs is also not considered. Political incentives aiming for a faster DAC deployment are not considered.

First, the operation-related costs and the lifetime expectancy of DAC plants are examined. For the capital-related costs, the specific investment costs are determined in dependency on different DAC capacity scales. Afterward, a proposal for levelized costs of CO_2 removal in the future is introduced as a reference value. An outline of the used parameters is given in Chapter 3.5.2.5.

3.5.2.1 Annual Operation-Related Costs

Fasihi et al. introduce a basis scenario and a conservative scenario. Both started with commercialization in the 2020s. However, the basis scenario considers a financial learning rate of 15 % per decade while the conservative scenario approaches a learning rate of 10 %. The basis scenario assumes a CDR rate of 15,356 $MtCO_2$/a in 2050. The conservative scenario considers only 50 % of the basis scenario's targeted CDR rate which results in 7,678 $MtCO_2$/a in 2050. (Fasihi et al., 2019) For this thesis, DAC-related data from the conservative approach of the research group is used. In the conservative approach, the annual operation-related costs are stated to be 4 % of the capital-related costs. (Fasihi et al., 2019)

3.5.2.2 Lifetime Expectancy of Project

The lifetime expectancy of a plant would usually be considered a technical aspect. However, it is listed here because the lifetime of the project is also assumed to be the depreciation time and is therefore important for project finance.

Across the base and conservative scenarios of *Fasihi et al.*, the lifetime expectancy of a DAC plant in 2020 is assumed to be at 20 years. It is projected to be extended to 30 years in the long term. (Fasihi et al., 2019) *Beuttler et al.* also consider lifetime extensions of their TVSA plants up to 30 years in the long term. (Beuttler et al., 2019) Therefore, a lifetime expectancy of up to 30 years is used within this thesis.

3.5.2.3 Specific Investment Costs

Depending on the capacity of the respective DAC plant, specific investment costs can vary. Thus, it is necessary to determine the specific investment costs according to the DAC plant capacity. Thus, the determination of capital-related costs can be accomplished. The relation between specific investment costs and the plant capacity for the calculation of the investment costs is introduced in Equation (3) of Chapter 2.6.

Fasihi et al. mention two specific investment cost values for DAC plant sizes of 3,600 tCO_2/a and 360,000 tCO_2/a. Their specific investment costs in 2020 are stated as 1,220 and 730 €/(tCO_2/a), respectively. (Fasihi et al., 2019) Those data were retrieved from a joint design study report by *Antecy B.V.* and *Shell Global Solutions International B.V.* about a methanol synthesis in 2015. (Roestenberg, 2015) While the report can be categorized as a white paper, obtaining financial data for DAC plants of varying scales is challenging within the DAC technology domain.

For the plant size of 360,000 tCO_2/a a price decrease is given with a decadic increment between 2020 and 2050. (Fasihi et al., 2019) For the research subject, it is assumed, that DAC plants are ordered in 2040 because current DAC plants need up to 2 years for construction until commissioning. (Climeworks AG, 2022a) Details on the price reduction of the DAC plant with a capacity of 3,600 tCO_2/a are not available in the paper of *Fasihi et al.*. (Fasihi et al., 2019) It is assumed, that the decadal reduction rate is similar to the one of the larger plant capacities. The specific investment costs ratio of the large-scaled plant between 2020 and 2040 is assigned to the small-scaled plant.

To estimate specific investment costs of smaller and larger DAC plant sizes, a logarithmic extrapolation is performed. It is based on the specific investment cost data for the years 2020 and 2040 of the plant capacities mentioned in the paragraph above. The trend lines of the extrapolation and their mathematical representation are shown in Figure 7. The considered capacity sizes for the optimization model can then be calculated with the help of the respective trend line extrapolation equations.

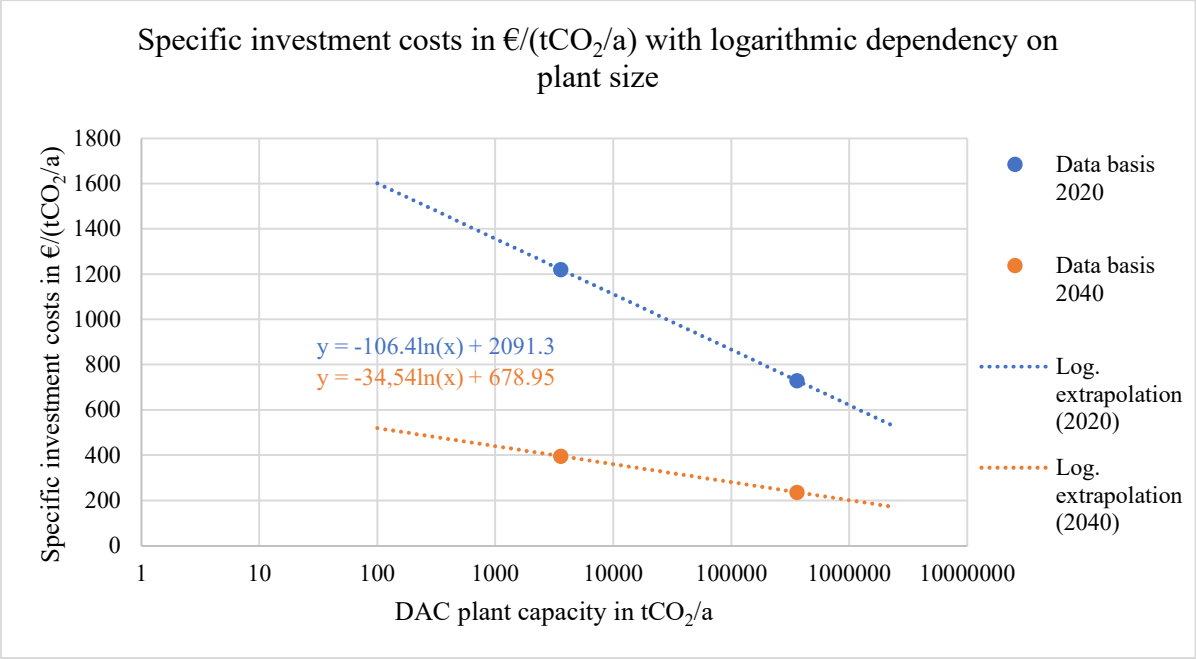

Figure 7: Diagram with the specific investment costs in €/(tCO₂/a) with a logarithmic dependency on the plant size. The blue points represent the data basis of the specific investment costs for pre-determined plant sizes in 2020. The orange dots are the data basis of the projected specific investment costs for pre-determined plant sizes in 2040. The dotted lines represent the logarithmic extrapolation trend lines that are built on the available data points. (Own illustration)

For small-scaled DAC plants, modules with a capacity of 300 tCO_2/a are assumed to be used. For a large-scale DAC plant, an initial guess for the maximum capacity is made. It is assumed that the maximum capacity in this case study is four times the size of the large-scale plant mentioned by *Fasihi et al.. (Fasihi et al., 2019)* This would result in a scale of 1.440 $MtCO_2/a$. The results of the logarithmic extrapolation of the specific investment costs of the data by *Fasihi et al.* in 2020 and 2040 to the preferred plant sizes are listed in Table 7. The price ratios between 2020 and 2040 are the same for each plant size.

Table 7: Specific investment costs in €/(tCO_2/a) for differently scaled DAC plants in the years 2020 and 2040. (Own illustration based on data by (Fasihi et al., 2019; Roestenberg, 2015) and own calculations)*

Capacity in tCO_2/a	**Specific investment costs in €/(tCO_2/a)**		**Price ratio for plant capacities between 2020 and 2040**
	2020	**2040**	
300	1,484*	482*	3.08
3,600	1,220	396*	
360,000	730	237	
1,440,000	583*	189*	

3.5.2.3.1 Interest Rate on Investment Costs

Fasihi et al. use a weighted average cost of capital (WACC) of 7 % for the calculation of the levelized costs of CO_2 removal ($LCoCO_2$). (Fasihi et al., 2019) The interest rate r_{int} on the investment costs according to the *VDI 2067* policy is adapted from *Fasihi et al.* and selected to be at 7 %. The r_{int} influences the AF which is used for the calculation of the $LCoCO_2$ in the optimization model according to Equations (2) and (4) (see Chapter 2.6).

3.5.2.4 Levelized Costs of CO_2 Removal

A wide range of current $LCoCO_2$ can be found in the literature. *Lackner & Azarabadi* state that a current commercially operating LT DAC plant of *Climeworks AG* isolates CO_2 at costs of 500 to 600 \$/tCO_2. (Lackner and Azarabadi, 2021) *Fasihi et al.* assume that a LT DAC plant can remove CO_2 for less than 300 €/tCO_2 in 2020. They also investigate $LCoCO_2$ for different full-load operation hours of DAC plants located in Morocco. In dependency on the utilization of waste heat or heat produced by HPs via electricity consumption, they calculated $LCoCO_2$ in the range of 40 to 69 €/tCO_2 in 2040 and 32 to 54 €/tCO_2 in 2050 for a continuously running DAC plant with a full-load operation time of 8,000 h/a. For a DAC plant within partial-load operation at 4,000 h/a, they modeled a $LCoCO_2$ of 67 to 97 €/tCO_2 in 2040 and 56 to 80 €/tCO_2 in 2050. (Fasihi et al., 2019)

Research groups expect CDR by DAC technology to become economically feasible at $LCoCO_2$ below 100 €/tCO_2. (Lackner and Azarabadi, 2021; Ozkan et al., 2022) In this thesis, it is assumed that $LCoCO_2$ of below 100 €/tCO_2 must be reached as a reference value within the potential analysis for a viable operation of the DAC plants.

The LT DAC plants additionally separate pure water which could also be sold and thus offset the $LCoCO_2$. However, this circumstance is not considered in this thesis.

3.5.2.5 Economic Parameter Summary

Two different specific investment costs are considered as they are assumed to occur at different DAC plant capacity scales for different sites in Hamburg which are addressed in Chapter 3.6. The lifetime of the DAC plants is expected to last 30 years. The annual operation-related costs in the amount of 4 % of the capital-related costs are used in a conservative approach. The capital-related costs are calculated according to Equation (3) with the help of the specific investment costs and the assumed DAC plant capacities. The interest rate is set to 7 % for the calculation of the AF and the $LCoCO_2$, respectively. Those are the parameters that are used in the optimization model.

For a discussion of the feasibility of the obtained $LCoCO_2$ in different scenarios of this thesis, a target value of 100 €/tCO_2 or below is determined. An overview of the economic data of the DAC plants is given in Table 8.

Table 8: Overview of economic parameters of DAC plants that are used in the optimization model. (Own illustration based on (Beuttler et al., 2019; Fasihi et al., 2019; Lackner and Azarabadi, 2021; Ozkan et al., 2022))

Economic parameter	**Value**
Specific investment costs in 2040 in €/(tCO_2/a): (small plants = 300 tCO_2/a)	482
Specific investment costs in 2040 in €/(tCO_2/a): (large plant = 1,440,000 tCO_2/a)	189
Lifetime of DAC plant in years:	30
Capital-related costs in €:	Specific investment costs * DAC plant power
Interest rate on capital-related costs:	1.07 (7 %)
Annual operation-related costs in €:	4 % of capital-related costs
Long-term target of levelized costs of CO_2 removal in €/tCO_2:	< 100

3.5.3 Technical Aspects

In this section, the technical aspects of the LT DAC plants are determined to mirror the technical and energetic behavior of the DAC technology and its process. It is decided on the electricity and heat demands for the model input. Further, the temperature level of the heat supply for the DAC plants and the overall process cycle time must be determined.

Those parameters depend strongly on the choice of solid sorbent material. Various materials are currently in research. *Azarabadi & Lackner* investigate solid sorbents in a techno-economic analysis. They list sorbent materials and their respective lifetime in cycles, cycle duration, and rate of degradation among other things. (Azarabadi and Lackner, 2019)

Sinha & Realff have executed a techno-economic study about solid sorbent-based DAC plants. They assume that the adsorbent material should be replaced twice a year as it is worn out fast. (Sinha and Realff, 2019) *McQueen et al.* also outline that the sorbent material in a LT DAC plant should be replaced at least once a year. (McQueen et al., 2021) The needed parameters for the optimization model are explained in the following.

3.5.3.1 Electricity and Heat Demand

A variety of current electricity and heat demands for TVSA DAC plants have been introduced in Chapter 2.4.1.1. It stands out that the most energy is consumed in the desorption phase and has to be supplied by heat. In this thesis, the energy demand data by *Fasihi et al.* are used. It is assumed that the overall energy demand is in line with the reported 2,000 kWh/tCO_2 by *Beuttler et al.*. (Beuttler et al., 2019) The heat demand is therefore set to 1,750 kWh. The electricity demand of 250 kWh/tCO_2 is similar to the electricity consumption assumed by the research group of *Hanna et al.*. (Fasihi et al., 2019; Hanna et al., 2021)

Further, *Fasihi et al.* developed scenarios that project a decrease in the electricity and heat demand until 2050. They assume a reduction rate of 10 and 14.3 % per decade, respectively. Those are in line with the expected reduction rates of *Climeworks AG* and other LT DAC plant manufacturers. (Fasihi et al., 2019) It is assumed that the reduced energy demand is related to the improvement of solid sorbent materials. As the sorbent material is suggested to be replaced once a year, it is assumed that the implementation of the newest sorbent technology can improve energy efficiency every year. Due to this assumption, a linear interpolation is executed for the year 2045. The energy demand values for the decades 2020 to 2050 and the interpolation towards the year 2045 are given in Table 9.

Table 9: Electricity and heat demand development of LT DAC plants until 2050. The energy demands in 2045 are calculated by linear interpolation and are used in this thesis. (Own illustration based on (Fasihi et al., 2019) and own calculation)*

Year	**Electricity demand in kWh/tCO_2**	**Heat demand in kWh/tCO_2**
2020	250	1,750
2030	225	1,500
2040	203	1,286
2045	192.5*	1,194*
2050	182	1,102

3.5.3.2 Temperature Level

The temperature level of LT DAC plants in the desorption phase must be compatible with the available heat source. The temperature level is influenced by the choice of solid sorbent. *Erans et al.* mention that a temperature level between 50 and 120 °C is achievable by amine-based solid sorbents. (Erans et al., 2022) The research group of *Sinha & Realff* assume a temperature range between 67 and 100 °C for a solid sorbent-based DAC plant. (Sinha and Realff, 2019) Other research groups such as *Sabatino et al.* elaborate in their DAC technology assessment that current DAC plants operate between 80 to 130 °C. (Sabatino et al., 2021) *Beuttler et al.* also declare that the TVSA plants of *Climeworks AG* operate at temperature levels between 80 and 120 °C in the desorption phase. They also state that *Global Thermostat* already reduced their plant's maximum operation temperature to 100 °C. They can operate at a minimum temperature of 80 °C. (Beuttler et al., 2019)

It can be assumed that a temperature level between 80 and 100 °C is applicable for the operation of the DAC plants in the optimization model. The DH system of the 4th generation by *Kicherer et al.* is anticipated to provide heat at a temperature range of 80 to 94 °C (see Chapter 3.4.2). Therefore, it is expected that LT DAC plants can be integrated into this DH system. The necessary temperature level for the proper operation in the desorption phase of the DAC plant should be met in this case.

3.5.3.3 Process Cycle Time

Process cycle times of LT DAC plants contain an adsorption and desorption phase. The process cycle times differ across the DAC plant manufacturers. According to *Fasihi et al., Global Thermostat* is capable to run a process cycle within 30 minutes using a steam purge while *Climeworks AG* DAC plants need up to 4 to 6 hours. The reason can be found in different sorbent materials with divergent CO_2-selectivity and the use of saturated steam as a heat transfer fluid. (Fasihi et al., 2019) The analysis of different solid sorbents by *Azarabadi & Lackner* result in process cycle times in the range of 6.5 minutes up to 8 hours. (Azarabadi and Lackner, 2019) Hence, it can be assumed that a solid sorbent material in 2045 is capable to execute one process cycle within 60 minutes. This cycle time is used for the optimization model.

3.5.3.4 Technical Parameter Summary

For the technical aspects of a LT DAC plant, the adsorbent material plays an important role. It influences the electricity demand and the heat consumption in the desorption phase as low pressure and heat are necessary to separate CO_2 from the filter (see Chapter 2.4.1.1). Due to the high wear of the sorbent material, it is assumed that the sorbent material is replaced yearly which results in an improvement of the energy efficiency. Thus, the electricity and heat demands are calculated and determined to be 192.5 kWh/tCO_2 and 1,194 kWh/tCO_2 in 2045, respectively (see Chapter 3.5.3.1). The temperature level and the process cycle time are also influenced by the choice of sorbent material. Due to an already existing variety of sorbent materials, it is assumed that a sorbent will exist in 2045 that can complete a process cycle within 60 minutes at a temperature level between 80 to 100 °C (see Chapters 3.5.3.2 and 3.5.3.3). An overview of the considered technical data and parameters is given in Table 10.

Table 10: Overview of economic parameters of DAC plants that are used in the optimization model. (Own illustration based on (Beuttler et al., 2019; Fasihi et al., 2019; Lackner and Azarabadi, 2021; Ozkan et al., 2022))

Technical parameter	**Value**
Electricity demand in 2045 in kWh/tCO_2:	192.5
Heat demand in 2045 in kWh/tCO_2:	1,194
Temperature level for desorption phase in °C:	80 to 100
Time for one process cycle in minutes:	60

3.6 Spatial Analysis for DAC Plants in Hamburg

For the potential roll-out of DAC plants in Hamburg, criteria must be met in terms of physical integration and connectivity. DAC plants must be positioned within the range of the DH system infrastructure. Because of the high population density in Hamburg, available space is a scarcity. The spatial analysis for DAC plants in Hamburg concentrates on open spaces as well as the availability of flat rooftops which are large enough for DAC modules within reach of the DH grid. Through this consideration, it is made sure that the necessary capacity of DAC plants can be physically integrated into the DH system and the city. However, only the integration of the actual DAC plant units is considered. Space demands for power generators, CO_2 transport infrastructure, or storage are not considered. Further assumptions and limitations of the analysis are explained in the next paragraph.

In general, costs for construction are assumed to be integrated into the specific investment costs (see Chapter 3.5.2.3). However, there are no further considerations made about the challenging installation of DAC plant modules on rooftops compared to the construction on an open field. Rent for the rooftops and open spaces is also not considered in this thesis as they need to be negotiated with the owners of the facilities. The compatibility and viability of the construction of a CO_2 pipeline infrastructure are also not in the scope of the thesis. The debate about the acceptance of DAC plants within the city of Hamburg is also not addressed. It is assumed that the citizens and government of Hamburg would agree to the installation of DAC plants in Hamburg. For a holistic approach, this would be necessary to investigate if the implementation of DAC plants in Hamburg should be realized.

The geographical position of the DH grid in 2045 is assumed to be laid out as mentioned in *Kicherer's* master thesis. It is based on the DH network expansion plan of *Wärme Hamburg GmbH*. (Kicherer, 2020) In the following subsections, different methods are presented to identify the capacity of open spaces and rooftop installations.

The specific space demands for small-scaled and large-scaled DAC plants are determined in Chapter 3.5.1. Their values can be seen in Table 6. Modular DAC plants in the size of a container shall be used for the implementation on buildings. Large-scale DAC plants shall be built on one or several open spaces.

3.6.1 Open Fields

An analysis of available open spaces in Hamburg with likely connectivity to the DH grid has already been performed in the master thesis by *Kicherer*. However, this analysis was executed to detect open spaces for solar thermal plants. A map of Hamburg with potential areas for solar thermal plants is shown in Figure 8. It contains the DH grid illustrated by the blue lines. Further, open fields for solar thermal plants are marked in brown. *Kicherer* identified open fields in the west of Hamburg that are likely to be connected to the DH grid. Those areas are stressed out by the red circles. (Kicherer, 2020)

The current land-use plan of Hamburg labels the three red-circled locations as land for agricultural use and green space. (Landesbetrieb Geoinformation und Vermessung, 2023a) It is assumed that those areas would be released to DAC plants, too. Depending on the scale of space demand of the DAC plants, modules could be piled up to save spatial resources. A detailed investigation would include the determination of competitive business cases on those sites as well as ownership regulations and a rent or lease price for the area. However, this is not part of this work.

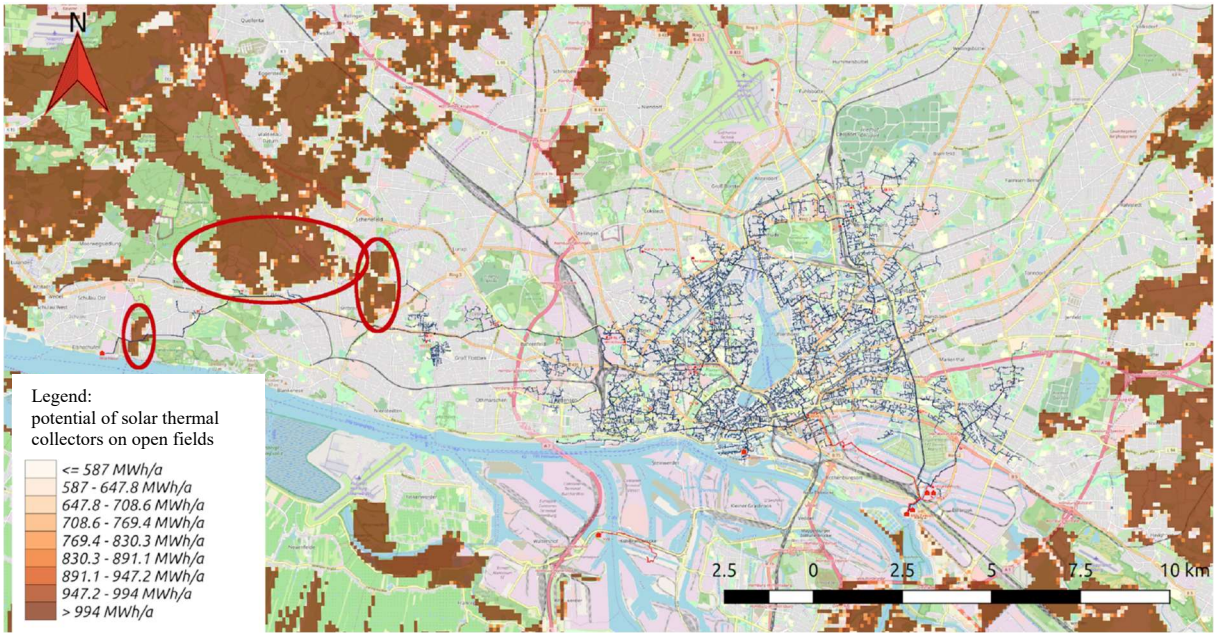

Figure 8: Potential for solar thermal systems on open fields in Hamburg and the district heating system of Hamburg. The blue lines show the DH grid of Hamburg. Brown areas would be open fields that would fit solar thermal systems. Suitable locations with a possible DH system connection are marked with red cycles. (Modified after (Kicherer, 2020))

3.6.2 Flat Rooftops

A geodata set of Hamburg is used to determine the available number of flat roofs in Hamburg to place DAC systems near the DH grid for connectivity. As a database, the geodata set *3D-Gebäudemodell LoD2-DE Hamburg* of the year 2022 is used in the City Geography Markup Language (CityGML) format. The total 3D building map of Hamburg is subdivided into hundreds of tiles in the CityGML format. (Landesbetrieb Geoinformation und Vermessung, 2023b) Each building has its building ID and can be filtered after its roof structure, which is represented by a roof type code. (Bayrische Vermessungsverwaltung, 2018) For more background information it is referred to the documentation of the 3D building model of Germany. (Federal Agency for Cartography and Geodesy, 2023)

Buildings are identified that might fit geometrically for a DAC module. However, the actual construction and installation are not considered here. An individual visual test of the suitability and a structural analysis would be necessary for each rooftop to be certain of the compatibility.

Data from 3D buildings in Hamburg have been processed before in an unpublished analysis of the *CC4E*. At the institute, the geodata is converted into another datatype called *CityJSON* for processing in *Python*. (Trosdorff, 2023) The analysis could be expanded and applied to the investigation of finding buildings near the DH infrastructure that would fit a generic container on their flat rooftops. The most important criteria for processing and filtering the tiles which are within reach of the DH infrastructure are described in the following.

First, several polygons with the approximate dimensions of the DH grid are spread out on the 3D building map. In this context, tiles are identified that intersect with the polygons of the DH system. Only the tiles mentioned above are considered and iterated in the process workflow explained in the following. A simplified representation of the workflow is given in Appendix 4.

The buildings in each investigated tile are filtered by their roof type to extract only buildings with a flat rooftop design. Then, the areas of the flat rooftops are calculated. In the next processing step, only buildings are further considered whose surface is larger than the surface area needed for a DAC module. *Beuttler et al.* propose that a 300 tCO_2/a DAC module would fit in a 40 feet container which is approximately equal to 30 m². (Beuttler et al., 2019) The suitable area of the rooftops is extended to be larger than 60 m² to enable maintenance work.

Afterward, the actual geometrical fit of a DAC module is examined. Therefore, the assumption is made that the areas of flat rooftops are equal to the floor plans of the respective buildings. In this context, the 3D model is converted into 2D polygons to enable a size comparison of the flat rooftops with the ground surface area of a container-sized DAC module. In the end, the number of suitable rooftops which would be large enough to fit at least one DAC module is given as a result for each tile.

An exemplary tile with filtered buildings according to a flat roof structure, an area of at least 60 m², and a suitable area that fits one DAC plant container module is shown in Figure 9. It shall visualize the methodological procedure. The light grey forms are buildings with another roof structure. The forms in the darker grey color are flat roofs with a size smaller than 60 m². The black-colored buildings are equal to or larger than 60 m². However, these do not fit a polygon of the dimension of a common container on their rooftops. The red-colored buildings fit the necessary dimensions of a container and their number represents the result of the spatial analysis.

Figure 9: An exemplary tile with filtered buildings according to a flat roof structure that fits one DAC plant container module. The light grey forms are buildings with another roof structure. The forms in the darker grey color are flat roofs with a size smaller than 60 m². Black-colored buildings are equal to or larger than 60 m², however, they do not fit a polygon of the dimension of a common container. Red-colored buildings fit the necessary dimensions. (Trosdorff, 2023)

3.7 Scenario Optimization Modeling

The input parameters for the development of different scenarios in this thesis have been determined in Chapters 3.2 to 3.5. The determined constant values and time series are used as a baseline for the optimization model. However, they are not the only input parameters that are needed for the optimization model. System requirements are stated in Chapter 3.7.1. The model must be filled with the definition of the decision variables, constraints, and an objective. This is performed in Chapters 3.7.2, 3.7.3, and 3.7.4, respectively.

In this chapter, the model-specific inputs for the optimization model are described. Therefore, the key points are explained to understand the model and its operating principles. The optimization method used in this thesis is deterministic. The modeling properties are defined to represent the real-world problem with the help of the previously determined parameters according to the targeted scenarios. The time resolution of the model is set to an hour per timestep. It is limited by the input time series of the power and heat systems. Together, they form the algebraic model which is solved by a solver according to the objective function.

The solved outputs of the optimization model are stated and described in Chapter 4. Some outputs are the solution of decision variables which must be defined at the beginning as input. This is executed in Chapter 3.7.2. However, to gain a better understanding of the upcoming procedure and content, an overview of the inputs and outputs of the optimization model is presented in Figure 10.

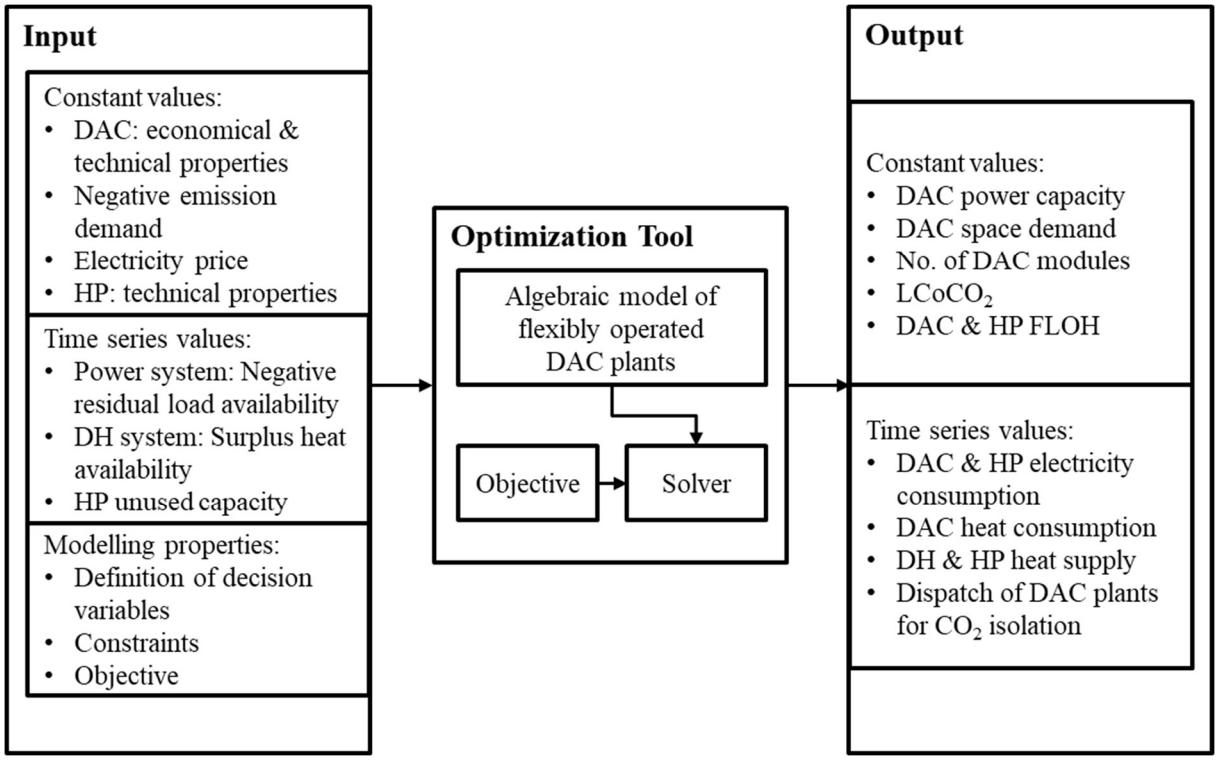

Figure 10: Overview of the optimization tool's procedure including inputs and outputs. Inputs are either constant values, time series containing hourly data for the year 2045, or properties of the model itself. The scenarios must be translated into an algebraic model. A defined objective and the model are handed over to a solver that solves the optimization problem. Output data of the optimization tool are constant values or time series of decision variables, the objective, and other computational results which are of interest for the follow-up processing. (Own illustration)

3.7.1 System and Model Requirements

For a start, the system requirements for the optimization model are described for the solution of the respective scenarios. The optimization model is programmed in *Python*. The development environment of *Visual Studio Code* is used. The code of the script for the optimization model is attached in the digital appendix B.1 *Flexible_DAC_plant_operation_optimization_model.py*. The necessary packages and libraries that are used for the optimization model are described in the next subsection. The created model is a MILP optimization and therefore needs a solver that can solve MILP problems. Modeling a real-world process has its challenges. The accuracy of the model depends on the quality of the parameters and the mathematical representation of the model dependencies in the form of constraints. Simplifying the real-world process results in uncertainties that are discussed in Chapter 5.4.

3.7.1.1 Python Packages and Libraries

The optimization is modeled with the help of the open-source software package called *Python Optimization Modeling Objects* (Pyomo). For the proper functionality of the *Pyomo* package, several libraries are required that must be installed and imported. *Numpy* and *Pandas* are used for mathematical operation and data analysis. In addition, *Matplotlib* is used for the graphical illustration of the time series.

3.7.1.2 Solver

To solve the optimization problem of this thesis, the solver *Gurobi* is used. It is capable to solve a variety of optimization models such as LP, NLP, MILP as well as MINLP. (Gurobi Optimization LLC., 2023a) It is a commercial solver, however, *Gurobi Optimization LLC* provides free licenses for academic use. (Gurobi Optimization LLC., 2023b) The explanation of the detailed mathematical solving processes is not part of this thesis. Information can be retrieved from *Synman & Wilke* as well as the datasheet of the solver. (Gurobi Optimization LLC., 2023a; Snyman and Wilke, 2018)

3.7.1.3 Time Series Input

Several time series are crucial for this optimization model. They are attached in the digital appendix *B.2 Input_time_series_MILP - Parameter - Additional_calculations.xlsx*. The first one concerns the expected residual load curve in the power system of Germany that is scaled down to the size of Hamburg (see Chapters 2.2.5 and 3.3). The residual load curve of Hamburg is defined as *electricity_hh*. Other time series contain the expected residual load curves of the DH system of Hamburg in 2045. They are called *DH_TES_cap_Xh* in the further definition of the constraints. Depending on the considered scenario, the short-term TES capacity is chosen to be 1 or 12 hours (see Chapters 3.4 and 3.4.2). The *X* in the name of the heat storage time series is related to either the 1- or 12-hour TES capacity. The input time series of the power and heat system are modified to set positive residual load values to zero. Thus, only negative residual loads can be used, and the DAC application can serve the power and heat system.

Furthermore, the time series of a river HP and a sewage water HP are used for an additional heat supply next to the already existing DH system's residual load. The time series of the HPs also differ depending on the short-term TES capacity scenarios (see Chapter 3.4.1.2). They are defined as *HP_river_th_availability_Xh* and *HP_sewage_th_availability_Xh*. The *X* in the name of the HPs' time series is related to the 1- or 12-hour TES capacity, too.

Timeslots of the HPs' time series that are unavailable for the DAC application are set to zero (see Chapter 3.4.1.2). The time series of the river HP is set to zero at timeslots with temperature restrictions (Kicherer, 2020). Further, the HPs are unavailable for the DAC application at timeslots when the HPs are already operated at full load in the DH system. The residual power to a full-load operation of the HPs can be used if the HPs are in partial load operation mode or are unused in the DH system.

The modifications of the time series in advance are essential for the constraints that follow in Chapter 3.7.3 as they are linked to the decision variables. These are defined to be non-negative real and non-negative integers (see Chapter 3.7.2). The time series are listed in Table 11.

Table 11: Overview of the input time series for the scenarios and model. (Own illustration)

Time Series	**Index**	**Unit**
Negative residual load of the power system scaled down to the size of Hamburg	*electricity_hh*	MWh/timestep
Negative residual load of the DH system at X hours = 1 to 12 hours TES capacity	*DH_TES_cap_Xh*	MWh/timestep
Free capacity of the river HP at X hours = 1 to 12 hours TES capacity	*HP_river_th_availability_Xh*	MWh/timestep
Free capacity of the sewage water HP at X hours = 1 to 12 hours TES capacity	*HP_sewage_th_availability_Xh*	MWh/timestep

3.7.2 Decision Variables

In this section, the decision variables are explained. All of them are defined to be non-negative. Once the decision variables are defined, their values can be calculated in each timestep of the time series by the optimization model. The resulting time series and values of the decision variables are part of the output of the optimization model. Their roles in the model are introduced here. The values of the decision variables can either change in each timestep or be constant throughout the time series. Almost all decision variables in this model are defined as NNR. One decision variable is defined as NNI. The model is therefore described as a mixed-integers optimization.

3.7.2.1 Energy Flows of the Heat Pumps and the District Heating System

The optimization model shall compute the optimum energy flows of the heat pumps and the thermal energy supply of the DH system for the DAC application. The heat supply of the DH system, the sewage water HP and the river HP shall be determined separately throughout the year. With the help of the decision variables *DH_system_th_supply*, *HP_river_th_supply*, and *HP_sewage_th_supply*, the optimization model can assign thermal energy units in MWh per timestep in a new time series. They are defined as NNR. However, they supply thermal energy which would be assigned with a negative algebraic sign. The input time series *HP_river_th_availability_Xh* and *HP_sewage_th_availability_Xh* have a negative algebraic sign. To provide a mathematically correct model, a sign conversion must be considered in the definition of the constraints. This is addressed in Chapter 3.7.3.

At the same time, the electricity consumption of the two HPs is of interest. The decision variables *HP_river_el_consumption* and *HP_sewage_el_consumption* are introduced to determine the respective electricity consumption per timestep for heat production. They are also defined as NNR. They have the technical correct algebraic sign. Their unit is also MWh per timestep.

3.7.2.2 Heat and Electricity Demand of DAC Plants

The heat and electricity consumption of the DAC process is addressed by the decision variables *DAC_th_consumption* and *DAC_el_consumption*. They are defined as NNR. They represent the consumption of heat and electricity and have therefore the technical correct algebraic sign. The energy consumption can vary according to the assigned maximum DAC plant capacity and the availability of heat and electricity in the DH system scenarios (see Chapter 3.7.3). Therefore, the energy consumption is adjustable in each timestep and must be determined for an optimum operation in 2045 in MWh.

3.7.2.3 Carbon Dioxide Removal Rate of DAC Plant

Another output of the optimization model is the dynamic dispatch of the DAC plants with the respective CO_2 removal rate in each timestep. The decision variable is called *DAC_CO2_out* and it is related to the heat and electricity consumptions represented by *DAC_th_consumption* and *DAC_el_consumption*. Therefore, *DAC_CO2_out* can also change throughout the year and has to be solved for each time step. The CDR rate of the DAC plants is also defined as NNR.

3.7.2.4 DAC Plant Capacity and Number of Modules

The overall optimum DAC plant capacity shall be determined by the model. The plant capacity is therefore constant in each timestep of the time series. It can be represented in tCO_2/timestep or tCO_2/a. The decision variable of the DAC plant capacity is given as *DAC_CO2_cap* and is defined as a NNR. As the overall DAC capacity shall be built in a modular way (see Chapter 3.5.1), it is necessary to define a NNI decision variable that prevents the construction of only half a DAC plant module. The number of plant modules is therefore given in the integer domain as the variable *DAC_number_of_plants*. It is only determined once in the model and has no unit.

3.7.2.5 Summary of Decision Variables

The model is built on the decision variables explained in the previous Chapters 3.7.2.1 to 3.7.2.4. A summary of the decision variables can be seen in Table 12. They are mentioned here with their respective unit, domain, and property to be capable of changing values in each timestep *i*. Each decision variable's time series is summed up for the representation of its solution in the results.

Table 12: Modelling properties of the decision variables defined in the model. (Own illustration)

Variable	Index	Unit	Domain
DH_system_th_supply	i	MWh/timestep	NNR
HP_river_th_supply	i	MWh/timestep	NNR
HP_sewage_th_supply	i	MWh/timestep	NNR
HP_river_el_consumption	i	MWh/timestep	NNR
HP_sewage_el_consumption	i	MWh/timestep	NNR
DAC_th_consumption	i	MWh/timestep	NNR
DAC_el_consumption	i	MWh/timestep	NNR
DAC_CO2_out	i	tCO_2/timestep	NNR
DAC_CO2_cap	-	tCO_2/a	NNR
DAC_number_of_plants	-	-	NNI

3.7.3 Scenario Constraints

The constraints of the model are defined here to build the framework of the scenarios. They are explained for a deeper understanding of the functionality of the considered scenarios. First, the constraints of the HPs are explained.

The initial input time series *HP_river_th_availability_Xh* and *HP_sewage_th_availability_Xh* have a negative algebraic sign as they represent the supply of thermal energy. Both time series are multiplied by -1 in each timestep *i* to match with the non-negative constraint of the decision variables *HP_river_th_supply* and *HP_sewage_th_supply*. The decision variables considering the thermal energy supply of the HPs for the DAC plants are limited in each timestep *i* to be smaller or equal to the maximum thermal energy capacity of the HPs that is available in each timestep *i*. These conditions can be seen in Equations (6) and (7) for both HPs.

$$HP\_river\_th\_supply[i] \leq (-1) \cdot HP\_river\_th\_availability\_Xh[i] \quad (6)$$

$$HP\_sewage\_th\_supply[i] \leq (-1) \cdot HP\_sewage\_th\_availability\_Xh[i] \quad (7)$$

The electricity demand of the heat pumps is determined by the optimization for the decision variables *HP_river_el_consumption* and *HP_sewage_el_consumption*. The relation between the electricity demand and the heat supply output of the HPs is defined by the COP. The parameter is named *HP_cop*. The variables of the electricity consumption are coupled in each timestep *i* to the decision variables *HP_river_th_supply* and *HP_sewage_th_supply*. The relation for both HPs is illustrated as a constraint in Equations (8) and (9).

$$HP\_river\_th\_supply[i] == HP\_river\_el\_consumption[i] \cdot HP\_cop \quad (8)$$

$$HP\_sewage\_th\_supply[i] == HP\_sewage\_el\_consumption[i] \cdot HP\_cop \quad (9)$$

Further, the DH system's heat supply for the DAC plants shall be detected and solved by the optimization model. Therefore, the variable *DH_system_th_supply* is implemented. The heat supply for the DAC application must be less or equal to the available surplus heat in the DH system at every timestep. This is represented by the constraint in Equation (10).

$$DH\_system\_th\_supply[i] \leq -1 \cdot DH\_TES\_cap\_Xh[i] \quad (10)$$

After the constraints of the HPs and the DH system have been introduced, the DAC plants' energy in- and outputs are examined. The CO_2 isolation rate per timestep *DAC_CO2_out* is not allowed to be higher than the hourly maximum capacity of the DAC plant *DAC_CO2_cap* that is determined in tCO_2/h. Otherwise, the DAC plant would remove more CO_2 than it should be capable of. This condition is shown in Equation (11).

$$DAC\_CO2\_out[i] \leq DAC\_CO2\_cap \quad (11)$$

For the total DAC plant capacity, the hourly *DAC_CO2_cap* is multiplied by 8,760 h/a. This results in a capacity represented in tCO_2/a. To address the total number of DAC plants, the total DAC plant capacity is divided by the size of the proposed DAC module *DAC_module_size* (see Chapter 3.5.1). The decision variable *DAC_number_of_plants* which represents the number of DAC plant modules is defined as an integer. This is due to the constraint that it is not realistic to install only half a module. This constraint is represented in Equation (12).

$$DAC\_number\_of\_plants == DAC\_CO2\_cap \cdot 8760 \,/\, DAC\_module\_size \quad (12)$$

The ratio of electricity and heat to remove one ton of CO_2 by the DAC plants is described by another constraint. It must be ensured that electricity and heat are both available in a certain ratio to extract a unit of CO_2 within one timestep. The ratio is described by the electricity demand of a DAC plant per tCO_2 *DAC_el_demand_per_tCO2* divided by the heat demand of the DAC plant per tCO_2 *DAC_heat_demand_per_tCO2*. If electricity is not available for the DAC application, the heat consumption of the DAC plant is also set to zero as it cannot be used alone to remove CO_2. No energy will be consumed by a DAC plant in a timestep when one or both energy sources are not available. However, if electricity is available, the DAC application could operate if the river or sewage water HP would be available (see Chapter 3.7.3.1). Timesteps of energy consumption by the DAC plants are determined in the optimization and the energy amounts are stored in the decision variables *DAC_th_consumption* and *DAC_el_consumption*. The constraint is represented in Equation (13).

$$DAC\_th\_consumption[i] \cdot \frac{DAC\_el\_demand\_per\_tCO2}{DAC\_heat\_demand\_per\_tCO2} == DAC\_el\_consumption[i] \quad (13)$$

The constraint depicted in Equation (14) aims for the conversion of the energy consumption optimized in the decision variables *DAC_th_consumption* and *DAC_el_consumption* to the respective CO_2 removal output per timestep *i*. The decision variables are represented in MWh/timestep (see Table 11). They are divided by the specific energy demands *DAC_heat_demand_per_tCO2* and *DAC_el_demand_per_tCO2* which have the unit MWh/tCO_2, respectively. The terms represented by the fractions are the tons of CO_2 that can be removed by the heat and electricity utilization in tCO_2/timestep. Both fractions result in the same value due to the constraint of Equation (13). As both energy sources are necessary to remove one unit of CO_2 (see Chapter 2.4.1), the sum of the two fractions must be divided by two to receive the correct CO_2 removal rate *DAC_CO2_out* in each timestep.

$$DAC\_CO2\_out[i] == \frac{\frac{DAC\_th\_consumption[i]}{DAC\_heat\_demand\_per\_tCO2} + \frac{DAC\_el\_consumption[i]}{DAC\_el\_demand\_per\_tCO2}}{2} \quad (14)$$

Further, the sum of the CO_2 removal time series *DAC_CO2_out* must be equal to the gross negative emission demand of Hamburg. This is necessary to achieve the proposed net negative emission rate. The parameter of the gross negative emission demand is called *gross_cdr_hh* in tCO_2/a. The constraint is shown in Equation (15).

$$\sum_{i=1}^{8760} DAC\_CO2\_out[i] == gross\_cdr\_hh \quad (15)$$

For CO_2 removal from the atmosphere, the energy feed-in to the DAC plant must be plausible. It must be ensured that the used electricity for the DAC application *DAC_el_consumption* is less or equal to available electricity in the grid. In addition, the HPs' electricity consumptions *HP_river_el_consumption* and *HP_sewage_el_consumption* must be considered. Therefore, the electricity demands of the river and sewage water HP are subtracted from the available electricity of the power system of Hamburg. The time series of the power system of Hamburg is called *electricity_hh*. It must be multiplied by -1 to convert the negative residual loads to positive values to oblige to the non-negative constraint of the variable *DAC_el_consumption*. The resulting constraint is illustrated in Equation (16).

$$DAC\_el\_consumption[i] \leq (-1) \cdot electricity\_hh[i] - HP\_river\_el\_consumption[i] - HP\_sewage\_el\_consumption[i] \quad (16)$$

3.7.3.1 Scenario-Specific Constraints

The previously explained constraints are the same in all scenarios. The following constraints differ in dependency on the considered thermal energy storage scenario. The heat feed-in for the DAC plant is either covered by the HPs *HP_river_th_supply* and *HP_sewage_th_supply* with the DH system's surplus heat supply *DH_system_th_supply* or solely by the available power of the HPs.

3.7.3.1.1 Scenarios without Seasonal TES

First, the constraints for the scenarios without seasonal TES are considered. The used heat for the DAC plants *DAC_th_consumption* must be equal to the heat from the DH system and the HPs' free capacity in each timestep. If the DH system does not supply heat at a specific timestep, the thermal input for the DAC plant can be provided by the HPs and vice versa. The heat supply provided by the DH system and the HPs must not exceed the heat consumption of the DAC plants. More heat would be produced than the DAC plants would demand. It must be prevented to produce unnecessary overshoot heat. Unnecessary heat production of the HPs would correlate with consuming too much electricity due to the constraints of Equations (8), (9), and (16) could be used in another electricity-consuming application. This is described in Equation (17).

$$DAC\_th\_consumption[i] == DH\_system\_th\_supply[i] + HP\_river\_th\_supply[i] + HP\_sewage\_th\_supply[i] \quad (17)$$

3.7.3.1.1 Scenarios with Seasonal TES

In the case of the availability of a seasonal TES, thermal energy is not supplied by the DH system for the DAC application (see Chapter 3.4.2). Therefore, the heat supply is covered only by the HPs. The heat consumption of the DAC application *DAC_th_consumption* and heat supply composition change compared to the scenarios without a seasonal TES. In the scenarios with a seasonal TES, *DAC_th_consumption* must be equal to the heat that can be provided by the heat pumps' free capacity. If the HPs cannot provide heat due to a lack of electricity or an already full-load operation in the DH system, the variable *DAC_th_consumption* is set to zero. The respective constraint for the scenario considering a seasonal TES is represented in Equation (18).

$$DAC\_th\_consumption[i] == HP\_river\_th\_supply[i] + HP\_sewage\_th\_supply[i] \quad (18)$$

3.7.4 Objective: Minimum $LCoCO_2$

In this section, the objective of the optimization and its elements are explained. The levelized costs of CO_2 removal ($LCoCO_2$) shall be minimized in all scenarios. The economic review of the optimization's output is executed by the annuity factor method after *VDI*. (Verein Deutscher Ingenieure e.V., 2012) Due to the incomplete information about DAC plants' economic parameters in the literature, the capital-related costs are simplified and don't take reinvestment costs and the residual value of the plant at the end of its lifetime into consideration. The determined parameters in Chapter 3.5.2 are used for the calculation of $LCoCO_2$. The investment costs of the DAC plants at different specific investment costs are calculated according to Equation (3) as CAPEX. For the annual OPEX, 4 % of the investment costs are set.

Demand-related costs are considered for the HPs and DAC plants. The annual demand-related costs for the HPs are calculated by the sum of the electricity demands *HP_river_el_consumption* and *HP_sewage_el_consumption* in MWh/a multiplied by the respective LCoE in €/MWh. The specific demand-related costs of the river HP per ton of CO_2 are called *HP_river_dr_cost* and are represented in €/tCO_2. For the calculation of *HP_river_dr_cost*, the annual demand-related costs in €/a are divided by the net negative emission output goal of Hamburg *net_cdr_hh* in tCO_2/a according to Equation (19).

$$HP\_river\_dr\_cost = \frac{LCoE \cdot \sum_{i=1}^{8760} HP\_river\_el\_consumption[i]}{net\_cdr\_hh} \left[\frac{€}{tCO_2}\right] \tag{19}$$

To reduce additional FLOHs for the sewage water HP, the operators are assumed to get a compensation fee *Comp_ fee* for each supplied thermal MWh in €/MWh. This additional demand-related cost is introduced because the sewage HP is already more utilized and operates at higher FLOHs than the river HP in the DH system (see Chapter 3.4.1.2). The annual demand-related costs in €/a are calculated by multiplying the annual *HP_sewage_el_consumption* by the sum of the LCoE and the compensation fee. The annual demand-related costs are then divided by *net_cdr_hh* to receive the specific demand-related costs of the sewage water HP per ton of CO_2. The specific demand-related costs of the sewage water HP in €/tCO_2 are called *HP_sewage_dr_cost*. They are illustrated in Equation (20).

$$HP\_sewage\_dr\_cost = \frac{\sum_{i=1}^{8760} HP\_sewage\_el\_consumption[i]}{net\_cdr\_hh} \cdot (LCoE + Comp\_fee) \quad \left[\frac{€}{tCO_2}\right] \tag{20}$$

As the lowest positive value of the LCoE is determined to be 1 €/MWh, the HPs heat production is more expensive than the heat supplied by the DH system. Thus, the surplus heat consumption of the DH system is prioritized in the optimization model. Potentially, the DH system could also claim demand-related costs in the form of LCoH. In default, it is assumed that the LCoH for surplus heat within the DH system is set to zero (see Chapter 3.4.1). In case the $LCoCO_2$ is higher than 100 €/tCO_2, the necessary negative LCoH for the surplus heat from the DH system is determined. The heat costs from the DH system are called *DH_cost_th*. They are calculated by multiplying the sum of the thermal energy supply of the DH system *DH_system_th_supply* by the LCoH. The calculation of *DH_cost_th* is depicted in Equation (21).

$$DH\_cost\_th = \frac{LCoH \cdot \sum_{i=1}^{8760} DH\_system\_th\_supply[i]}{net\_cdr\_hh} \quad \left[\frac{€}{tCO_2}\right] \tag{21}$$

The DAC plants also consume electricity. The time series of the decision variable *DAC_el_consumption* is summed up to acquire the total electricity consumption in 2045. The total energy consumption is multiplied by the LCoE to calculate the total electricity costs of the DAC plant. For the specific electricity costs per removed ton of CO_2, the total electricity costs of the DAC application are divided by the parameter of the net CDR rate of Hamburg *net_cdr_hh* in 2045. The calculation of the specific electricity costs per removed ton of CO_2 is called *DAC_cost_el*. It is represented in Equation (22).

$$DAC\_cost\_el = \frac{LCoE \cdot \sum_{i=1}^{8760} DAC\_el\_consumption}{net\_cdr\_hh} \quad \left[\frac{€}{tCO_2}\right] \tag{22}$$

For the calculation of the $LCoCO_2$ of the DAC application, the CAPEX, OPEX, and demand-related costs for heat and electricity are considered. The demand-related costs for the heat supply by the HPs and DH system as well as the electricity costs for the DAC plant per ton of CO_2 have been introduced in Equations (19) to (22). They are added to the CAPEX and OPEX in Equation (23). This expression is similar to Equation (4). The condition of linear relations between the decision variables is satisfied in all equations, constraints, and the objective function. Thus, the optimization is based on a MILP problem instead of a MINLP.

$$LCoCO_2 = \frac{CAPEX \cdot AF + OPEX}{net\_cdr\_hh} + DAC\_cost\_el + DH\_cost\_th + HP\_river\_dr\_cost + HP\_sewage\_dr\_cost \quad \left[\frac{€}{tCO_2}\right] \tag{23}$$

With: $LCoCO_2$ = levelized costs of CO_2 removal [€/tCO_2]
CAPEX = investment costs [€]
AF = annuity factor [-]
OPEX = annual operational expenditures [€]
net_cdr_hh = annual mass of net CO_2 removal [tCO_2]
DAC_cost_el = demand-related electricity costs of the DAC plant [€/tCO_2]
DH_cost_th = demand-related heat costs of the DAC plant from the DH system [€/tCO_2]
HP_river_dr_cost = demand-related costs of the river HP for heat production [€/tCO_2]
HP_sewage_dr_cost = demand-related costs of the sewage water HP for heat production [€/tCO_2]

3.7.5 Summary of Inputs and Expected Outputs of the Scenarios

In this section, the concerned inputs are listed once more, and the upcoming outputs of the optimization model are explained to understand the results of Chapter 4. Uniform input parameters that are used in all considered scenarios are illustrated in Table 13. The input time series of Chapter 3.7.1.3 are chosen and applied according to the scenarios depicted in Table 1.

Table 13: Uniform parameter inputs and assumptions for all scenarios. (Own illustration)

Parameter	**Value**
Resolution time of time series in minutes	60
Electricity: negative residual load in MWh in 2045	-12,440,659.058
DH system: negative residual load in MWh in 2045	-415,916.404
Temperature level of DH system in °C	80 to 94
Approx. FLOH of river HP in DH system in h/a	1,875
Approx. FLOH of sewage w. HP in DH system in h/a	4,513
Annual OPEX in % of investment costs	4
Project lifetime in years	30
interest rate in %	7
Specific heat demand in kWh/tCO_2	1,194
Specific electricity demand in kWh/tCO_2	192.5
Process cycle time in minutes	60
Capacity size of a DAC module in tCO_2/a	300
Target value of an optimum $LCoCO_2$ in €/tCO_2	< 100
Hamburg's gross negative emissions in tCO_2 in 2045	485.239
Hamburg's net negative emissions in tCO_2 in 2045	471.167

The main output of the optimization model is the solution of the $LCoCO_2$ in each scenario. Next to the $LCoCO_2$, the DAC plant capacity, the correlating investment costs, the number of DAC modules, and the space demand are considered. Other outputs such as the FLOHs of the river and the sewage water HPs as well as the FLOH of the DAC plants are also of interest to check on the plausibility of the scenarios. For the calculation of the FLOHs of the HPs and DAC plants, the thermal energy supply of the HPs and the CO_2 isolation of the DAC plants are considered as outputs. These are calculated according to Equation (5). A compensation fee for the sewage water HP is determined to limit its FLOHs. An increase of less than 0.01 €/tCO_2 for the $LCoCO_2$ is proposed.

The total electricity demand of the HPs and the DAC plants contains the sum of the decision variables *HP_river_el_consumption*, *HP_sewage_el_consumption*, and *DAC_el_consumption*. The heat consumption of the DAC plants *DAC_th_consumption*, the respective heat supply of the HPs, and the DH system are also determined by the optimization model. The used energy share from the total available negative residual load of the power and DH system is also calculated. Further, the optimum LCoE and LCoH are also investigated to reach the proposed $LCoCO_2$ below 100 €/tCO_2 (see Chapter 3.5.2.4).

4 Results

In this section, the outputs of the optimization model are stated for each scenario. The influence of the parameters, decision variables, and constraints on each other in the respective scenarios are also described in this Chapter. However, the evaluation of the results and scenarios in the context of the research subject is located in Chapter 5.

First, the overall energy consumption of the DAC application is presented in Chapter 4.1. As the gross negative CO_2 emission demand by DAC technology is fixed, the input energy for the DAC plants is the same in all scenarios. Next, the demand-related costs containing the optimum LCoE and LCoH for the proposed $LCoCO_2$ are addressed. Furthermore, the optimum compensation fee for the sewage water HP in each scenario is reported in Chapter 4.2.

The composition of the heat supply by the HPs and the DH system is presented in Chapter 4.3 as they are influenced by the demand-related costs. The resulting FLOHs of the HPs are also addressed. Additionally, the used surplus heat share of the DH system and the used share of negative residual loads from the power system of Hamburg are described.

Afterward, the calculated DAC plant capacity and the respective FLOH, investment costs, and space demand are presented in Chapter 4.4. Further, the results from the spatial analysis are displayed in Chapter 4.5. Finally, the resulting $LCoCO_2$s are mentioned for all scenarios in Chapter 4.6.

For a better understanding, the time series of five exemplary TES capacity scenarios of the DH system are attached in Appendix 5 to Appendix 9. The data frames and figures of the time series of all scenarios are attached in the digital appendix B.3 *Collection of scenarios and their time series (inputs, variables, and other outputs).xlsx* and B.4 *Figures of the scenarios' time series*. An overview of the results of all scenarios is listed in Appendix 10 to Appendix 12 which are categorized according to the DH system designs.

4.1 Energy Consumption and CO_2 Isolation of DAC Plants

Since the net and gross CDR rate and the energy demand of the DAC plants are the same in all scenarios, the energy consumptions of the DAC plants are uniform across the scenarios. The electrical energy consumption *DAC_el_consumption* results in 93,408.509 MWh/a at a specific electricity demand of 192.5 kWh/tCO_2. The thermal energy consumption of the DAC plants *DAC_th_consumption* is solved to be 579,375.378 MWh/a with the specific heat demand of 1,194 kWh/tCO_2.

Although the total energy consumption of the DAC plants is calculated to be the same across all scenarios, the availability of surplus heat and free heat generator capacity of the DH system of Hamburg varies across the TES capacity scenarios (see Chapter 4.3). Thus, CO_2 is isolated at different timesteps and different amounts in the time series *DAC_CO2_out* of the main TES capacity scenario. This can be seen in three exemplary scenarios in Figure 11.

The differences in the CO_2 isolation dispatches of the 1- and 12- hours short-term scenarios can be seen for example in April 2045. The differences between the 12-hour short-term TES with and without a seasonal TES cannot be distinguished visually. However, the time series data show that a slightly higher DAC power capacity is in place when a seasonal TES exists, and no surplus heat of the DH system is available (see Chapter 4.4.1).

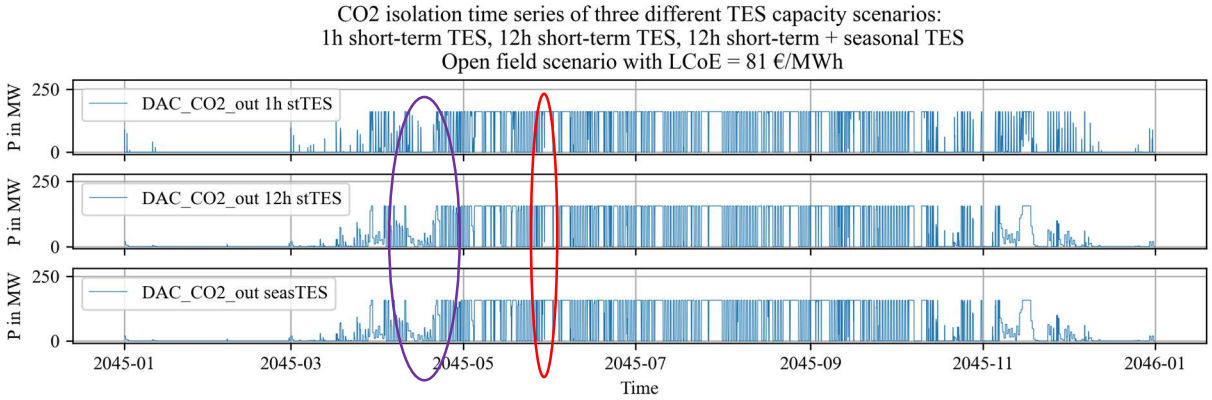

Figure 11: Exemplary time series of CO_2 isolation dispatch of the DAC plants using the 1-hour short-term TES (top), 12-hour short-term TES (middle), and 12-hour short-term and seasonal TES (bottom) of the DH system. The CO_2 isolation dispatch schedules of the 1- and 12-hour short-term scenarios vary significantly in April 2045 (purple circle). Differences between the 12-hour short-term TES and the 12-hour short-term with a seasonal TES can be seen on 1st June (red circle). (Own illustration)

4.2 Demand-Related Costs and Their Impact

In this section, the impacts of the varying electricity prices, surplus heat prices, and the compensation fees for the sewage water HP in the optimization of the scenarios are described. The results of the demand-related costs influence other outputs of the optimization model. However, other in- and outputs influence the demand-related costs, too. Therefore, the demand-related costs are presented for the different scenarios here with references to other chapters that contain results of other outputs of the optimization model.

4.2.1 Electricity and Heat Prices

An impact on the dispatch schedule within a TES capacity scenario is not detected for the assumed LCoE of 1 and 81 €/MWh. Within a TES scenario, the usage of surplus heat from the DH system and the usage of HPs is solved in the same way for the given LCoE range (see Chapter 4.3). For scenarios resulting in an $LCoCO_2$ above 100€/tCO_2, optimum LCoE and LCoH are detected to achieve an $LCoCO_2$ below 100 €/tCO_2. The results for the optimum LCoE and LCoH are listed in Table 14.

Table 14: Optimum LCoE and LCoH of the scenarios to operate DAC plants at $LCoCO_2$ below 100 €/tCO_2. (Own illustration)

Scenario in 2045	LCoE in €/MWh	LCoH in €/MWh
OF-stTES1h-wo/SeasTES-elOptimum	<= 75	0
OF-stTES12h-wo/SeasTES-elOptimum	<= 81	0
OF-stTES12h-w/SeasTES-elOptimum	<= 55	0
FR-stTES1h-wo/SeasTES-elOptimum	<= -124	0
FR-stTES12h-wo/SeasTES-elOptimum	<= -113	0
FR-stTES12h-w/SeasTES-elOptimum	<= -115	0
FR-stTES1h-wo/SeasTES-thOptimum	1 [81]	<= -133 [-192]
FR-stTES12h-wo/SeasTES-thOptimum	1 [81]	<= -119 [-177]

In the following, the reason for different optimum LCoEs in the TES capacity scenarios is explained. The solved scenarios containing a 12-hour short-term TES capacity of the DH system allow a higher percentage of the overall available surplus heat to be consumed by the DAC application. This can be explained by peak load heat generation within the DH system. The peak load heat generation in the 1-hour short-term TES capacity scenario is not feasible to be consumed as a higher DAC plant capacity would be necessary. Thus, the HPs are used more in the 1-hour TES scenario than in the 12-hour TES capacity scenario (see Chapter 4.3). This is the reason why the optimum LCoE can be higher in the 12-hour short-term TES capacity scenario compared to the 1-hour short-term TES capacity.

For a large-scale DAC plant on an open field, an optimum LCoE can be realized within the range of 1 to 81 €/MWh in all TES capacity scenarios. The optimum in the 12-hour short-term TES capacity scenario is given at 81 €/MWh which is also the upper boundary of the LCoE range. In the 1-hour short-term TES scenario, the LCoE can be at a maximum of 75 €/MWh or lower to obtain the targeted $LCoCO_2$ as less surplus heat from the DH system can be used. The scenario with a seasonal TES must provide the heat only by HPs due to the lack of surplus heat of the DH system (see Chapter 4.3). Therefore, the optimum and maximum LCoE must decrease further to 55 €/MWh or below.

For the scenarios containing several small-scale DAC plants on flat rooftops, a negative LCoE is necessary for the optimum LCoE to bring down the $LCoCO_2$ to below 100 €/tCO_2 (see Chapter 4.6). This is caused by the higher investment costs for the DAC plants. A negative LCoE results in increased usage of the HPs and a decreased usage of the surplus heat of the DH system due to the cost-reducing effect on the $LCoCO_2$. In the scenarios *FR-stTES1h-wo/SeasTES-elOptimum* and *FR-stTES12h-wo/SeasTES-elOptimum*, the surplus heat of the DH system is no longer prioritized. The heat supply composition becomes similar to the one in the scenarios containing a seasonal TES (see Figure 13 in Chapter 4.3). Both scenarios' time series are also illustrated in Appendix 8 and Appendix 9.

In the 1-hour short-term TES capacity scenario, the HPs must compensate for the infeasible usage of peak surplus heat of the DH system. Therefore, the time series of *HP_river_th_supply* and *HP_sewage_th_supply* are solved to supply 192.853 MWh/timestep and 64.284 MWh/timestep at maximum in the scenario *FR-stTES1h-wo/SeasTES-elOptimum*. In the scenario *FR-stTES12h-wo/SeasTES-elOptimum*, the maximum used heat supply by the river and sewage water HPs are 185.658 and 61.886 MWh/timestep.

The increased peak load generation and utilization of the HPs in the 1-hour short-term TES capacity DH system results in a more negative LCoE of -124 €/MWh than the one for the 12-hour short-term capacity TES scenario which is solved to be -113 €/MWh. The scenario considering a seasonal TES needs a higher DAC power capacity due to the missing surplus heat of the DH system (see Chapter 4.4.1) than in the 12-hour short-term TES capacity scenario without a seasonal TES. This would explain the slightly lower LCoE of -115 €/MWh that would be necessary to solve the modeled scenario according to the $LCoCO_2$ goal.

In addition, the DH systems without a seasonal TES that need negative demand-related costs have been tested on a negative LCoH in the scenarios *FR-stTES1h-wo/SeasTES-thOptimum* and *FR-stTES12h-wo/SeasTES-thOptimum*. At an LCoE of 1 and 81 €/MWh, *FR-stTES1h-wo/SeasTES* can be solved using negative LCoHs of -133 and -192 €/MWh, respectively. In the scenario with a 12-hour short-term TES capacity, the LCoH would be at -119 or -177 €/MWh for an LCoE of 1 or 81 €/MWh. The circumstance that a more negative LCoH would be necessary for the smaller short-term TES capacity is in line with the findings above.

4.2.2 Compensation Fee

The compensation fee is a demand-related cost associated with the sewage water HP. It limits the excessive utilization of the sewage water HP and prevents too many additional FLOHs. The compensation fee is not applied to the river water HP. Thus, the river water HP is prioritized and can achieve higher FLOHs. The compensation fee is limited to an additional increase of the $LCoCO_2$ up to 0.01 €/tCO_2.

The two DH system scenarios, which do not incorporate a seasonal TES system, do not rely solely on heat provided by the HPs to fulfill the total heat demand of the DAC application. In the DH system scenario including a seasonal TES, the heat supply for the DAC plants is exclusively dependent on the utilization of HPs. This results in a higher FLOH of the HPs in the DH system scenarios with a seasonal TES (see Chapter 4.3). This affects the sewage water HP particularly.

Due to the higher FLOH of the sewage water HP, the compensation fee per thermal energy unit can be set to 0.33 €/MWh for a $LCoCO_2$ increase of less than 0.01 €/tCO_2. The DH system scenarios without a seasonal TES, however, could implement a slightly higher compensation fee of 0.39 €/MWh to reduce the FLOHs of the sewage water HP to a minimum. This is due to the prioritization of the DH system's surplus heat as the LCoH is set to zero.

In the scenarios *FR-stTES1h-wo/SeasTES-elOptimum* and *FR-stTES12h-wo/SeasTES-elOptimum*, the optimum LCoE has been determined to be equal or below -124 and -113 €/MWh, respectively. Thus, the prioritization of the DH system's surplus heat is shifted towards the HPs' utilization. Therefore, the HPs' FLOHs are increased in both scenarios (see Chapter 4.3).

In the scenario *FR-stTES1h-wo/SeasTES-elOptimum*, the river HP is used more, but the FLOHs of the sewage water HP are the same as they are in the other sub-scenarios considering a 1-hour short-term capacity and multiple DAC plants on flat rooftops. Therefore, the compensation fee is set to be 0.39 €/MWh as well although the LCoE is negative.

In the scenario *FR-stTES12h-wo/SeasTES-elOptimum,* however, the FLOHs of the sewage water HP are increased. The FLOHs of the sewage water HP are in the same range as in the scenarios containing a seasonal TES (see Chapter 4.3). Thus, the compensation fee for the sewage water HP results in 0.33 €/MWh. A list of the scenarios and their respective compensation fees is depicted in Figure 12. The effect of the compensation fee on the FLOH distribution between the river and sewage water HPs is addressed in the next chapter.

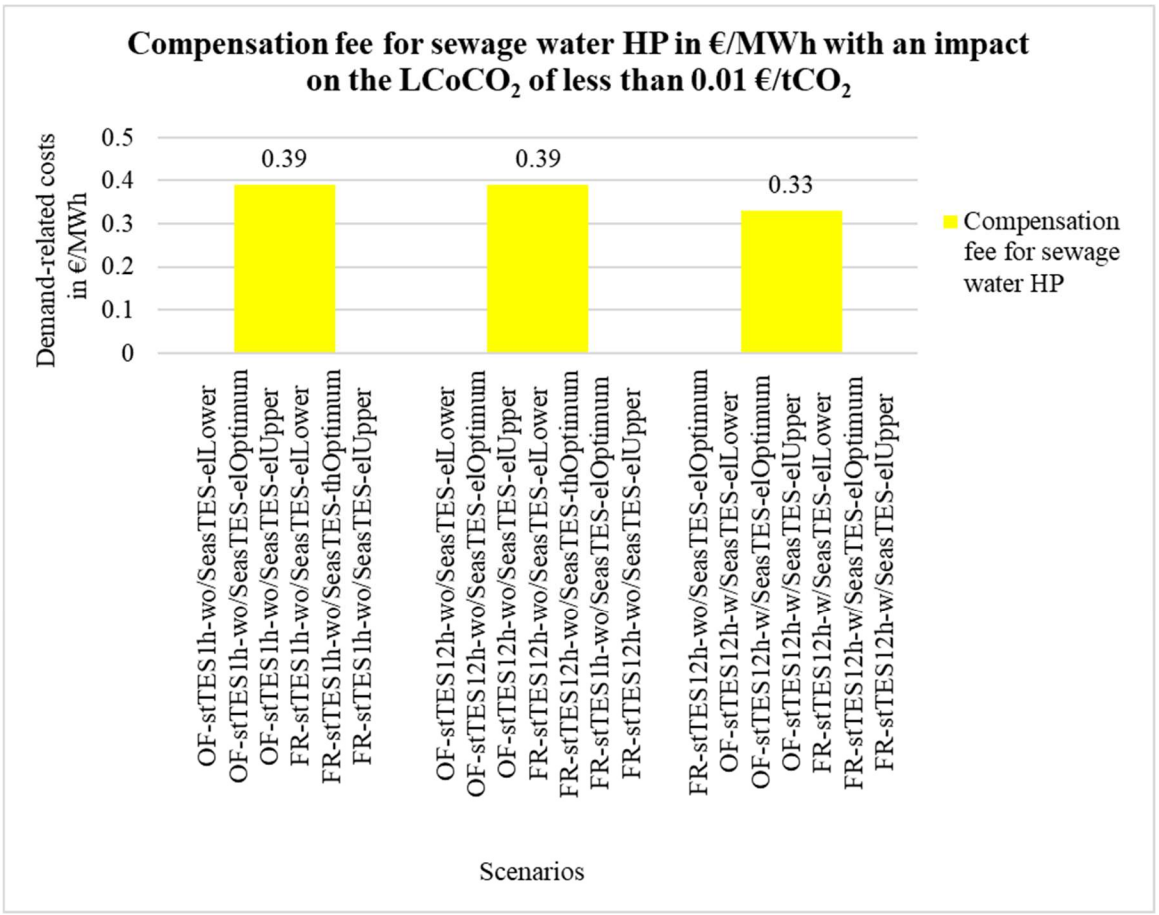

Figure 12: Overview of the compensation fee to limit the FLOH of the sewage water heat pump. The values are affected by the overall needed heat supply by the HPs, the costs for electricity for the HPs, and the surplus heat of the DH system in the scenarios. (Own illustration)

4.3 Energy Flows and Composition of the Heat Supply for DAC Plants

In this section, the results of the optimization model concerning the heat supply for the DAC plants in the scenarios are addressed. The three main scenarios consider different DH system designs. Thus, the composition of the heat varies that is supplied to the DAC applications.

The concerned energy supplies and consumptions are limited to the DH system and HPs for the DAC plants. The necessary energy flows are only considered to the point of CO_2 isolation. Necessary energy for CO_2 transport and storage is not considered in this thesis. An overview of the heat supply by the DH system, river and sewage water HPs is illustrated in Figure 13 for all scenarios. Further, the total FLOHs of the HPs are depicted. The total FLOHs of the HPs are calculated by the previous utilization within the DH system (see Table 13) plus the additional utilization for the DAC application.

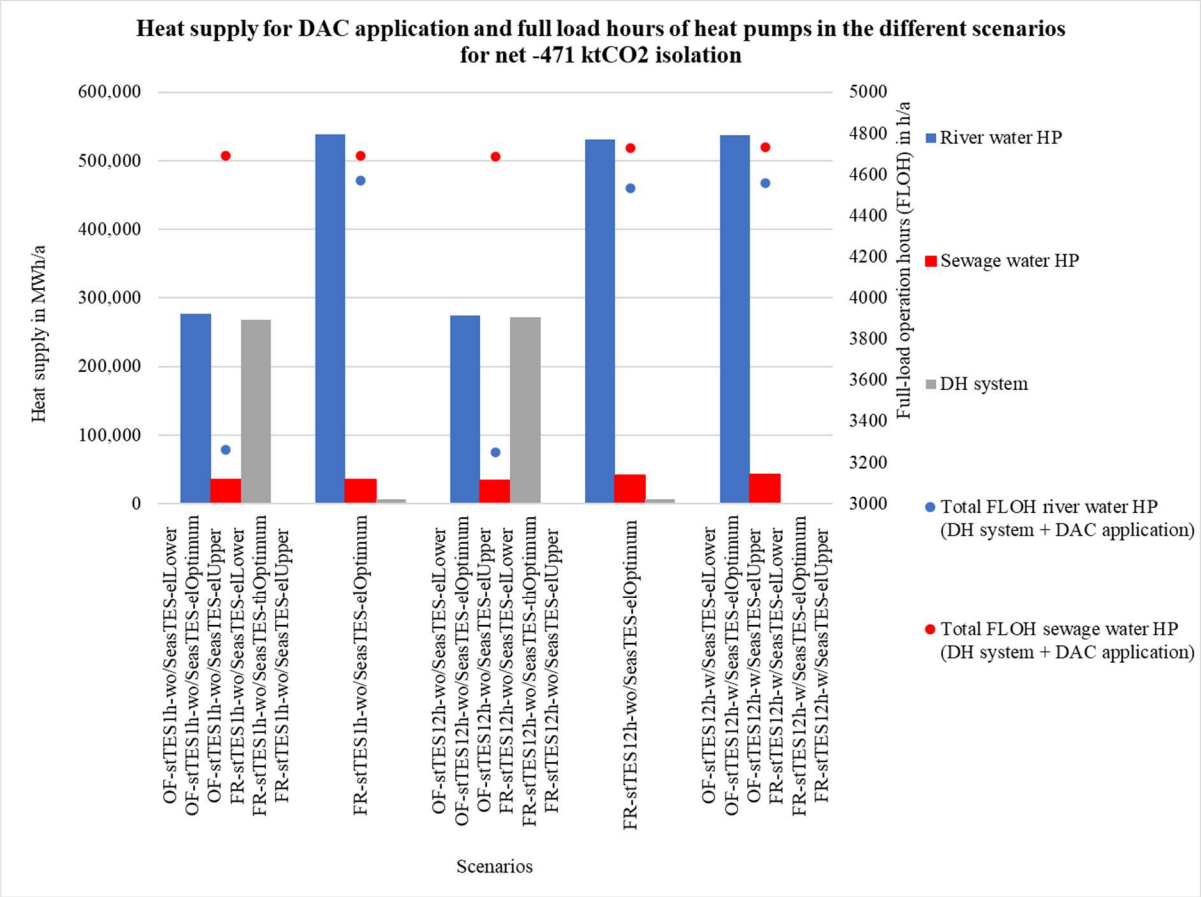

Figure 13: Heat supply for DAC plants in the specific scenarios distinguished by surplus heat of the DH system and heat pumps and their respective full-load operation hours. (Own illustration)

The used share of the total available surplus heat of the DH system is illustrated for each scenario in Figure 14. In the scenarios containing a short-term TES capacity of 1 and 12 h, the utilization of surplus heat is depending on the simultaneous availability of electricity for the DAC application (see Equation (13)). The maximum usable share of the DH system's surplus heat is detected to be 66.995 and 66.359 % for the 1-hour TES scenario and 12-hour TES scenarios, respectively. This has been performed by applying a maximum LCoE of $81*10^{15}$ €/MWh in the model.

The provided heat by the HPs is also linked to electricity availability and consumption. Therefore, the electricity consumption differs in the scenarios and is reviewed in the following subsections. The used shares of the negative residual loads of the power system of Hamburg are depicted in Figure 14.

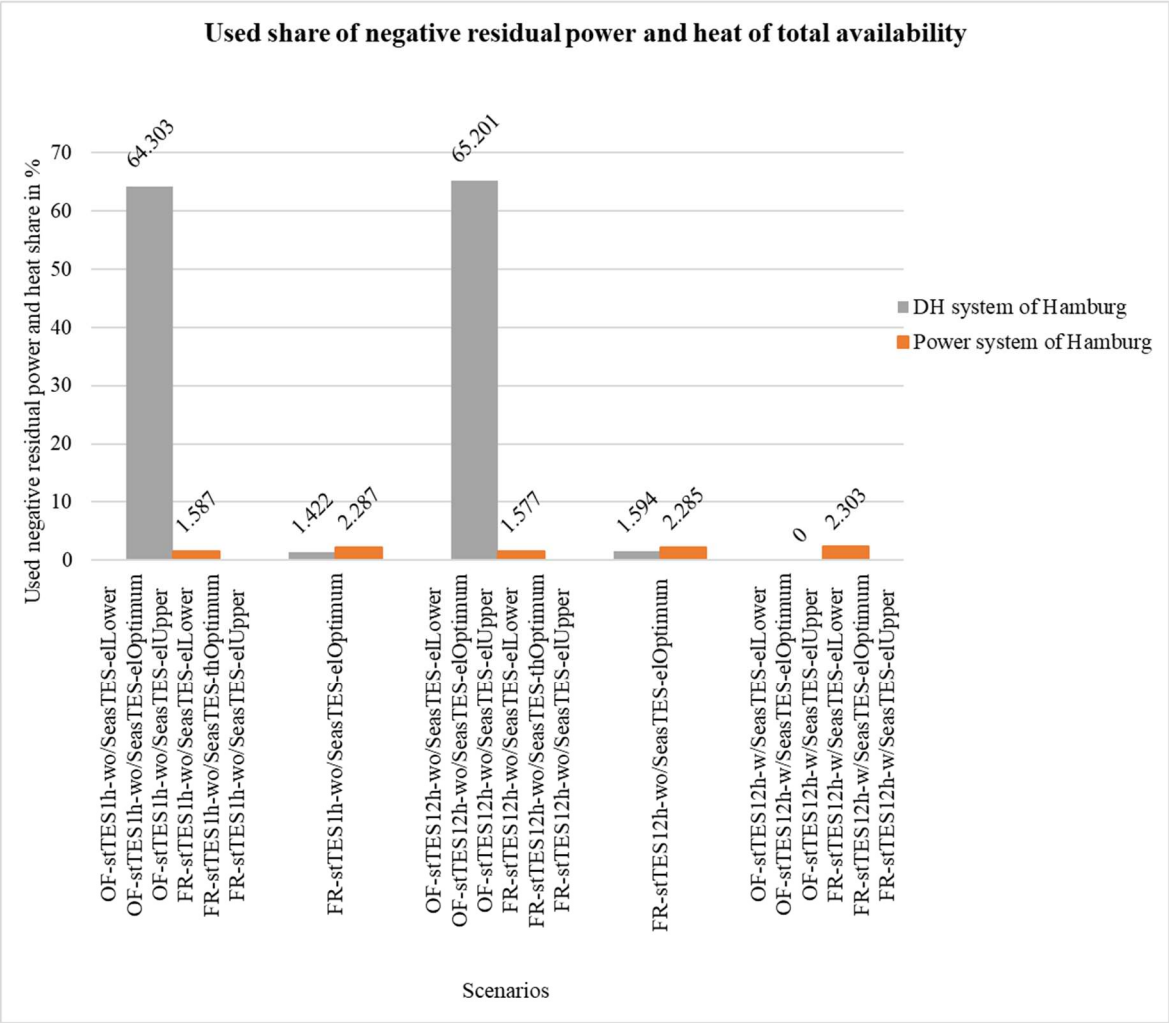

Figure 14: Used share of electricity of the total available negative residual load in the power system that is scaled down to the size of Hamburg in each scenario. Further, the used share of the DH system's surplus heat is depicted in grey per scenario. The maximum usage of surplus heat is limited to 66.995 and 66.359 % in the scenarios considering 1- and 12-hour short-term TES capacity due to the constraint of having electricity available at the same time for the DAC plants. (Own illustration)

4.3.1 1-Hour Short-Term TES Capacity Scenario

In the 1-hour short-term TES capacity scenario, the heat supply composition is the same for all sub-scenarios with a large-scale DAC plant installed on an open field. This is also true for the flat rooftop scenarios considering a positive LCoE for the HPs. According to the results of the optimization model, the river HP supplies 277,366.981 MWh in 2045 in these scenarios. The sewage water HP adds another 34,560.518 MWh. The electricity demand is related to the heat supply. The river HP utilizes 92,455.660 MWh and the sewage water HP consumes 11,520.173 MWh of electrical energy. The additional FLOHs of the river and sewage water HP are 1,386 and 178 h/a, respectively. This results in a total FLOH of 3,261 and 4,691 h/a of the river and sewage water HPs when the heat supply of the HPs for the DH system is also taken into account.

The DH system supplies 267,447.879 MWh of surplus heat. This is 64.303 % of the total available surplus heat of the DH system's design. The total electricity consumption of the HPs and the DAC plants

is solved to be 197,384.342 MWh. This is a consumed share of 1.587 % of all negative residual loads in the power system of Germany that was scaled down to the size of Hamburg.

An exception within the 1-hour short-term TES capacity scenario is the sub-scenario *FR-stTES1h-wo/SeasTES-elOptimum*. In this scenario, a negative LCoE has been detected for a $LCoCO_2$ below 100 €/tCO_2 (see Chapter 4.2.1). Due to the negative LCoE, the prioritization of the DH system's surplus heat shifts to the HPs electricity consumption and thus their heat supply. Thus, the surplus heat of the DH system decreases to 5,914.502 MWh in 2045. This is a share of 1.422 % of the available surplus heat. The river HP supplies 179,633.453 MWh and the sewage water HP stays constant at 11,520.173 MWh. The heat quantities are equal to 2,695 FLOH for the river HP and 178 h/a for the sewage water HP. In total, the river HP operates at 4,570 h/a, and the sewage water HP reaches 4,691 FLOH. The river HP consumes 179,633.453 MWh of electricity and the sewage water HP requires 11,520.173 MWh. In total, 284,562.135 MWh of electrical energy is consumed by the HPs and the DAC application which is equal to 2.287 % of the total available negative residual load in the power system of Hamburg.

4.3.2 12-Hour Short-Term TES Capacity Scenario without Seasonal TES

Similar to the situation in the 1-hour short-term scenario, the heat supply composition remains consistent across all sub-scenarios with a large-scale DAC plant installed on an open field in the 12-hour short-term TES capacity scenario. This is also the case for the flat rooftop scenarios considering an LCoE of 1 and 81 €/MWh for the HPs and electricity consumption of the DAC plants. The river HP supplies 274,816.854 MWh in 2045 in these scenarios. The sewage water HP contributes 33,375.979 MWh. Therefore, the river HP consumes 91,605.618 MWh and the sewage water HP consumes 11,125.326 MWh of electrical energy. The respective additional FLOHs of the river and sewage water HP are calculated to be 1,374 and 172 h/a. This results in a total FLOH of 3,249 and 4,685 h/a of the river and sewage water HPs. The HP utilization is slightly lower than in the 1-hour short-term TES capacity scenarios.

The DH system supplies 271,182.545 MWh of surplus heat. This is 65.201 % of the total available surplus heat of the DH system's design. The higher surplus heat share results from the smoothened peak surplus heat generation. This can be seen in the time series *DH_TES_cap_1h* and *DH_TES_cap_12h* in Appendix 5 and Appendix 6. The combined operation of the HPs and the DAC plants results in a total electrical energy consumption of 196,139.454 MWh. This is a share of 1.577 % of all negative residual loads in the power system of Hamburg.

There is also an exception within the 12-hour short-term TES capacity without a seasonal TES scenario. This is the sub-scenario *FR-stTES12h-wo/SeasTES-elOptimum*. In this scenario, a negative LCoE is necessary as well to achieve a $LCoCO_2$ below 100 €/tCO_2 (see Chapter 4.2.1). The same explanation can be applied that is stated for the scenario *FR-stTES1h-wo/SeasTES-elOptimum* in Chapter 4.3.1. Due to the negative LCoE, the prioritization of the DH system's surplus heat shifts to the HPs electricity consumption. Thus, the surplus heat of the DH system decreases to 6,628.271 MWh in 2045. This is a share of 1.594 % of the available surplus heat.

Due to the better availability of the surplus heat of the DH system within the 12-hour short-term TES capacity scenario, the used share of the DH system's surplus heat can be a little bit higher than in the scenario *FR-stTES1h-wo/SeasTES-elOptimum*. An explanation can be found in the decreased necessary river HP's maximum power capacity which also results in a decreased DAC plant capacity. A higher

DAC plant capacity would result in higher $LCoCO_2$ that cannot be compensated by further utilization of the HPs although they operate at a negative LCoE.

In the scenario *FR-stTES12h-wo/SeasTES-elOptimum*, the river HP supplies 531,298.027 MWh and the sewage water HP adds another 41,449.079 MWh. The heat quantities are equal to 2,657 FLOH for the river HP and 214 h/a for the sewage water HP. In total, the river HP operates at 4,532 h/a, and the sewage water HP reaches 4,727 FLOH. The utilization of the river heat pump (HP) is lower in this scenario compared to the *FR-stTES1h-wo/SeasTES-elOptimum* scenario. The sewage water HP's utilization is increased compared to the other scenarios concerning a 12-hour short-term TES capacity. It is economically more feasible to increase the sewage water HP's FLOHs than the FLOHs of the river HP. This can be explained similarly to the explanation in the paragraph before.

A further increase in the maximum supplied heat capacity of the river HP would cause an increase in the DAC plant power capacity. It is more cost-effective if the sewage water HP's heat supply is increased instead. The additionally paid compensation fee for the increased utilization of the sewage water HP causes fewer costs than a potential increase of the river HP's maximum capacity which would result in an increased DAC plant capacity (see Chapter 4.4.1).

The river HP consumes 177,099.342 MWh of electricity and the sewage water HP needs 13,816.360 MWh. In total, 284,324.212 MWh of electrical energy is consumed by the HPs and the DAC application which is equal to 2.285 % of the total available negative residual load in the power system of Hamburg. That is 0.002 % less than in the scenario *FR-stTES1h-wo/SeasTES-elOptimum* due to the more feasible DH system's surplus heat to reduce the overall investment costs of a higher DAC plant power capacity.

4.3.3 12-Hour Short-Term TES Capacity Scenario with Seasonal TES

In the 12-hour short-term TES with seasonal TES capacity scenario, the heat supply composition consists only of the river and sewage water HP. It is the same ratio in all sub-scenarios. It does not depend on the investment costs and demand-related costs of the DAC plants.

As the DH system is excluded from heat supply in these scenarios, the share of surplus heat is 0 %. The river HP consumes 178,902.762 MWh and the sewage HP uses 14,222.364 MWh of electricity. In total, the DAC plants and the HPs consume 286,533.635 MWh of electricity. That is a share of 2.303 % from the negative residual loads of the power system of Hamburg. The HP's thermal energy supply is the only heat source. Thus, it is the highest electricity consumption of the three main scenarios, too. The river HP supplies 536,708.287 MWh and the sewage water HP provides 42,667.091 MWh of heat. The river HP achieves additional FLOHs of 2,684 h/a and the sewage water HP runs at an extra 220 h/a. In total, that results in 4,559 h/a for the river HP and 4,733 h/a for the sewage water HP.

The thermal energy supply provided by the HPs is greater than in any sub-scenario of the other two DH system scenarios. The maximum used heat supply capacity of the river HP within a timestep is solved to be 187.314 MWh/timestep. This is slightly higher than in the scenario *FR-stTES12h-wo/SeasTES-elOptimum* which considers a negative LCoE optimum and thus prioritizes the utilization of the HPs as well. In that scenario, the river HP's maximum produced thermal energy is slightly lower at 185.658 MWh/timestep due to the more feasible option of using some surplus heat of the DH. The higher maximum used heat supply of the river HP when heat is only supplied by HPs results in a higher DAC plant capacity (see Chapter 4.4.1). The larger DAC plant capacity is more cost-intense than the savings by a negative LCoE.

4.4 DAC Plants' Dimensions and Costs

This section discusses the power capacity of the DAC plants and the resulting FLOHs in the various DH system scenarios in Chapter 4.4.1. Additionally, it highlights the total investment costs in Chapter 4.4.2, which depend on the location and scale of the DAC application. The demand for spatial resources of the different DAC plant scales is addressed in Chapter 4.4.3.

4.4.1 Power Capacity and Full-Load Operation Hours

DAC plant power capacities within a respective DH system scenario are solved to the same result in the optimization model. The plant capacity is solved to be constant despite different specific investment costs and demand-related costs. The resolution of the DAC plant capacity is limited by the module size of 300 tCO_2/a. Changes below 300 tCO_2 could therefore not be detected.

In the 1-hour short-term TES capacity scenario, the plant capacity is solved to be 1,415,100 tCO_2/a. In the scenario with a 12-hour short-term TES capacity and without a seasonal TES, the required capacity of the DAC plants is calculated to be 1,362,300 tCO_2/a. It is lower due to the less extensive heat generation peaks of the DH system caused by the larger short-term TES capacity.

In the third scenario using a seasonal TES at a 12-hour short-term TES capacity, the DAC plant capacity is solved to a size of 1,374,300 tCO_2/a. This is smaller than the DAC plant capacity in the 1-hour short-term scenarios. However, it is larger than the DAC plant in the 12-hour short-term TES capacity scenario without a seasonal TES. This is due to the increased utilization of the HPs due to the missing DH system's surplus heat. The increase in the maximum used HP capacity leads to an increase in the DAC plant capacity. However, the used maximum capacity of the river HP is not exploited to its availability maximum.

The proposed output of the DAC plants is a CDR rate of -471 $ktCO_2$ in 2045 across all scenarios. Thus, the DAC plant capacity deviations correlate with the FLOHs of the DAC plant. Their FLOHs are calculated according to Equation (5). The FLOHs are 3,004 h/a in all 1-hour short-term TES capacity scenarios. In the 12-hour short-term TES capacity scenarios without a seasonal TES, the FLOHs are solved to be 3,120 h/a. In the 12-hour short-term TES capacity scenarios with a seasonal TES, the FLOHs of the DAC plants result in 3,093 h/a. The capacities and FLOHs are depicted in Figure 15.

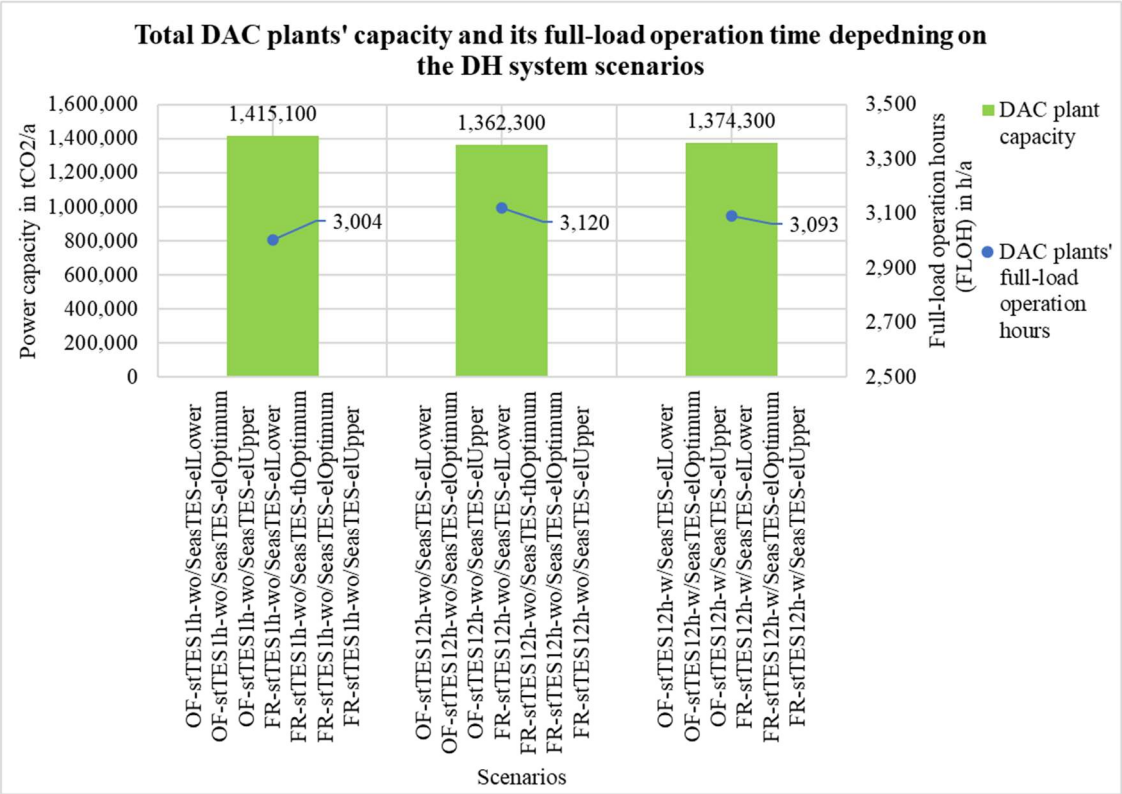

Figure 15: Optimized DAC plant capacity in tCO_2/a and the corresponding full-load operation hours in h/a of the DAC plants in the respective scenarios. (Own illustration)

4.4.2 Capital-Related Costs

The capital-related costs depend on the required capacity of the DAC plants and the respective specific investment costs. The DAC plant capacity varies only at the level of different DH systems (see Chapter 4.4.1). The specific investment costs depend on the position of the DAC plants. A large-scale DAC plant on an open field is assumed to be available at specific investment costs of 189 €/(tCO_2/a) while several small-scale DAC plant modules are assumed to cost 482 €/(tCO_2/a) (see Chapter 3.5.2.3).

The scenarios with a 1-hour short-term TES capacity have the highest DAC plant capacity with 1,415,100 tCO_2/a. The capacity multiplied by 189 for a DAC plant on an open field or 482 €/tCO_2/a) for several plants on flat rooftops results in 267,453,900 € and 682,078,200 €, respectively.

In the scenarios with a 12-hour short-term TES capacity but without a seasonal TES, the investment costs are calculated to be 257,474,700 € for a large-scale DAC plant on an open field. The difference to the DH system scenario with less short-term TES capacity is limited to approximately 10.0 million €. The same capacity installed on flat rooftops would cost 656,628,600 €. The difference in the DH system scenarios without a seasonal TES is given at approximately 25.5 million €.

In the DH system scenarios considering a seasonal TES, the investment costs are solved to be 259,742,700 € for a large-scale DAC plant located on an open field. This is approximately 2.3 million € more than in the scenarios that do not consider a seasonal TES at the same short-term TES capacity. When considering the installation of the same capacity of 1,374,300 tCO_2/a on flat rooftops, the investment costs would amount to 662,412,600 €. This would result in an increase of 5.8 million € compared to the DH system scenarios without a seasonal TES which has a 12-hour short-term TES capacity. The investment costs of the scenarios are depicted in Figure 16.

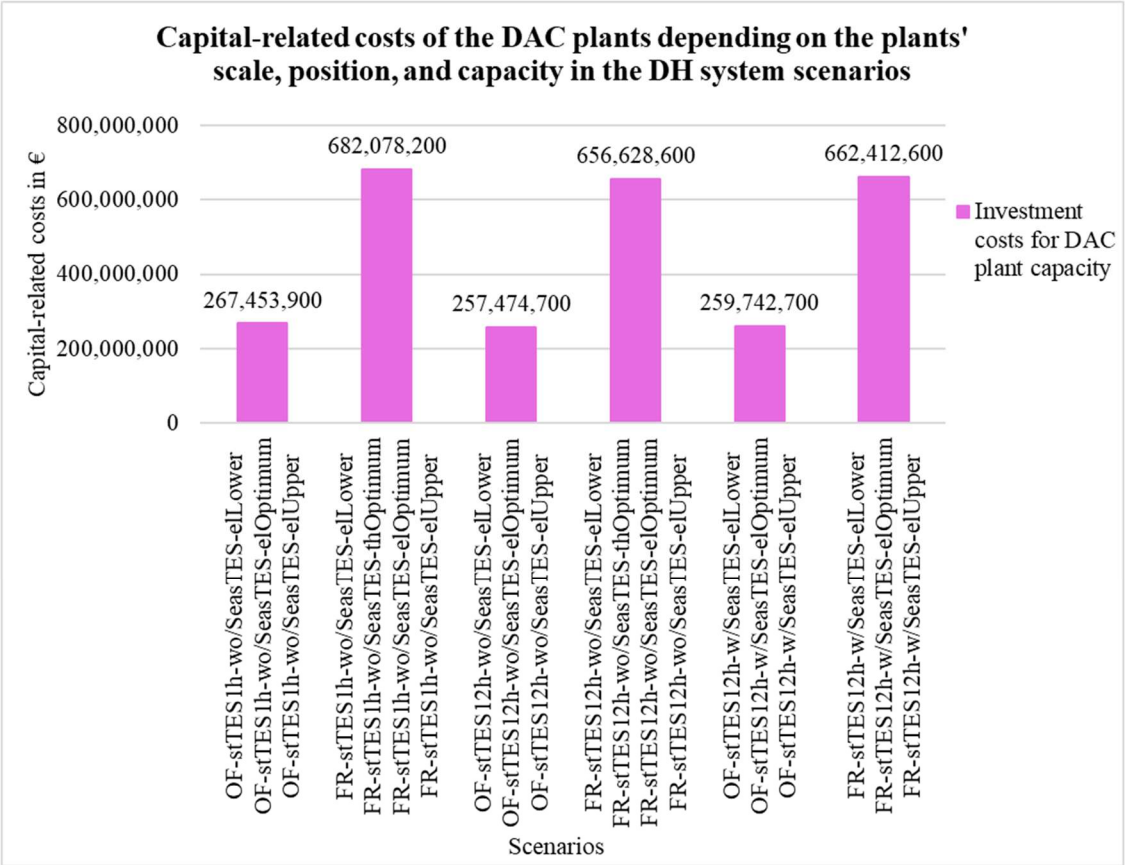

Figure 16: Investment costs of the DAC plants in the respective scenarios. In the considered cases, the specific investment costs have a more significant impact on the investment costs than the DH systems' designs that influence the plant's capacity. The specific investment costs depend on the position and scale of the DAC plant which is either on an open field or a flat rooftop. (Own illustration)

4.4.3 Spatial Requirements

Within a specific DH system design option, the space demands of a large-scale DAC plant on an open field are solved to be the same due to the same DAC plant capacities. The area demands of the DAC plants constructed on open fields are solved to be 110,377.8 m² in the DH system scenarios with a 1-hour short-term TES capacity. This is the highest area demand of the DAC plants installed on open fields. In the 12-hour short-term TES capacity scenarios with and without a seasonal TES, the area demand of an open field DAC plant results in 106,259.4 and 107,195.4 m², respectively. The results of the spatial resource demand of a DAC plant on an open field can be rounded to 0.106 km², 0.107 km², and 0.110 km².

To construct small-scale DAC plant modules on flat rooftops, the DAC plant capacities and the specific area demands per tCO_2/a power capacity of 0.1 m²/(tCO_2/a) result in thousands of DAC plant modules. In the 1-hour short-term TES capacity scenario, the number of necessary DAC plant modules is calculated to be 4,717 units. In the 12-hour short-term TES capacity scenario without a seasonal TES, the number decreases to 4,541 DAC plant modules in the size of a common container. In the 12-hour short-term TES capacity scenario considering a seasonal TES, the number of DAC plants is solved to be 4,581 units.

4.5 Spatial Analysis

In this section, the results of the spatial availability analysis of open fields and flat rooftops in Hamburg are presented. Therefore, the total space demand of the DAC plants is stated according to the solution of the scenarios that are applied to the optimization model. A detailed investigation would include the determination of competitive business cases on those sites as well as ownership regulations. Challenges and costs for buying, renting, or leasing these areas and implementing a CO_2 infrastructure are not considered in the results but are reviewed in Chapter 5.5. The results of the spatial analysis are also discussed in Chapter 5.6.4.

4.5.1 Open Fields

Available open field areas for solar thermal collectors near the DH system have been detected by *Kicherer* in the western side of Hamburg. The transfer of these areas for the construction of DAC plants on the open field near the DH system has been discussed in Chapter 3.6.1. The assumption is made that these areas would also be allocated for the implementation of DAC plants.

The area consumption of a DAC plant on an open field is equal to 0.106, 0.107, and 0.110 km² (see Chapter 4.4.3). An area step size of 0.2 km² could be measured as a minimum according to the scale in Figure 17. Therefore, areas of the size of 0.2 km² are inserted as red squares within the three suitable areas that are highlighted with red circles. This illustrates the compatibility and approximate scale of the area demand of a large-scale DAC plant in the respective areas. The total DAC plant capacity can thus be fitted in each of the three suitable areas.

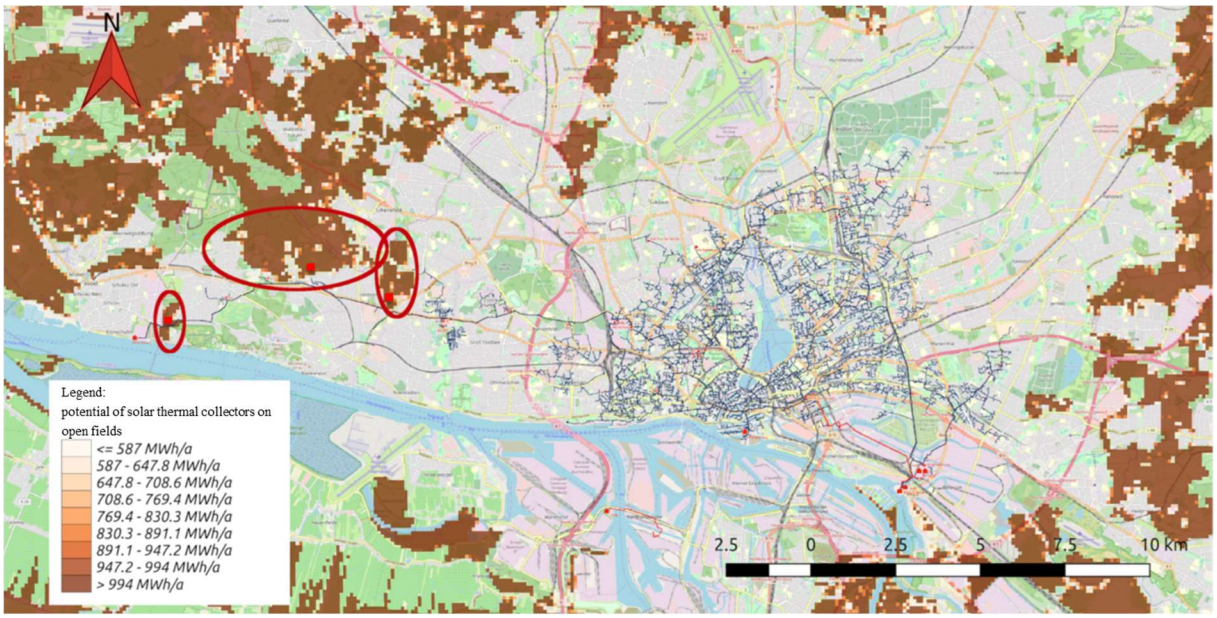

Figure 17: Potential for solar thermal systems on open fields in Hamburg and the district heating system of Hamburg. The blue lines show the DH grid of Hamburg. Brown areas would be open fields that would fit solar thermal systems. Suitable locations with a possible DH system connection are marked with red cycles. (Modified after (Kicherer, 2020))

4.5.2 Flat Rooftops

The number of flat rooftops in Hamburg is identified according to the procedure explained in Chapter 3.6.2. The results are presented here. The tiles intersecting with the DH system have been determined. There are 144 of them that are identified. They are depicted in Figure 18.

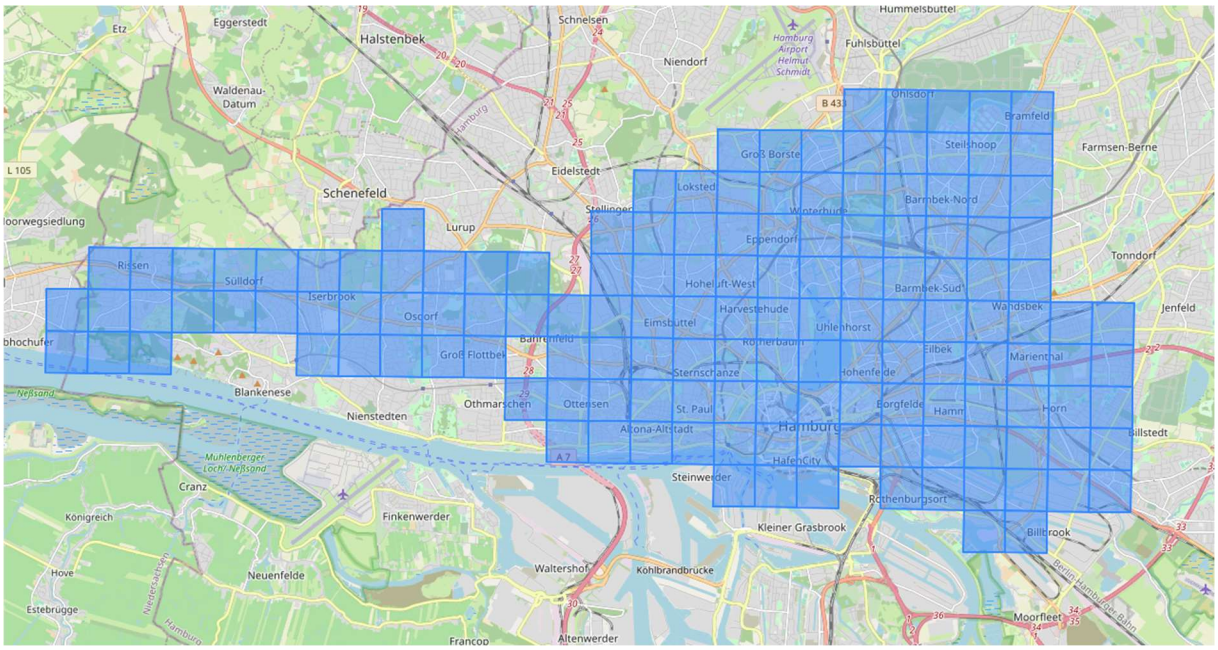

Figure 18: Tiles of the 3D building map which intersect with the DH system of Hamburg (Trosdorff, 2023)

The spatial analysis results in 144 tiles in the 3D building model intersecting with the DH systems area. They include 105,897 buildings. 54,822 buildings have a flat roof of which 34,785 are equal to or larger than 60 m². From the respective flat rooftop polygons, 22,785 buildings can fit container polygons. Thus, 21.5 % of the considered buildings in the tiles are geometrically suitable for an installation of a DAC plant module. The 22,875 flat rooftops should be large enough, to enable maintenance work on the DAC plant modules due to the size of at least 60 m² per suitable building. The maximum number of DAC plant modules in the flat rooftop scenarios is determined to be lower with 4,717 units (see Chapter 4.4.3). However, the results of this analysis are not comprehensive which is discussed in Chapter 5.5.2.

4.6 Minimum $LCoCO_2$ Objective

In this section, the calculated levelized costs of CO_2 isolation of the DAC plants of all regarded scenarios are considered. The minimum $LCoCO_2$ is determined by the objective function of the optimization in Equation (*23*). The defined scenarios, used parameters, developed constraints, and optimized decision variables lead to the respective minimum $LCoCO_2$. In the following, the $LCoCO_2$s are presented according to the designs of the DH system and further explained and distinguished according to the sub-scenarios. An overview of the $LCoCO_2$ of each scenario and the scenario-specific parameters leading to the respective $LCoCO_2$ is illustrated in Table 15.

Table 15: Optimized levelized costs of CO_2 isolation in each scenario. $LCoCO_2$ highlighted in blue are below 100 €/tCO_2 and are achieved within the range of assumed energy costs. $LCoCO_2$ highlighted in orange are also below the proposed 100 €/tCO_2, however, they are only achieved by applying negative energy prices in the optimization model. $LCoCO_2$ highlighted in red are achieved within the range of assumed energy costs but resulted in CDR costs above 100 €/tCO_2. (Own illustration)

Thermal energy storage (TES) capacity in the district heating (DH) system of Hamburg	**Position and scale of DAC plants**	**$LCoCO_2$ in €/tCO_2**			
1 h short-term TES	Open field (OF) Specific investment costs = 189 €/(tCO_2/a)	68.88	102.39	99.88 (at 75)	-
	Flat rooftop (FR) Specific investment costs = 482 €/(tCO_2/a)	174.99	208.51	99.68 (at -124)	99.50 [99.52] (at -133 [-192] when LCoE = 1 [81])
12 h short-term TES	Open field (OF) Specific investment costs = 189 €/(tCO_2/a)	66.32	99.62	99.62 (at 81)	-
	Flat rooftop (FR) Specific investment costs = 482 €/(tCO_2/a)	168.48	201.78	99.87 (at -113)	99.99 [99.91] (at -119 [-177] when LCoE = 1 [81])
12 h short-term + seasonal TES (No surplus heat, only unused heat pump capacities)	Open field (OF) Specific investment costs = 189 €/(tCO_2/a)	67.09	115.75	99.93 (at 55)	-
	Flat rooftop (FR) Specific investment costs = 482 €/(tCO_2/a)	170.15	218.80	99.61 (at -115)	-
Energy prices (LCoE for DAC & HP; LCoH for DAC)		LCoE = 1 €/MWh	LCoE = 81 €/MWh	LCoE = (Optimum) €/MWh	LCoH = (Optimum) €/MWh

4.6.1 1-Hour Short-Term TES Capacity Scenario

In the 1-hour short-term TES capacity scenario with a large-scale DAC plant on an open field, the $LCoCO_2$ range is solved to be between 68.88 and 102.39 €/tCO_2 when the range of LCoE between 1 and 81 €/MWh is applied. The upper limit of the LCoE range leads to a $LCoCO_2$ above 100 €/tCO_2 and is thus unprofitable. The optimum LCoE would be at 75 €/MWh or below to achieve an $LCoCO_2$ of 99.88 €/tCO_2 or below.

In the scenarios considering DAC plants installed on flat rooftops, the $LCoCO_2$ is higher than in the scenarios of a DAC plant on an open field when the LCoE is within the range of 1 to 81 €/MWh. This is only due to the increased specific investment costs as the DAC plant capacity is the same within a DH system's design.

DAC plants on flat rooftops in the 1-hour short-term TES capacity scenario can operate and remove CO_2 at costs of 174.99 and 208.51 €/tCO_2 when the electricity price is in the range of 1 to 81 €/MWh. This price is not within the profitability range of the proposed $LCoCO_2$. To achieve a $LCoCO_2$ below 100 €/tCO_2, the LCoE would need to be adjusted to negative values. Specifically, it would need to reach -124 €/MWh or lower (see Chapter 4.2.1). This would result in CDR costs of 99.68 €/tCO_2 in the scenario *FR-stTES1h-wo/SeasTES-elOptimum*.

In the scenario *FR-stTES1h-wo/SeasTES-thOptimum*, an optimum LCoH is considered. The surplus heat of the DH system would need to be supplied at costs of -119 €/MWh if the LCoE would be available at 1 €/MWh. A price of 99.99 €/tCO_2 could be achieved for the $LCoCO_2$. In case the LCoE is at the upper boundary of 81 €/MWh, the LCoH would have to be further decreased to below -177 €/MWh. This would result in a $LCoCO_2$ of 99.91 €/tCO_2.

4.6.2 12-Hour Short-Term TES Capacity Scenario without Seasonal TES

In the scenarios considering the integration of DAC plants in a DH system with 12-hour short-term TES capacity, a higher share of feasible surplus heat is used (see Chapter 4.3). This results in a lower required DAC plant capacity and thus in lower investment costs (see Chapter 4.4). This also influences the $LCoCO_2$ to be smaller compared to the 1-hour short-term TES capacity scenarios.

The $LCoCO_2$ in the scenario *OF-stTES12h-wo/SeasTES-elLower* is optimized to 66.32 €/tCO_2. Compared to the scenario *OF-stTES1h-wo/SeasTES-elLower* from Chapter 4.6.1, the $LCoCO_2$ is 2.56 €/tCO_2 cheaper. In the case of *OF-stTES12h-wo/SeasTES-elUpper*, the $LCoCO_2$ is solved to 99.62 €/tCO_2. At LCoE of 81 €/MWh, the $LCoCO_2$ of the scenarios *OF-stTES1h-wo/SeasTES-elUpper* and *OF-stTES12h-wo/SeasTES-elUpper* differs by 2.77 €/tCO_2. The $LCoCO_2$ of the scenario *OF-stTES12h-wo/SeasTES-elUpper* is already below 100 €/tCO_2. Therefore, the upper limit of the LCoE is also the optimum value that is allowed for the proposed $LCoCO_2$. Thus, the scenarios *OF-stTES12h-wo/SeasTES-elUpper* and *OF-stTES12h-wo/SeasTES-elOptimum* are solved in the same way.

In the scenarios *FR-stTES12h-wo/SeasTES-elLower* and *FR-stTES12h-wo/SeasTES-elUpper*, the $LCoCO_2$ is solved to be between 168.48 and 201.78 €/tCO_2. A LCoE of 1 to 81 €/MWh is used as a basis, respectively. Compared to the scenario *FR-stTES1h-wo/SeasTES-elLower* from Chapter 4.6.1, the $LCoCO_2$ of the scenario *FR-stTES12h-wo/SeasTES-elLower* is 6.51 €/tCO_2 cheaper. The scenario *FR-stTES12h-wo/SeasTES-elUpper* results in a $LCoCO_2$ difference of 6.73 €/tCO_2 lower than scenarios *FR-stTES1h-wo/SeasTES-elUpper*.

As the $LCoCO_2$ already results in a value above the proposed value of 100 €/tCO_2 at a LCoE of 1 €/MWh, the optimum LCoE must be in the negative price range. In the optimization model, this could be achieved by a LCoE of -113 €/MWh or below (see Chapter 4.2.1). Thus, the $LCoCO_2$ is traded down to 99.87 €/tCO_2 in the scenario *FR-stTES12h-wo/SeasTES-elOptimum*.

In an alternative approach, the $LCoCO_2$ in the flat rooftop scenarios is brought down by a negative LCoH instead. The necessary LCoH would have to be in the range of -119 to -177 €/MWh for the surplus heat consumption if the LCoE is fixed to the range of 1 to 81 €/MWh, respectively (see Chapter 4.2.1). The energy prices of the scenario *FR-stTES12h-wo/SeasTES-thOptimum* would result in $LCoCO_2$s of 99.99 and 99.91 €/tCO_2.

4.6.3 12-Hour Short-Term TES Capacity Scenario with Seasonal TES

In the DH system scenarios considering the integration of a seasonal TES, heat is only supplied by the river and sewage water HPs. The total DAC plant capacity is higher than in the 12-hour short-term TES capacity scenario which does not consider a seasonal TES but is lower than the DAC plant capacity in the 1-hour short-term TES capacity scenario.

When the demand-related costs for electricity are limited to 1 €/MWh in the DH system scenario with a seasonal TES, they are similar to those of the other two DH system scenarios that additionally supply surplus heat at costs of 0 €/MWh. Thus, the $LCoCO_2$ of the sub-scenarios at the LCoE of 1 €/MWh only differ mostly due to the DAC plant capacities. Hence, the $LCoCO_2$s of both scenarios *OF-stTES12h-w/SeasTES-elLower* and *FR-stTES12h-w/SeasTES-elLower* are between the $LCoCO_2$s of the other two DH system scenarios considering the respective DAC plant location sub-scenarios with the LCoE given at 1 €/MWh. The $LCoCO_2$ of the scenarios *OF-stTES12h-w/SeasTES-elLower* and *FR-stTES12h-w/SeasTES-elLower* are solved to be 67.09 and 170.15 €/tCO_2, respectively.

In the scenario of this subsection, a surplus heat supply provided by the DH system is excluded. As the heat for the DAC plants is solely produced by the HPs, each supplied thermal energy unit consumes electricity in the ratio of the HPs' COP. The electricity consumption in this scenario is therefore increased in contrast to the other two DH system scenarios without a seasonal TES (see Chapter 4.3). Additionally, this circumstance leads to an increase in the absolute demand-related costs, particularly when the LCoE is set at the upper threshold of 81 €/MWh compared to the other two DH system designs. The $LCoCO_2$ is solved to 115.75 and 218.80 €/tCO_2 for the scenarios *OF-stTES12h-w/SeasTES-elUpper* and *FR-stTES12h-w/SeasTES-elUpper*, respectively. These $LCoCO_2$ values are higher compared to the ones of the other two DH systems considering the same framework conditions in their sub-scenarios. It stands out that the LCoE has a more significant impact on the DH system that includes a seasonal TES.

The detection of the optimum LCoEs to achieve the proposed range for the $LCoCO_2$ has been considered in Chapter 4.2.1. However, it is taken up again here to explain the $LCoCO_2$s of the scenarios *OF-stTES12h-w/SeasTES-elOptimum* and *FR-stTES12h-w/SeasTES-elOptimum* that are depicted in Table 15. The maximum LCoE of 55 €/MWh is the optimum value for the sub-scenario *OF-stTES12h-w/SeasTES-elOptimum* to achieve a $LCoCO_2$ of 99.93 €/tCO_2. In this sub-scenario, the LCoE is required to be the smallest compared to the scenarios *OF-stTES12h-wo/SeasTES-elOptimum* and *OF-stTES1h-wo/SeasTES-elOptimum*. This is due to the highest electricity consumption of the HPs within the DH system design.

In the scenario *FR-stTES12h-w/SeasTES-elOptimum*, a $LCoCO_2$ of 99.61 €/tCO_2 can be achieved when a LCoE of -115 €/MWh is applied. Here, the LCoE must be 2 €/MWh lower compared to the scenario *FR-stTES12h-wo/SeasTES-elOptimum*. However, the LCoE is allowed to be higher than the LCoE of the scenario *FR-stTES1h-wo/SeasTES-elOptimum*. The mentioned scenarios have similar heat supply compositions due to the prioritization of the utilization of the HPs and thus have similar LCoEs (see Chapters 4.2.1 and 4.3).

Among the various thermal energy storage scenarios for the DH system that use a LCoE of 1 €/MWh, the absence of seasonal TES leads to the most significant differences in the $LCoCO_2$ between the 1-hour and 12-hour short-term TES capacity scenarios (see Table 15). The scenarios considering a DAC plant on an open field have a difference of 2.56 €/tCO_2. The DAC plants on flat rooftops deviate in 6.51 €/tCO_2. The difference in $LCoCO_2$ within the specific DH system scenario can be explained by the different specific investment costs for the DAC plants.

In the case of a LCoE at 81 €/MWh, the most significant difference in $LCoCO_2$ occurs between the 12-hour short-term TES capacity scenarios. The decision of whether a seasonal TES is implemented or not leads to a difference of 16.13 €/tCO_2 for DAC plants constructed on an open field. The variation in $LCoCO_2$ is less significant when multiple DAC plants are situated on flat rooftops, as indicated by a detected deviation of 17.02 €/tCO_2. The most significant difference of the $LCoCO_2$ induced by deviating DH system designs is shifted toward the comparison of the DH systems with and without a seasonal TES. This can be explained by the highest electricity consumption of the DAC application in the DH system design considering a seasonal TES due to the restriction of only using HPs. In the DH system with a seasonal TES, the LCoE has the most influence on the $LCoCO_2$ due to the highest electricity consumption. All $LCoCO_2$ differences occurring due to the DH system designs are illustrated in Table 16 for completeness.

Table 16: Comparison of the $LCoCO_2$ differences between the DH system designs at the same LCoEs and DAC plant properties. (Own illustration)

Scenario properties	**Δ $LCoCO_2$ = 1 h - 12 h short-term TES without seasonal TES in €/tCO_2**	**Δ $LCoCO_2$ = 1 h - 12 h short-term TES with seasonal TES in €/tCO_2**	**Δ $LCoCO_2$ = 12 h with seasonal TES - 12 h short-term TES without seasonal TES in €/tCO_2**
DAC plant on open field LCoE = 1 €/MWh	2.56	1.79	0.77
DAC Plant on flat roofs LCoE = 1 €/MWh	6.51	4.84	1.67
DAC Plant on open field LCoE = 81 €/MWh	2.77	-13.36	16.13
DAC Plant on flat roofs LCoE = 81 €/MWh	6.73	-10.29	17.02

4.6.4 Impact of Specific Investment Costs

The assumed specific investment boundary costs for the different-scaled DAC plants have the most significant impact on the $LCoCO_2$ across the deviating parameters that are considered in the scenarios (see Table 15). The $LCoCO_2$ differences in the same DH system scenario with deviating specific investment costs are between 102.16 and 106.11 €/tCO_2. The influence of the specific investment costs could be reduced if the DAC plant capacity would be decreased and the FLOHs of the DAC plant be increased. The relation is also illustrated in Table 17 for the occurrences in the respective DH system scenarios of this thesis.

Table 17: Comparison of the $LCoCO_2$ differences of the DAC plants installed on flat rooftops and open spaces in the individual DH system designs. The DAC plant capacity and the respective FLOHs influence the difference between the $LCoCO_2$ values. (Own illustration)

Thermal energy storage (TES) capacity in the district heating system of Hamburg	**Δ $LCoCO_2$ in €/tCO_2 at the same LCoE**	**Total DAC plant capacity in tCO_2/a**	**Full-load operation hours in h/a**
1 h short-term TES	106.11	1,415,100	3,004
12 h short-term TES	102.16	1,362,300	3,120
12 h short-term + seasonal TES	103.06	1,374,300	3,093

5 Discussion

In this section, the general limitations and constraints of this thesis are reviewed in Chapter 5.1. The choice of parameters, assumptions, and methods are highlighted and discussed in more detail in Chapters 5.2 to 5.5.

The data basis consisting of the DH system designs of Hamburg and the power system of Germany is discussed in the context of compatibility in Chapter 5.2. Furthermore, the assumptions for the respective systems are discussed and evaluated. In Chapter 5.3, the findings of the literature research on DAC technology and negative emission demands in Germany are evaluated. Afterward, the methodology and assumptions of the optimization model are examined and assessed in Chapter 5.4. It follows the evaluation of the spatial analysis methodology and its constraints in Chapter 5.5. The results and findings of the optimized scenarios are discussed considering the research subject of this thesis in Chapter 5.6. The evaluation of the results and classification in the context of scientific literature are also addressed there.

5.1 General Limitations of this Work

Only the DAC plant's process until the point of CO_2 isolation is addressed in this thesis. The post-processing steps consisting of the transport and storage of CO_2 are not part of this thesis. The implementation of a CO_2 infrastructure, the accompanying costs, as well as the carbon footprint for construction, operation, and maintenance, are therefore not examined.

Sites for the CCS process are not considered in the scope of this work. The scope of the CO_2 infrastructure, implementation challenges, and costs to bring the CO_2 to the CCS sites are not considered. At the time of writing, CCS sites are not allowed in Germany (see Chapter 2.4.4).

In the spatial analysis, only the physical implementation is considered. However, setting up DAC plants on open fields or flat rooftops of urban buildings would result in consequences beyond the scope of fluctuating specific investment costs and specific space demands. The locations for the DAC plant integration would lead to different construction costs and challenges. Less effort is expected to build a plant in a location of an open field rather than to access thousands of smaller sites on top of buildings within the city. The varying specific space demand would also result in deviating property demands and costs for rent or buying. A large CO_2 network would have to be implemented across the city in the case of DAC plants located on buildings with thousands of access points. One large-scale DAC plant would only need a few access points to a CO_2 pipeline. This would also have to be considered for the connection of the DAC plants to the heat and power grid, respectively. Further, the public acceptance of the implementation of DAC plants within the city is not addressed in this thesis.

The findings of this thesis are not directly applicable or transferable to other DH systems. Each DH system is unique and is faced with different requirements and serves other consumer behavior. (Triebs et al., 2021) The methodology of this thesis, however, could be used to investigate the implementation of DAC plants in the design plans of DH systems for other cities. For the compatibility of the designs of the DH system and the DAC application, assumptions are made that are addressed and discussed in Chapter 5.2.1.

The parameters and data that are used within this thesis are obtained by literature research and do not consist of measured data of a real-world application. The real-world application is converted into a theoretical consideration. Simplifications and assumptions are made in advance to investigate the research subject. This thesis does not consider the influence of weather conditions and plant failures, which are significant factors that can impact real-world processes.

Further, this thesis only considers the economic viability in 2045 as a snapshot. A larger period is not examined. The profitability of this operation mode can change throughout the project lifetime of the DAC plant. The time series for the power system and heat system of Hamburg beyond 2050 will differ. Changing consumer behaviors and weather conditions influence energy consumption and production. More years must be evaluated to make a statement about whether the flexible operation mode of DAC plants is feasible beyond 2045. More details on specific limitations of the data basis, parameters, and assumptions are mentioned in the following Chapters.

5.2 Data Basis and Assumptions

The data basis is a power system of Germany and a DH system design approach of Hamburg (see Chapter 2.2 and 2.3). They are evaluated in the following Chapters 5.2.1 and 5.2.2. In the following paragraph, the compatibility of the heat and power system's designs is examined.

The time series of the heat and power systems are based on different weather models and consider different areas. The weather conditions for 2050 used by Kicherer et al. are based on the TRY 2045 of Hamburg by the German National Meteorological Service. (Kicherer et al., 2021) The weather conditions can be expected in 2045 as well. This results in the same heat load profile of the DH system in 2045. The TRY is based on weather data of the period 1995 to 2012 for comparison and evaluation of typical weather patterns. (Deutscher Wetterdienst, 2023)

The weather conditions in the optimized power system of Germany by *REMod* are based on other years. The projected weather conditions are built on those of the years 2011 to 2015. (Sterchele et al., 2020) In the thesis, it is assumed that the weather time series are compatible because weather forecasts can vary widely at national and local levels. However, it would be necessary to use time series that are based on the same weather years and the same forecast calculation algorithm.

Whether the power system or the DH system is served more by the operation mode of the DAC plants could not be distinguished. The resolution time of the time series of the heat and power system is limited to 1 hour. A higher resolution time could result in a change in the necessary process cycle time of the DAC plants due to deviating residual loads in the LFC areas that are balanced e.g., in 15-minute periods by the TSOs. (50Hertz Transmission GmbH et al., 2023)

As the resolution time is given at 1 hour, storage capacities for at least 1 hour are assumed to be in place. Different battery energy storage system capacities could be implemented in the power system, too. Therefore, the significance of this study is limited to the case of a storage capacity of at least 1 hour within the power and heat system.

5.2.1 DH System of Hamburg

The developed findings about the DH system designs of Hamburg in 2045 by *Kicherer* are assumed to be valid. This is assumed due to the subsequent publication of the respective master thesis in a peer-reviewed paper by *Kicherer et al.* (see Chapter 2.3.1). However, as the DH system design is proposed for 2050, it remains uncertain whether one of the proposed DH system designs will be implemented in 2045.

In a real-world DH system application, the heat generation mix differs throughout the year (see Figure 3). The heat generators provide heat at different temperature levels. (Kicherer, 2020) Temperature level changes in the DH system due to varying heat generator mix compositions throughout the year have not been examined within this thesis. Further investigation would be necessary to ensure that the temperature level does not drop below 80 °C to be used by the DAC application. The dynamic temperature level changes would have to be assigned to the time series of the DH system to ensure a stable operation for the DAC plants. Further, in a real-world problem, heat transport and storage losses would occur. However, these characteristics have not been stated by *Kicherer* in detail. Therefore, they have been neglected in this thesis as well to reduce the scope of the research subject.

5.2.1.1 Short-Term TES Scenarios

Kicherer worked out different scenarios with short-term TES capacities of 1, 2, 6, and 12 hours (see Chapter 2.3.1). Only the extremum short-term capacities are considered to investigate the technical suitability in the worst and best case. However, this thesis does not answer whether a 1- or 12-hour short-term TES capacity should be implemented as the different short-term capacities go along with different costs, challenges, and reliability that have to be balanced for the DH system in another research work. It could therefore be of interest to extend the research of the DAC application of this thesis to the remaining short-term TES capacities as well.

A higher short-term capacity results in greater flexibility of the DH system. A statement can be made that greater flexibility benefits the DAC application. However, the influence on the $LCoCO_2$ is lower compared to the influence of the specific investment costs for the DAC plant capacity and the demand-related costs. The implementation costs for different short-term TES are not considered. The costs for peak load heating sources due to the lack of seasonal TES must also be clarified outside of this thesis.

5.2.1.2 Seasonal TES Scenarios

The implementation of a seasonal TES should be considered according to *Kicherer*. The seasonal TES capacity is therefore included in one of the main scenarios. 90 GWh of waste heat would be available if no storage losses would be assumed in the seasonal TES. The prediction of timeslots, when it is suitable to store or supply heat in and by a seasonal TES, cannot be answered within the scope of this thesis. The remaining negative residual heat loads are not considered to be available for DAC operation in this scenario (see Chapter 3.4.2).

A follow-up investigation on the utilization of the remaining surplus heat amounts could be executed when the designs of the DH system of Hamburg would be edited in more detail. In that case, the competing costs for storing surplus heat could be included in the optimization model. The changed schedule of heat production within the DH system could then be examined.

5.2.1.3 Heat Pricing

Potentially, the DH system could claim demand-related costs in the form of LCoH. It is assumed that the LCoH for surplus heat within the DH system could be zero (see Chapter 3.4.1). The DH systems cannot sell surplus heat to another DH system operator but only to consumers within their network. (Triebs et al., 2021) Therefore it is assumed that the DH system operators would be willing to provide their unused heat without an extra charge at times of surplus heat generation to the DAC application. This assumption is made based on the understanding that must-run generators would need to implement a cooling application, which would result in additional costs for the operators, as outlined in Chapter 3.4.1.1. These assumptions are considered to be plausible due to similar procedures in pricing surplus electricity in the power system stated by *Fraunhofer IEE et al.* (see Chapter 3.3.1). (Fraunhofer IEE et al., 2021)

However, the DH system operators would have to operate more cost-intense peak load heat generators at times of positive residual loads if a seasonal TES is missing. (Kicherer, 2020) The costs for the peak load generators would decide whether integration of a seasonal TES would be economically viable and consequently result in the construction of a seasonal TES. The seasonal TES would be a competitive customer for surplus heat.

The identified unused heat generator capacities are expected to be implemented in the DH system designs regardless of the DAC application. In this thesis, the unused heat generator capacities such as heat pumps supply heat at costs that only cover the demand-related costs. Operation-related costs such as maintenance would also be added to the LCoH provided by the HPs in a more detailed investigation. Charges for access to the heat grid and its utilization are also not considered.

5.2.1.4 River and Sewage Water Heat Pumps

In this thesis, the COP for the HPs is assumed to be 3.0 on average. Other research groups such as *Cames et al.* or *Fasihi et al.* use more optimistic COPs of 3.5 in their projections for the utilization of HPs for DAC plants. (Cames et al., 2021; Fasihi et al., 2019)

Kicherer et al. assume a COP of 3.0 for their DH system designs of Hamburg. (Kicherer et al., 2021) The research work of *Kicherer et al.* and the master thesis of *Kicherer* build the data basis for this thesis. Therefore, the COP of 3.0 is chosen according to *Kicherer et al.* to avoid inconsistencies in the integration of DAC plants in the DH system of Hamburg. However, this is assumed to be a conservative approach.

Further, an average COP of 3.0 is also a simplification. In a real-world process, the COP changes across the year. (Bach et al., 2016) This is due to changing inlet temperatures of the river and sewage water. (Kicherer et al., 2021) For a more accurate analysis, a dynamic COP would have to be applied to the time series of the HPs according to the inlet temperatures of the river and sewage water.

5.2.2 Power System of Germany

The reliability of the studies concerning power system designs in 2050 as well as the updated version aiming to advance the power system design to 2045, conducted by *Sterchele et al.* in 2020 and 2021, is presumed. These reports were developed in cooperation with the *Fraunhofer ISE*. They used the well-established *REMod* optimization tool. (Sterchele et al., 2020; Sterchele et al., 2021) However, the provided time series of the power system in 2045 is incomplete and only considers inflexible power producers and inflexible consumers (see Chapter 2.2.5). (Kaiser, 2022)

Competing flexible electricity consumers could not be considered in this thesis. In a holistic view, the dispatch schedule of the DAC plants must be adapted to timesteps when its operation is the best choice when other flexible operators act in the market. Other consumers could be prioritized when other products are needed urgently by society or industry. Since the time series only contains an hourly resolution, it must be assumed that the power system of Germany has multiple battery energy storage systems with a total storage capacity of 1 hour.

In this thesis, the electricity supply by the German power system for the DAC application in Hamburg is equipped with several assumptions and simplifications that would have to be recognized for the knowledge transfer of this theoretical work to a practical application. The overall balance of the power system is also not further investigated. The residual load curve is given for the total power system in Germany. Localization of the power production and consumption sites is not performed. For simpler handling, further grid losses for the electricity supply to Hamburg are neglected. An additional assumption is made that curtailments in the transmission and distribution grid do not occur. These are constraints that need to be considered if the research subject should be extended.

As the scope of the study by *Sterchele et al. in 2021* refers to the power system of Germany, it must be reduced to the scale of Hamburg. (Sterchele et al., 2021) As Hamburg is low in available space and high in energy consumption, Hamburg is not able to produce surplus electricity itself. It requires power supply from other federal states. An allocation of electricity shares based on a per-capita approach is performed. It is referred to Chapter 5.3.1 where the uncertainties of a per-capita approach are discussed in the context of deriving negative CO_2 emission targets for Hamburg from the proposed scale for Germany.

5.2.2.1 Electricity Price

A range of electricity prices is considered due to uncertainties in the price prediction until 2045. The price range depends on the developments of the power system concepts and ongoing political incentives such as industrial DR and DSM. Since the DAC application is assumed to be a flexibility service, it would be proposed to add a dynamic electricity price time series to the dynamic dispatch time series of the HPs and the DAC plants. However, this is not considered as a dynamic electricity price time series for 2045 is not available for this research work. An assignment of dynamic prices to the adapted residual load time series of the power system is not performed.

Data about the average wholesale price in 2045 are retrieved from the study by *Fraunhofer IEE et al.* in 2021. The average wholesale electricity price in the reform scenario is stated for 2050. (Fraunhofer IEE et al., 2021) The assumption is made that the price could occur in 2045 as the goal of GHG neutrality is brought forward 5 years to 2045. (*Federal Climate Change Act.* Federal Ministry of Justice, 2021)

The study by *Fraunhofer IEE et al.* has been published before the Russian invasion of Ukraine in 2022. Thus, no geopolitical events are considered in the prices of their study. The geopolitical developments concerning the Russian invasion of Ukraine resulted in a recently risen energy price which is not considered in any publicly available price development scenario projected until 2045. Therefore, the quality of data about electricity prices in 2045 is limited. It is recommended to redo the calculation of the scenarios when new studies about the power market design and new electricity prices are available.

The study of *Fraunhofer IEE et al.* calculates the average electricity price and includes the cost-intense positive residual peak loads. However, *Fraunhofer IEE et al.* state that lower LCoE than the average wholesale price can be achieved during periods of negative residual loads. (Fraunhofer IEE et al., 2021) If explicitly negative residual loads are used in the research subject of this thesis, lower LCoEs can be applied. Dynamic pricing of electricity and incentives for flexibility services support the assumption of an electricity price range. However, electricity cost projections will always face high uncertainties which are addressed by a price range in this thesis.

A LCoE of 0 €/MWh is stated by *Fraunhofer IEE et al.* as the minimum value that should be paid for electricity. (Fraunhofer IEE et al., 2021) A LCoE of 0 €/MWh and the same assumed price for surplus heat of 0 €/MWh would result in an undefined state of no prioritization of the heat supply in the optimization model of this thesis. A constraint for this state should be added in follow-up work. Therefore, the lowest electricity price is set to 1 €/MWh to achieve explicit prioritization.

5.2.2.1.1 Negative Electricity Prices

Negative LCoE must be prevented in the future for the economic survival of the RE operators according to *Fraunhofer IEE et al.*. (Fraunhofer IEE et al., 2021) However, balancing services are tendered for the LFC area of the TSOs and are financially compensated to provide their services. (*Energiewirtschaftsgesetz.* Federal Ministry for Economic Affairs and Climate Action, 2005) However, further research is necessary to ensure that the implementation of DAC plants as a balancing service would be technically and regulatory possible and financially viable.

5.3 Literature Research and Assumptions

In the following section, the findings of the literature research in the field of negative CO_2 emission demand and DAC technology are evaluated. Additionally made assumptions are also discussed.

5.3.1 Negative CO_2 Emission Demand in Germany

The investigated studies in Chapter 3.2 suggest a similar negative GHG emission goal forecast to achieve a climate-neutral Germany in 2045. Deviations occur in the composition of NETs. This results in uncertainties regarding the deployment rate of DAC plants.

Another limitation occurs as the negative GHG emission demand becomes larger after 2045 as net negative GHG emissions in Germany are targeted. (*Federal Climate Change Act.* Federal Ministry of Justice, 2021) For a comprehensive study, the negative emission demands for Germany must be considered across the lifetime of the project.

As the scope of the research subject focuses on Hamburg, a scale-down of Germany's negative GHG emission goal to the magnitude of Hamburg's size is required. Therefore, a per-capita approach is considered. However, future developments of the German population could deviate from the assumed variant 2 that is used and introduced in Chapter 3.2. Variant 2 considers a moderate birth rate, lifetime expectancy, and migration. (Federal Statistical Office Germany, 2019) Other variants from the 15th coordinated population projection can occur and thus induce deviations in the per-capita ratio of Hamburg and Germany. This results in another uncertainty. For a comprehensive review of the profitability of the DAC plants, the negative CO_2 emission demand in Hamburg would have to be adapted for each considered year. The population of both Hamburg and Germany will undergo annual changes. The investigation of deviating negative CO_2e emission goals and shares to be removed by Hamburg could be executed in further research.

In this thesis, gross negative emissions are only determined for the DAC plant and the process of isolating CO_2. Further CO_2e emissions will occur due to CO_2 transport and storage from Hamburg to a CCS site. These emissions would have to be added to the gross negative CO_2 emission demand in a comprehensive review. However, there are no released CCS sites in Germany, yet (see Chapter 2.4.4). Hence, the most favorable option is currently presumed to be the exportation of CO_2.

In future research, additional CO_2 emissions generated by transportation could be explored for exemplary CCS sites, such as those located in the North Sea. (Bui et al., 2018) The CO_2 leakage from pipelines, transport, and storage is mentioned to be between 11 to 52 % of the relative GHG emissions of a DACCS application. They occur due to the electricity consumption of CO_2 compression and recompression for transport and injection at the CCS site. However, they depend on the energy mix. (Terlouw et al., 2021)

In this thesis, the electricity supply by negative residual loads is assumed to have the same carbon footprint as surplus energy. Differences in the carbon footprint between excess electricity and normal power production by REs are stated by *Deutz & Bardow*. (Deutz and Bardow, 2021b) This assumption was made to simplify the CO_2e emissions from the energy mix provided for the DAC plants. The provided time series of the power system consists of inflexible power generators and consumers. No detailed information about the electricity mix is provided for the power system. (Kaiser, 2022) However, this assumption is not accurate and the additional CO_2 emissions by the energy mix would have to be considered for the gross CDR rate.

In a holistic view of the power system, the power system would contain flexible power providers and consumers such as battery energy storage systems or other flexible reserves e.g., electrolysis. (Kaiser, 2022) Thus, further research would be necessary to identify which timesteps would provide real surplus electricity and which have a higher carbon footprint according to the composition of power generator units in the power system. A further increase in the gross negative CO_2 emission demand would be expected in a more detailed study.

5.3.2 Techno-Economic Parameters of DAC Plants

Fasihi et al. researched available and published data and literature about DAC plants in 2019. In their paper, they assess financial and technical information. They examine different DAC plant capacities and different learning rates. The learning rates correlate with respective large-scale deployment rates of DAC technology up to 2050. (Fasihi et al., 2019)

In this thesis, a conservative approach for the energetic reduction rate developments and financial learning rates has been used for DAC plants (see Chapter 3.5.2.1). These are taken from *Fasihi et al.*. (Fasihi et al., 2019) Although *Fasihi et al.* adopted a conservative approach, the future developments of LT DAC technology in the global market remain uncertain. Current LT DAC plants are displayed with various energy requirements in literature due to the TRL of 6 to 7 (see Chapters 2.4, 2.4.1.1, and 3.5.3.1). Various development pathways of the DAC technology could be investigated in terms of deployment rates, energy demands, financial learning rates, OPEX, lifetime expectancies, and interest rates in future research and sensitivity analyses.

5.3.2.1 DAC Plants Spatial Requirements

The research topic is centered on harnessing negative residual loads, surplus energy, and unused power capacities from existing systems in the year 2045. Therefore, the space requirements of the energy producers for the DAC application are not considered. Only the dimensions of the actual DAC plants are considered. The assumed specific space demands of a large-scaled and small-scaled modular DAC plant are close to each other (see Chapter 3.5.1). It could be argued and assumed that the spatial requirements of a large-scale DAC plant could be lower since the plant size of this thesis is 13 times larger than the one stated by *Deutz & Bardow* for a large-scale plant (see Table 6).

5.3.2.2 Economic Data of DAC Plants

In this section, only economic data for the DAC technology itself are considered. Additional costs for constructing the CO_2 infrastructure, enabling CO_2 transport, and its storage are not examined in the scope of this thesis. Inflation until 2045 is also not considered. If CCS sites are allowed in Germany at a later point in time, the costs for the construction and operation of a CCS site and CO_2 infrastructure can be added for a comprehensive DACCS analysis.

The specific investment costs for different DAC plant scales were retrieved from *Fasihi et al.*. (Fasihi et al., 2019) However, the primary source for this data is a joint design study report by *Antecy B.V.* and *Shell Global Solutions International B.V.* about a methanol synthesis in 2015. (Roestenberg, 2015) Finding comparable financial data for DAC plants of different scales is difficult within the literature on DAC technology. As the report of *Roestenberg* would be classified as a white paper, further literature research is recommended to obtain a better quality of data.

The assumed initial DAC plant capacity of 1,440,000 tCO_2/a for a logarithmic extrapolation of the specific investment costs in the methodology (see Chapter 3.5.2.3) is larger than the DAC plant capacities computed by the optimization model. The lowest DAC plant capacity is optimized to 1,362,300 tCO_2/a in the scenarios with a 12-hour short-term TES capacity without a seasonal TES. The largest DAC plant capacity is achieved in the 1-hour short-term TES capacity scenarios with 1,415,100 tCO_2/a. (see Chapter 4.4.1) For higher accuracy, the extrapolation could be adjusted to the corresponding DAC plant capacities of the modeled scenarios. It is assumed that the lower DAC plant capacity in the scenarios would result in a slightly higher specific investment cost whose impact would be marginal due to a logarithmic extrapolation approach. The influence should be reviewed in future research.

5.4 Optimization Modeling

The accuracy of the optimization model depends on the quality of the input data and the formulation of the mathematical representation of the real-world problem. (Hart et al., 2017) The time resolution of the model is set to an hour per timestep. It is limited by the hourly resolution of the input time series of the power and heat systems (see Chapters 2.2.5 and 2.3.1).

To convert the real-world process into a mathematical representation, simplifications and assumptions are made in Chapter 3. This results in uncertainties. For example, the real-world process of a DAC plant depends on weather conditions. *Erans et al.* state that the relative humidity, ambient temperature, and CO_2 concentration influence the performance of DAC plants. (Erans et al., 2022) The team of the *CC4E* also researched the impact of ambient conditions on their demonstration DAC plant. (Zachariassen, 2023) However, these findings have not been addressed in this thesis and implemented in the optimization model. The time series of weather conditions and future CO_2 concentrations in Hamburg and their impacts on DAC plants could be added to the optimization model in future research for an improved representation of the DAC plants process.

The optimization model of this thesis does not consider the influences of competing flexibly operated technologies in the heat and power system. Additional actors might need to be incorporated and taken into account to formulate a more precise assessment of whether the selected timeslots for operating the DAC plants are optimal for the system. All available flexible consumers and generators participating in the system must be considered to achieve a balance of the residual load in the power system.

The optimization model *REMod* is more sophisticated and can investigate the balancing effects of multiple flexibly operated consumers and generators of the power system in parallel in the studies by *Sterchele et al.*. (Sterchele et al., 2020; Sterchele et al., 2021) The model is more complex and is based on a NLP optimization. (Fraunhofer Institute for Solar Energy Systems ISE, 2023) However, necessary resources such as the computation time increase with the rising complexity of the optimization problem. (Hart et al., 2017)

The optimization model of this thesis does not include all data that would be required for a holistic investigation of whether the potential of the flexibly operated DAC plant is feasible across the lifetime of the project. Nevertheless, the results of this thesis show that the proposed CDR rate in a system-serving operation mode of the DAC plant can be achieved in 2045. The $LCoCO_2$ might vary, but an implementation of a DAC plant on an open field is considered financially promising.

5.4.1 Assumptions for the Objective Modeling

Due to the incomplete information about the economic parameters of DAC plants in literature, the capital-related costs are simplified and do not take reinvestment costs and the residual value of the plant at the end of its lifetime into consideration. These parameters would be required for a comprehensive review of the economics of a plant by *VDI*. (Verein Deutscher Ingenieure e.V., 2012) The costs for the thermal energy supply provided by the DH system and the HPs are also simplified and do not contain taxes, grid charges, and other levies that need to be identified in future investigations.

5.4.2 Evaluation of Optimization Tool

During the modeling process, efforts have been made to ensure the plausibility of the obtained results. The FLOHs of the HPs are within the range of the expected values for a real-world implementation stated by the *Authority for Environment and Energy* (see Chapters 3.4.1.2 and 5.6.2). (Authority for Environment and Energy, 2019)

The FLOHs of the DAC plants and the correlated $LCoCO_2$s are also in the expected range. However, the results of $LCoCO_2$s of this thesis are difficult to compare with literature due to deviating assumptions for energy demands, demand-related costs, carbon footprints of the energy mix, net and gross negative CO_2 emission ratios, investment costs, and FLOHs. As most of the techno-economic characteristics are orientated in the study by *Fasihi et al.*, the results are compared with their study.

Fasihi et al. state $LCoCO_2$s of 67 and 56 €/tCO_2 for 2040 and 2050 when FLOHs of 4,000 h/a are achieved. For the expressed $LCoCO_2$ values, they assume using waste heat free of charge. Specific investment costs of 237 and 199 €/(tCO_2/a) are mentioned for 2040 and 2050, respectively. LCoE of 21 and 18 €/MWh are assumed. (Fasihi et al., 2019)

The best-case scenario of this thesis is represented by the scenario *OF-stTES12h-wo/SeasTES-elLower*. The $LCoCO_2$ is solved to be 66.32 €/tCO_2 (see Chapter 4.6). The FLOHs of the DAC plant are stated to be 3,120 h/a (see Chapter 4.4.1). The scenario is based on a LCoE of 1 €/MWh and specific investment costs of 189 €/(tCO_2/a). The amount of specific energy demand in this thesis is interpolated for the year 2045 of the energy consumptions stated by *Fasihi et al.* in 2040 and 2050 (see Chapter 3.5.3.1).

Despite lower LCoE and specific investment costs, the $LCoCO_2$ is in a similar range to the $LCoCO_2$ stated by *Fasihi et al.* for 2040. This can be explained by the lower FLOHs of the DAC application in this thesis. The $LCoCO_2$s of the optimized scenarios are therefore assumed to be plausible. This supports the assumption that the optimization model has been appropriately programmed.

A validation of the model would be conducted by comparing the computed results with measured data from the past. However, this is not possible as the developed optimization problem does not exist in such a form in real-life to validate the simulation. The used data and underlying assumptions are purely theoretical, lacking any reference to historical data for validation. This represents a weakness of both the model and the thesis which needs careful consideration.

However, planning, scheduling, and solving scenarios with a LP optimization is appreciated as an accessible, low-cost, and effective method by literature as input data and time series can be easily exchanged. (Hart et al., 2017; Kurucz et al., 1996) The optimization model of this thesis can be further extended. It may be a starting point to examine other parameters of DAC plants, time series, or scenarios in future research.

5.5 Spatial Analysis in Hamburg

In this section, the methodology and constraints of the spatial analysis are evaluated. In the spatial analysis for DAC plants in Hamburg, only the integration of the actual DAC plant units is considered. Challenges, costs, and workload differences for installing DAC plant modules on rooftops compared to the construction on an open field are not considered in detail. In general, costs for construction are assumed to be integrated into the specific investment costs depending on the DAC plant sizes (see Chapter 3.5.2.3).

Rent or purchasing prices for thousands of rooftops or one open space are expected to vary as they need to be negotiated with the owners of the facilities. This would have to be taken into account in future investigations of individual scenarios. Further, the different DAC plant scales are attributed to different specific space demands which results in different space demands at the same DAC plant capacity. The space demand differences are outlined in the results (see Chapter 4.5). However, the monetary impact is not elaborated in the scope of this thesis.

The compatibility and viability of the construction of a CO_2 pipeline infrastructure in the city of Hamburg are also not part of the scope of the thesis. This needs to be addressed in a more comprehensive review. Additionally, the debate about the public acceptance of DAC plants in Hamburg would have to be addressed.

5.5.1 DAC Plants on Open Fields

Open spaces for DAC plants have been identified in Chapter 4.5.1. A detailed investigation would further include the determination of competitive business cases on those sites as well as ownership regulations. Additionally, rent or purchasing prices for the area would have to be identified.

The concentration of a DAC plant in a single location is anticipated to facilitate access to the site. This would result in lower construction and maintenance costs compared to the construction of thousands of DAC plant units on individual rooftops distributed along the DH grid of Hamburg. However, these advantages are not monetarily considered in the optimization model except for the specific investment cost differences of the considered DAC plant scales. A more detailed breakdown of the costs would be necessary for follow-up work.

DAC plant modules could also be piled up to save further spatial resources if they are delivered in containers. This would result in the same total space demand computed for the DAC plants on flat rooftops and probably in an increase in the specific investment costs.

5.5.2 DAC Plants on Flat Rooftops

Buildings are identified that might fit geometrically for a DAC module stored in a container. The necessary suitable area of the rooftops is extended to be larger than 60 m² to enable maintenance work. The result of the flat rooftop analysis is the number of flat roofs that fit at least one DAC module. A lot of the identified buildings are large enough to potentially fit more than one DAC module on it (see Figure 9). The number of DAC plants in the size of a container that could be installed on rooftops could therefore be larger than the number of flat rooftops. However, it is assumed that a pile-up of containers would not be possible on flat rooftops due to static issues.

Challenges and costs occurring during the actual construction and installation are not detected and considered by the used method for the spatial analysis. An individual test of the suitability and structural analysis is recommended for each rooftop to be certain of the compatibility with DAC plant modules in a container. A safe work environment and installation on the building must be ensured. The number of qualified flat rooftops is expected to decrease further when more detailed investigations would be pursued as structural restrictions are likely to occur. The compatibility and viability of the construction of a largely distributed CO_2 pipeline infrastructure are not considered in this thesis. These are aspects that must be considered in a holistic approach if considerations of the implementation of DAC plants in Hamburg should be intensified at a later point in time.

5.6 Evaluation of Scenario Results

The influences of the parameters on the decision variables and other outputs have been presented in Chapter 4. In this section, the results are evaluated and further discussed in terms of plausibility and reliability. The energy flows of the power and heat system are highlighted. Afterward, the FLOHs of the HPs in the different DH system scenarios are reflected in the context of the technically feasible range. The plausibility, reliability, and requirements for the detected demand-related costs are discussed. Further, the DAC plant designs, capacities, and respective $LCoCO_2$s of the scenarios are discussed and evaluated according to the assumptions made in the scenario developments. It is examined whether individual scenarios are more promising or recommendable due to the made assumptions and obtained results.

5.6.1 Energy Flows of the Power and Heat System

The electricity consumption of the DAC application is estimated to range from 1.577 to 2.303 % of the assumed negative residual loads of the power system allocated for Hamburg (see Chapter 4.3). Whether a higher or lower negative residual load consumption by the DAC application is beneficial for the power system's stability, cannot be answered in the context of this thesis. Other flexible generators and consumers would have to be taken into account in a comprehensive review of the power system.

If all power producers and consumers would be considered, a more advanced optimization model could generate a stabilized residual load curve of the total power system as it is accomplished by *Sterchele et al.* in 2020 with the help of *REMod*. (Sterchele et al., 2020) However, the DAC application is capable to achieve the proposed CDR rate for Hamburg consuming solely electricity at times of negative residual load occurrences in the power system.

In most sub-scenarios that include a 1-hour short-term TES capacity without a seasonal TES, the surplus heat consumption achieved 64.303 % from a maximum available surplus heat of the DH system of 66.995 % in the respective periods. A similar result is presented by most sub-scenarios considering a 12-hour short-term TES capacity without a seasonal TES. These achieve 65.201 % of the maximum available 66.259 % (see Figure 14).

In both mentioned DH system scenarios, this is assumed to have a significant effect on the stabilization of the DH system. All consumers and producers are already implemented in the considerations of *Kicherer* and *Kicherer et al.* except for a seasonal TES and the DAC application. Nevertheless, it is not feasible for the DAC application to utilize all the surplus peak load heat generation. This would require an increased DAC plant capacity that would not be cost-effective. However, it is assumed that further surplus heat from unused periods would be consumed by the DAC application if electricity would be constantly available.

The heat demand of the DAC plants in the scenarios is determined to be 579,375.378 MWh/a (see Chapter 4.1). The DH system designs of *Kicherer* and *Kicherer et al.* provide a maximum surplus heat of -415,916.404 MWh in 2045 (see Chapter 2.3.1). Thus, the total heat demand for the flexibly driven DAC plants cannot be covered by the surplus heat of the DH system alone, even if all surplus heat were accessible during potential DAC plant operation periods. Therefore, the investigation of additional heat sources within the DH system was a necessary step in the methodology to cover the heat demand of the DAC application for the proposed CDR rate.

5.6.2 Full-Load Operation Hours of Heat Pumps

In 2019, plans for the DH system of Hamburg in 2025 intended a range between 3,300 and 5,300 h/a FLOHs for a sewage water HP. (Authority for Environment and Energy, 2019) It is assumed that 5,300 h/a are the maximum FLOHs that can be reached by sewage water HPs and river HPs on a technical level. The already used FLOHs of the river and sewage water HP in the considered DH system scenarios have been determined to be 1,875 h/a and 4,513 h/a, respectively (see Chapter 3.4.1.2).

Due to the sewage water HP operating at a higher full load operation rate compared to the river HP, an additional compensation fee is included. The FLOHs of the river HP are increased, and the additional utilization of the sewage water HP is reduced to a minimum. The condoned impact of the compensation fee on the $LCoCO_2$ has been limited to less than 0.01 €/tCO_2. The practicability of such a measure must be investigated in future research.

The results state that the maximum FLOHs of the river HP occur in the scenario *FR-stTES1h-wo/SeasTES-elOptimum* at 4,570 h/a (see Chapter 4.3.1). The maximum FLOHs of the sewage water HP are reached in the scenarios of the DH system that consider a seasonal TES at 4,733 h/a (see Chapter 4.3.3). These values are the sum of the utilization in the DH system and the DAC application. Both maximum FLOHs of the respective HPs are below the maximum value of 5,300 h/a which is assumed to be technically feasible. Thus, the HPs do not exceed the maximum feasible FLOHs in any scenario of this thesis. The utilization of the HPs is therefore in a plausible and technically feasible range.

However, the HPs may be more involved in the heat supply for the DH system in subsequent years as weather conditions and heat load demands will differ. These cases would have to be examined for a comprehensive investigation if the HPs heat supply will be sufficient throughout the lifetime of the DAC plants.

In DH system scenarios where short-term TES capacity ranges from 1 to 12 hours without seasonal TES and with a positive levelized cost of energy (LCoE), the river HP is utilized for a total of 3262 and 3249 h/a, respectively (see Chapter 4.3.1 and 4.3.2). These scenarios allow for a greater margin to adjust for variations in FLOHs of the HPs in subsequent periods.

5.6.3 Demand-Related Costs

LCoEs ranging from 1 to 81 €/MWh are regarded as the best- and worst-case scenarios for the demand-related costs associated with a flexibly driven DAC application functioning as an industrial DR (see Chapter 3.3.1). Feasible scenarios are determined by optimizing the LCoEs to fall within the range of this electricity price range (see Chapter 5.2.2.1). If the optimized LCoE is solved to be a negative value, another business case must be considered for the DAC application. In these cases, DAC plants would have to operate as a balancing service. However, this business case needs further elaboration. In the following subsections, the reliability of the scenarios with negative energy prices is discussed.

5.6.3.1 Negative LCoE Scenarios

Negative LCoEs are determined in the scenarios *FR-stTES1h-wo/SeasTES-elOptimum*, *FR-stTES12h-wo/SeasTES-elOptimum*, and *FR-stTES12h-w/SeasTES-elOptimum*. These would be necessary to bring the $LCoCO_2$ down below 100 €/tCO_2 if only this parameter is allowed to be changed. However, whether the compensation fees for the balancing service could reach prices down to -124 €/MWh (see Chapter 4.2.1) has to be examined in future research.

Additionally, the DAC application in this thesis is set to have a process cycle time of 1 hour due to the resolution time of the time series of the heat and power system (see Chapter 3.5.3.3). The necessary runtime for a process cycle may therefore be too long for balancing service. (50Hertz Transmission GmbH et al., 2023) However, the compatibility and requirements for the registration of DAC plants as a balancing service in 2045 could not be examined in detail in this thesis. Hence, the realizability of this business case remains uncertain due to the lack of information for the time being. Therefore, the scenarios *FR-stTES1h-wo/SeasTES-elOptimum*, *FR-stTES12h-wo/SeasTES-elOptimum*, and *FR-stTES12h-w/SeasTES-elOptimum* are impracticable in this thesis.

However, current LT DAC plants can reach a process cycle time of 30 minutes. (Fasihi et al., 2019) Other materials have also been tested and demonstrated to achieve process cycle times of less than 7 minutes. (Azarabadi and Lackner, 2019) A follow-up study could therefore investigate the viability of DAC plants with the respective techno-economic characteristics as a balancing service.

5.6.3.2 Negative LCoH Scenarios

The scenarios *FR-stTES1h-wo/SeasTES-thOptimum* and *FR-stTES12h-wo/SeasTES-thOptimum* require a negative LCoH to attain a $LCoCO_2$ below the suggested reference (see Chapter 4.2.1). It remains uncertain how the price for surplus heat in the DH system of Hamburg in 2045 will be determined. However, negative LCoH would be economically infeasible for the DH system operators. Additionally, the increased heat demand within the DH system in the winter season would have to be compensated by additional heat generation that must be paid for at periods when positive residual heat loads occur. (Kicherer, 2020) In these scenarios, the DH system operators would have to pay twice for residual loads in case of surplus heat and lack of heat. It is assumed that the DH system operators would prioritize the implementation of a seasonal TES system in the scenarios with a negative LCoH which would result in the DH system design that includes a seasonal TES. Therefore, the scenarios *FR-stTES1h-wo/SeasTES-thOptimum* and *FR-stTES12h-wo/SeasTES-thOptimum* are classified to be less likely to occur in the future. They are therefore not further considered to be a realistic option in the context of the research subject of this thesis.

5.6.4 DAC Plants on Open Spaces vs. Flat Rooftops

In this section, the results of the different DAC plant designs of the scenarios are discussed and evaluated. The area consumption of a DAC plant on an open field is equal to 0.106, 0.107, and 0.110 km² (see Chapter 4.4.3). The space availability in each of the three proposed areas would be sufficient (see Figure 17). Further investigations would be necessary to determine the best qualified open space next to other recommended investigations listed in Chapters 5.5 and 5.5.1.

In the spatial analysis of flat rooftops for DAC plants, 22,785 buildings are identified to be geometrically suitable (see Chapter 4.5.2). The 22,875 flat rooftops should be large enough, to enable maintenance work on the DAC plant modules due to the size of at least 60 m² per suitable building. As the buildings are filtered to be at least 60 m², it is also possible that on several buildings more than one DAC plant module could be installed. It must be further investigated if the respective buildings' static is stable enough to carry a DAC plant module. However, this is considered a promising result as the maximum number of DAC plant modules in the flat rooftop scenarios is determined to be 4,717. Further constraints of the analysis are listed in Chapter 5.5.2.

Both spatial analyses display technically achievable results. However, access to one open field site is expected to be less challenging than access and construction of thousands of DAC plants across Hamburg. The implementation of DAC plants in an open space would result in less effort and lower costs in construction and maintenance. Compared to scenarios involving the distribution of DAC plant units on individual flat rooftops throughout the DH grid of Hamburg, the construction of a CO_2 pipeline network would be relatively simpler. These aspects are not considered in detail in this thesis. However, they affect the choice of recommendation if scenarios should be further investigated in follow-up research.

5.6.5 Economic Feasibility

In this section, the achieved $LCoCO_2$s of the scenarios are evaluated in light of the proposed reference $LCoCO_2$. Research groups expect CDR by DAC technology to become economically feasible at $LCoCO_2$ below 100 €/tCO_2. (Lackner and Azarabadi, 2021; Ozkan et al., 2022) The scenarios in this potential analysis must reach the proposed $LCoCO_2$ to be considered as an economically feasible option.

The $LCoCO_2$ exceeds the required reference value in scenarios that involve multiple DAC plants on flat rooftops with a positive LCoE (see Chapter 4.6). The results of the scenarios are interpreted to be technically and physically possible (see Chapters 5.6.1 to 5.6.4). However, they are not considered to be feasible in terms of economics.

The scenarios *FR-stTES1h-wo/SeasTES-thOptimum* and *FR-stTES12h-wo/SeasTES-thOptimum* can achieve a $LCoCO_2$ below 100 €/tCO_2. Nonetheless, they are presumed to be less likely to be technically realized due to the prioritization of an implementation of a seasonal TES in the event of negative LCoH (see Chapter 5.6.3.2).

A negative LCoE in the scenarios *FR-stTES1h-wo/SeasTES-elOptimum*, *FR-stTES12h-wo/SeasTES-elOptimum*, and *FR-stTES12h-w/SeasTES-elOptimum* would help to achieve an economically feasible $LCoCO_2$ (see Chapter 4.6). However, a negative LCoE is presumed in these scenarios. From the current perspective, it is uncertain whether DAC plants could operate as a balancing service to achieve a negative LCoE and thus reduce the $LCoCO_2$ below 100 €/tCO_2 (see Chapter 5.6.3.1).

The $LCoCO_2$ of the scenarios *OF-stTES1h-wo/SeasTES-elUpper* and *OF-stTES12h-w/SeasTES-elUpper* are determined with the maximum LCoE of 81 €/MWh. They exceed the reference $LCoCO_2$ (see Chapter 4.6). However, the scenario *OF-stTES1h-wo/SeasTES-elUpper* comes close to the threshold of viability with 102.39 €/tCO_2. The scenario *OF-stTES12h-wo/SeasTES-elUpper* already achieves a $LCoCO_2$ below 100 €/tCO_2 despite the LCoE being set to the upper limit of the electricity price range.

The $LCoCO_2$s of the scenarios *OF-stTES1h-wo/SeasTES-elLower*, *OF-stTES12h-wo/SeasTES-elLower*, and *OF-stTES12h-w/SeasTES-elLower* are all solved to be below 69 €/tCO_2 (see Chapter 4.6). Consequently, these scenarios would be economically feasible. However, the LCoE of 1 €/MWh is the most optimistic assumption of the positive electricity price range.

The maximum allowed LCoE for the DAC application positioned on an open field has been determined in each DH system design in Chapter 4.2.1. The $LCoCO_2$s of the scenarios *OF-stTES1h-wo/SeasTES-elOptimum*, *OF-stTES12h-wo/SeasTES-elOptimum*, and *OF-stTES12h-w/SeasTES-elOptimum* achieve $LCoCO_2$s below 100 €/tCO_2 using LCoEs of 55, 75, and 81 €/MWh, respectively. The optimized LCoEs are assumed to be realistic as they are within the positive electricity price range. Additionally, the LCoEs are closer to the worst-case than to the best-case limit of the positive electricity price range (see Chapter 5.6.3). These scenarios would be economically viable.

6 Conclusion

All scenarios with DAC plants on flat rooftops and open fields are interpreted to be technically feasible, regardless of the DH system design of Hamburg in 2045. The results show that DAC plants could be implemented in deviating DH system designs on a technical level. The proposed CDR rate for Hamburg in 2045 is achievable in the flexibly driven operation mode of DAC plants. A DAC plant capacity between 1,362,300 and 1,415,100 tCO_2/a would be necessary for different DH system designs to isolate CO_2 using surplus heat and unused heat generator capacities. The DAC application would achieve FLOHs between 3,120 and approximately 3,000 h in 2045, respectively.

The investigated DAC applications can consume significant shares of the available surplus heat of the DH system designs of Hamburg when it is provided free of charge. Unused heat generation capacities of a sewage water HP and river HP can be used to provide thermal energy for the DAC application without overload. Additionally, the DAC application and HPs are solely operated in periods of negative residual loads in the power system. It is possible to use the additional infrastructural effort of the DH system of Hamburg for the proposed DAC application.

Construction sites for the DAC application have been identified on open spaces and flat rooftops of buildings near the DH grid. The physical implementation is considered to be possible with some limitations that require further research demand. However, extra effort would be required to identify buildings with mandatory static stability. Further research would also be required to ensure safe and cost-effective construction. The installation process itself of thousands of DAC modules on roofs could also be a significant obstacle. Construction costs for a more sophisticated CO_2 transport network in Hamburg have not been considered in detail but are also expected to be substantially higher compared to establishing a single access point for a large-scale DAC plant on an open field.

The potential for flexibly operated DAC plants on flat rooftops is further constrained by anticipated costs that exceed the economic feasibility range mentioned in the literature, which is below 100 €/tCO_2. $LCoCO_2$s between 168.48 to 218.80 €/tCO_2 have been determined for flexibly operated DAC plants on flat rooftops with deviating LCoEs and DH system designs. Additional challenges such as the implementation of a more sophisticated CO_2 pipeline network have not been monetarily considered, yet. For this DAC plant deployment, the optimum demand-related costs would have to be negative to achieve a $LCoCO_2$ in the proposed cost range. Whether the DAC technology could be implemented as a balancing service for a negative LCoE remains uncertain. Using negative LCoH for the surplus heat instead to bring down the $LCoCO_2$ is presumed to be improbable. A negative LCoH would be economically infeasible for the DH system operators. The prioritization would likely lean towards a seasonal TES.

A large-scale DAC plant on an open field with lower specific investment costs is determined to be able to operate economically feasible at FLOHs between 3,004 and 3,120 h in 2045. $LCoCO_2$ between 66.32 and 115.75 €/tCO_2 have been simulated in dependency on the demand-related costs and the DH system design of Hamburg in 2045. The economic efficiency of the DAC application depends on the achievable LCoE. The required optimum LCoE depends on the TES capacities that will be integrated into the DH system of Hamburg in 2045. If the LCoE can be reduced from the upper limit of 81 to 55 €/MWh, the DAC application can operate viable regardless of the proposed DH system design. Consequently, the DAC application could continue to operate viable even if a seasonal TES would be implemented subsequently. In a DH system with a short-term TES capacity of 12 hours without a seasonal TES, the maximum LCoE could be as high as the considered average wholesale electricity

price of 81 €/MWh which would make the DAC application independent from political incentives such as industrial DR or dynamic pricing.

The significant differences in the total investment costs and in the $LCoCO_2$s of the two DAC plant designs as well as the expected challenges of a physical implementation support the proposal that further investigations of an implementation of DAC plants in Hamburg should be pursued on open spaces. In conclusion, the potential of multiple DAC plant positioned on flat rooftops is considered to be technically feasible, but economically not viable.

The findings of this thesis show that an implementation of a flexibly operated DAC plant in the DH system of Hamburg can be technically, physically, and economically feasible in 2045. A flexibly driven large-scale DAC plant with lower FLOHs on an open field has an achievable economic break-even point if the demand-related costs can be partially compensated through political incentives like industrial DR. The DAC application can operate viably using solely unused heat generator capacities if a seasonal TES is implemented. If the DH system is designed to store heat in a 12-hour short-term TES capacity without a seasonal TES, compensation for the demand-related electricity costs would not be required.

6.1 Outlook

This thesis investigated the technical, physical, and financial feasibility of a flexibly driven DAC plant in 2045. For a comprehensive review, the economic feasibility of the DAC plant project could be investigated if time series data for the DH system and power system are available throughout its lifetime. The examination of surplus heat availability and the identification of sufficient unused flexible heat generator capacities after 2045 would be necessary. Next to these investigations, public acceptance of DAC plants in Hamburg would also require careful consideration.

The 12-hour short-term TES capacity is expected to be the most cost-intense scenario for the DH system operators due to the large storage capacity which has not been further considered in this thesis. Therefore, the DH system designs of the scenarios with a 2- and 6-hour short-term TES capacity should be considered. For the scenario considering a seasonal TES, a detailed investigation should be initiated to identify and predict periods when it is suitable to store heat in a seasonal TES and when to provide heat for the DAC application. The remaining negative residual heat loads of 90 GWh minus the losses could then be added as surplus heat in the DH system scenarios that include a seasonal TES.

The efficiency of the DAC application further depends on relative humidity, CO_2 concentration, and temperature in a real-life process. The influence of weather conditions could be examined and implemented in the optimization model as recent investigations have been pursued by the *CC4E*. The dynamic dispatch of the HPs and DAC plants should be reconsidered with dynamic electricity pricing. A dynamic COP of the used HPs could be investigated to achieve a more detailed representation. Further, the practicability of implementing a compensation fee to reduce the FLOHs of the sewage water HP compared to the river HP must be examined in further research.

Further research could be executed to offset the $LCoCO_2$ by DAC plants and form additional assets. For example, LT DAC applications produce pure water as a byproduct. The asset of the byproduct is not further considered in this thesis although it could be sold to decrease the $LCoCO_2$. The implementation of flexibly operated DAC plants in a business case as a balancing service would need further research as specific regulations and technical requirements must be fulfilled. In this context, the amount of the payment for a balancing service would have to be determined.

Additionally, costs for construction and integration of the required CO_2 infrastructure should be considered in future investigations. The identification of qualified CCS sites is also required to examine the costs for the CO_2 network. The distance from Hamburg to the CCS site is important for the additional cost estimation and energy demand of CO_2 transport. In this context, the carbon footprint of the energy mix should be considered in more detail. When CCS sites are identified in Germany at a later point in time, the costs, energy demands, and carbon footprint for a DACCS application could be reconsidered and added for a comprehensive analysis. Further research is necessary to identify area acquisition prices for the DAC application sites in Hamburg. This could be done by extending the optimization model.

An economic viability gap is detected for the DAC application constructed on flat rooftops. Further investigations are recommended to find a break-even point for a profitable $LCoCO_2$ by parameter adjustment in these scenarios. Deviating LCoEs, specific investment costs, and space demands have been considered in this thesis. A sensitivity analysis of other input parameters could enhance the understanding of the effect of the input parameters on the resulting decision variables and objective. Parameters such as the interest rate on the CAPEX, OPEX, lifetime of a DAC plant project, heat and electricity demands of the DAC plants, CDR rates, and deviating COPs for the HPs could be examined in follow-up work.

References

50Hertz Transmission GmbH, Amprion GmbH, TenneT TSO GmbH and TransnetBW GmbH (2023) *www.regelleistung.net > General info > What is control energy? (Prequalification)* [Online]. Available at https://www.regelleistung.net/en-us/General-info/What-is-control-energy-Prequalification (Accessed 2 May 2023).

Authority for Environment and Energy (2019) *Wärmewende & Energiepark Hafen* [Online], Hamburg. Available at https://www.hamburg.de/contentblob/12957152/7374b07373873dce6dd7af51f012383c/data/d-waermewende.pdf (Accessed 22 June 2023).

Azarabadi, H. and Lackner, K. S. (2019) 'A sorbent-focused techno-economic analysis of direct air capture', *Applied Energy*, vol. 250, pp. 959–975.

Bach, B., Werling, J., Ommen, T., Münster, M., Morales, J. M. and Elmegaard, B. (2016) 'Integration of large-scale heat pumps in the district heating systems of Greater Copenhagen', *Energy*, vol. 107, pp. 321–334.

Bayrische Vermessungsverwaltung (2018) *Kundeninformation LoD2 Gebäudemodelle: Stand 3/2018* [Online]. Available at https://www.ldbv.bayern.de/file/pdf/6723/Kundeninformation_LoD2.pdf (Accessed 10 May 2023).

Beuttler, C., Charles, L. and Wurzbacher, J. (2019) 'The Role of Direct Air Capture in Mitigation of Anthropogenic Greenhouse Gas Emissions', *Frontiers in Climate*, vol. 1.

Block, S. (2022) *Auslegung, Analyse und Bewertung von Direct Air Capture (DAC)-Anlagen zur Nutzung für Power-to-X-Prozesse und zur Erzielung "negativer Emissionen" in Deutschland* [Online], Wuppertal, Wuppertal Institut für Klima Umwelt Energie gGmbH. Available at https://epub.wupperinst.org/files/7944/WSA25_Block.pdf.

Boldrini, A., Jiménez Navarro, J. P., Crijns-Graus, W. and van den Broek, M. A. (2022) 'The role of district heating systems to provide balancing services in the European Union', *Renewable and Sustainable Energy Reviews*, vol. 154, p. 111853.

Buffa, S., Cozzini, M., D'Antoni, M., Baratieri, M. and Fedrizzi, R. (2019) '5th generation district heating and cooling systems: A review of existing cases in Europe', *Renewable and Sustainable Energy Reviews*, vol. 104, pp. 504–522.

Bui, M., Adjiman, C. S., Bardow, A., Anthony, E. J., Boston, A., Brown, S., Fennell, P. S., Fuss, S., Galindo, A., Hackett, L. A., Hallett, J. P., Herzog, H. J., Jackson, G., Kemper, J., Krevor, S., Maitland, G. C., Matuszewski, M., Metcalfe, I. S., Petit, C., Puxty, G., Reimer, J., Reiner, D. M., Rubin, E. S., Scott, S. A., Shah, N., Smit, B., Trusler, J. P. M., Webley, P., Wilcox, J. and Mac Dowell, N. (2018) 'Carbon capture and storage (CCS): the way forward', *Energy & Environmental Science*, vol. 11, no. 5, pp. 1062–1176 [Online]. Available at https://pubs.rsc.org/en/content/articlelanding/2018/ee/c7ee02342a.

Bürger, V., Hesse, T., Köhler, B., Palzer, A. and Engelmann, P. (2019) 'German Energiewende—different visions for a (nearly) climate neutral building sector in 2050', *Energy Efficiency*, no. 12, pp. 73–87.

Cames, M., Chaudry, S., Göckeler, K., Kasten, P. and Kurth, S. (2021) *E-fuels versus DACCS: Total costs of electro-fuels and direct air capture and carbon storage while taking into account direct and upstream emissions and environmental risks,* Öko-Institut e.V. [Online]. Available at https://www.transportenvironment.org/wp-content/uploads/2021/08/2021_08_TE_study_efuels_DACCS.pdf (Accessed 10 February 2023).

Castro-Muñoz, R., Zamidi Ahmad, M., Malankowska, M. and Coronas, J. (2022) 'A new relevant membrane application: CO2 direct air capture (DAC)', *Chemical Engineering Journal*, vol. 446, p. 137047.

Chen, S., Gong, F., Zhang, M., Yuan, J., Liao, S., Chen, H., Li, D., Tian, S. and Hu, X. (2021) 'Planning and Scheduling for Industrial Demand-Side Management: State of the Art, Opportunities and Challenges under Integration of Energy Internet and Industrial Internet', *Sustainability*, no. 13.

Climeworks AG (2022a) *Climeworks takes another major step on its road to building gigaton DAC capacity* [Online]. Available at https://climeworks.com/news/climeworks-announces-groundbreaking-on-mammoth (Accessed 21 April 2023).

Climeworks AG (2022b) *Climeworks completes the commercial operations of its 1st gen technology in Hinwil, Switzerland, the world's first commercial DAC facility* [Online]. Available at https://climeworks.com/news/climeworks-completes-commercial-operations-in-hinwil (Accessed 21 April 2023).

DENA (2021a) *dena-Leitstudie Aufbruch Klimaneutralität: Abschlussbericht* [Online]. Available at https://www.dena.de/fileadmin/dena/Publikationen/PDFs/2021/Abschlussbericht_dena-Leitstudie_Aufbruch_Klimaneutralitaet.pdf (Accessed 8 June 2023).

DENA (2021b) *Tech for Net Zero Allianz: Klimaneutralität 2045 – Neue Technologien für Deutschland"* [Online]. Available at https://www.dena.de/fileadmin/dena/Publikationen/PDFs/2021/TfNZ_Klimaneutralitaet_2045_-_Neue_Technologien_fuer_Deutschland.pdf (Accessed 19 July 2023).

Deutscher Wetterdienst (2023) *Wetter und Klima - Deutscher Wetterdienst - Leistungen - Testreferenzjahre (TRY)* [Online]. Available at https://www.dwd.de/DE/leistungen/testreferenzjahre/testreferenzjahre.html (Accessed 12 July 2023).

Deutz, S. and Bardow, A. (2021a) 'Life-cycle assessment of an industrial direct air capture process based on temperature–vacuum swing adsorption', *Nature Energy*, vol. 6, no. 2, pp. 203–213.

Deutz, S. and Bardow, A. (2021b) 'Supplementary information: Life-cycle assessment of an industrial direct air capture process based on temperature- vacuum swing adsorption', *Nature Energy*, vol. 6, no. 2, pp. 203–213.

Eid, C., Codani, P., Perez, Y., Reneses, J. and Hakvoort, R. (2016) 'Managing electric flexibility from Distributed Energy Resources: A review of incentives for market design', *Renewable and Sustainable Energy Reviews*, vol. 64, pp. 237–247.

Erans, M., Sanz-Pérez, E. S., Hanak, D. P., Clulow, Z., Reiner, D. M. and Mutch, G. A. (2022) 'Direct air capture: process technology, techno-economic and socio-political challenges', *Energy & Environmental Science*, vol. 15, no. 4, pp. 1360–1405.

Fasihi, M., Efimova, O. and Breyer, C. (2019) 'Techno-economic assessment of CO2 direct air capture plants', *Journal of Cleaner Production*, vol. 224, pp. 957–980.

Federal Agency for Cartography and Geodesy (2023) *Dokumentation Dokumentation - 3D Gebäudemodell Deutschland - LoD2-DE* [Online]. Available at https://sg.geodatenzentrum.de/web_public/gdz/dokumentation/deu/LoD2-DE.pdf (Accessed 20 April 2023).

Federal Ministry for Economic Affairs and Climate Action (2005) *Energiewirtschaftsgesetz* (EnWG).

Federal Ministry for Economic Affairs and Climate Action (2023) *Federal cabinet adopts evaluation report on the Carbon Dioxide Storage Act* [Online], BMWI. Available at https://www.bmwk.de/Redaktion/EN/Pressemitteilungen/2022/12/20221221-federal-cabinet-adopts-evaluation-report-on-the-carbon-dioxide-storage-act.html (Accessed 26 April 2023).

Federal Ministry of Justice (2021) *Federal Climate Change Act*.

Federal Statistical Office Germany (2019) *Künftige Bevölkerungsentwicklung in Deutschland: 15. koordinierte Bevölkerungsvorausberechnung - Ergebnisse für Deutschland und Bundesländer* [Online]. Available at https://www.destatis.de/DE/Themen/Gesellschaft-Umwelt/Bevoelkerung/Bevoelkerungsvorausberechnung/_inhalt.html#_iriy438zx (Accessed 5 May 2023).

Fraunhofer IEE, Fraunhofer ISE and Becker Büttner Held (2021) *Neues Strommarktdesign: Neues Strommarktdesign für die Integration fluktuierender Erneuerbarer Energien* [Online]. Available at https://www.klimaneutrales-stromsystem.de/pdf/Strommarktdesignstudie_BEE_final_Stand_14_12_2021.pdf (Accessed 19 July 2023).

Fraunhofer Institute for Solar Energy Systems ISE (2023) *REMod – National Energy System Model with Focus on Intersectoral System Development - Fraunhofer ISE* [Online]. Available at https://www.ise.fraunhofer.de/en/business-areas/power-electronics-grids-and-smart-systems/energy-system-analysis/energy-system-models-at-fraunhofer-ise/remod.html (Accessed 6 April 2023).

Fridgen, G., Keller, R., Körner, M.-F. and Schöpf, M. (2020) 'A holistic view on sector coupling', *Energy Policy*, no. 147.

Fujikawa, S., Selyanchyn, R. and Kunitake, T. (2021) 'A new strategy for membrane-based direct air capture', *Polymer Journal*, vol. 53, no. 1, pp. 111–119.

German Environment Agency (2023) *Renewable energies in figures* [Online]. Available at https://www.umweltbundesamt.de/en/topics/climate-energy/renewable-energies/renewable-energies-in-figures (Accessed 22 March 2023).

Gorjão, L. R., Vanfretti, L., Witthaut, D., Beck, C. and Schäfer, B. (2020) 'Data-driven model of the power-grid frequency dynamics', *IEEE Access*, no. 8, pp. 43082–43097 [Online]. Available at https://ieeexplore.ieee.org/stamp/stamp.jsp?arnumber=8963682.

Gorjão, L. R., Vanfretti, L., Witthaut, D., Beck, C. and Schäfer, B. (2022) 'Phase and Amplitude Synchronization in Power-Grid Frequency Fluctuations in the Nordic Grid', *IEEE Access*, no. 10, pp. 18065–18073.

Gudmundsson, O., Dyrelund, A. and Thorsen, J. E. (2021) 'Comparison of 4th and 5th generation district heating systems', *E3S Web of Conferences*, vol. 246, p. 9004.

Gunantara, N. (2018) 'A review of multi-objective optimization: Methods and its applications', *Cogent Engineering*, vol. 5, no. 1, p. 1502242.

Gurobi Optimization LLC. (2022) *Mixed-Integer Programming (MIP) – A Primer on the Basics - Gurobi Optimization* [Online]. Available at https://www.gurobi.com/resources/mixed-integer-programming-mip-a-primer-on-the-basics/ (Accessed 27 February 2023).

Gurobi Optimization LLC. (2023a) *Gurobi Optimizer Reference Manual: Version 10.0* [Online]. Available at https://www.gurobi.com/wp-content/plugins/hd_documentations/documentation/10.0/refman.pdf (Accessed 11 April 2023).

Gurobi Optimization LLC. (2023b) *Academic Program and Licenses - Gurobi Optimization* [Online]. Available at https://www.gurobi.com/academia/academic-program-and-licenses/ (Accessed 11 April 2023).

Gutknecht, V., Snæbjörnsdóttir, S. Ó., Sigfússon, B., Aradóttir, E. S. and Charles, L. (2018) 'Creating a carbon dioxide removal solution by combining rapid mineralization of CO2 with direct air capture', *Energy Procedia*, vol. 146, pp. 129–134.

Hanna, R., Abdulla, A., Xu, Y. and Victor, D. G. (2021) 'Emergency deployment of direct air capture as a response to the climate crisis', *Nature communications*, vol. 12, no. 1, p. 368.

Hart, W. E., Laird, Carl D. Watson, Jean-Paul, Woodruff, D. L., Hackebeil, G. A., Nicholson, B. L. and Siirola, J. D. (eds) (2017) *Pyomo — Optimization Modeling in Python*, 2nd edn, Springer.

Hart, W. E., Watson, J.-P. and Woodruff, D. L. (2011) 'Pyomo: Modeling and solving mathematical programs in Python', *Mathematical Programming Computation*, no. 3, pp. 219–260.

Henning, H.-M. and Palzer, A. (2014) 'A comprehensive model for the German electricity and heat sector in a future energy system with a dominant contribution from renewable energy technologies—Part I: Methodology', *Renewable and Sustainable Energy Reviews*, vol. 30, pp. 1003–1018.

Hepburn, C., Adlen, E., Beddington, J., Carter, E. A., Fuss, S., Mac Dowell, N., Minx, J. C., Smith, P. and Williams, C. K. (2019) 'The technological and economic prospects for CO2 utilization and removal', *Nature*, vol. 575, no. 7781, pp. 87–97.

IEA, International Energy Agency (2022) *Direct Air Capture: A key technology for net zero,* International Energy Agency [Online]. Available at https://iea.blob.core.windows.net/assets/78633715-15c0-44e1-81df-41123c556d57/DirectAirCapture_Akeytechnologyfornetzero.pdf (Accessed 19 July 2023).

IPCC (2021) *Technical Summary: In Climate Change 2021: The Physical Science Basis. Contribution of Working Group I to the Sixth Assessment Report of the Intergovernmental Panel on Climate Change,* IPCC.

IPCC (2022a) *Climate Change 2022: Impacts, Adaptation and Vulnerability. Contribution of Working Group II to the Sixth Assessment Report of the Intergovernmental Panel on Climate Change: Summary for Policymakers,* IPCC.

IPCC (2022b) *Climate Change 2022: Mitigation of climate change. Contribution of Working Group III to the Sixth Assessment Report of the Intergovernmental Panel on Climate Change: Cross-sectoral perspectives,* IPCC.

Kaiser, M. (2022) e-mail and interview Moritz Rickert, 5 December.

Keith, D. W., Holmes, G., St. Angelo, D. and Heidel, K. (2018) 'A Process for Capturing CO2 from the Atmosphere', *Joule*, vol. 2, no. 8, pp. 1573–1594.

Kicherer, N. (2020) *Entwicklung einer Strategie für die langfristige Transformation des Hamburger Wärmenetzes*, Masterarbeit, Hamburg, Hochschule für Angewandte Wissenschaften Hamburg.

Kicherer, N., Lorenzen, P. and Schäfers, H. (2021) 'Design of a district heating roadmap for Hamburg', *Smart Energy*, vol. 2, p. 100014.

Kohlhepp, P., Harb, H., Wolisz, H., Waczowicz, S., Müller, D. and Hagenmeyer, V. (2019) 'Large-scale grid integration of residential thermal energy storages as demand-side flexibility resource: A review of international field studies', *Renewable and Sustainable Energy Reviews*, vol. 101, pp. 527–547.

Kolb, S., Dillig, M., Plankenbühler, T. and Karl, J. (2020) 'The impact of renewables on electricity prices in Germany - An update for the years 2014–2018', *Renewable and Sustainable Energy Reviews*, vol. 134.

Kondziella, H. and Bruckner, T. (2016) 'Flexibility requirements of renewable energy based electricity systems – a review of research results and methodologies', *Renewable and Sustainable Energy Reviews*, vol. 53, pp. 10–22.

Kurucz, C. N., Brandt, D. and Sim, S. (1996) 'A linear programming model for reducing system peak through customer load control programs', *IEEE Transactions on Power Systems*, vol. 11, no. 4.

Lackner, K. and Azarabadi, H. (2021) 'Buying down the Cost of Direct Air Capture', *Industrial & Engineering Chemistry Research*, vol. 60, no. 22, pp. 8196–8208.

Landesbetrieb Geoinformation und Vermessung (2023a) *MetaVer - Verfügbare Kartendienste: Flächennutzungsplan Hamburg* [Online]. Available at https://metaver.de/kartendienste?lang=de&topic=themen&bgLayer=sgx_geodatenzentrum_de_web_light_grau_EU_EPSG_25832_TOPPLUS&E=546735.14&N=5936634.37&zoom=11&layers=5f4f6a7093482c1125d61d4811f3b9b1&swipe_ratio=0.89&layers_opacity=91c85f899e56014969935fefd68830b9 (Accessed 19 April 2023).

Landesbetrieb Geoinformation und Vermessung (2023b) *3D-Gebäudemodell LoD2-DE Hamburg - MetaVer* [Online]. Available at https://metaver.de/trefferanzeige?docuuid=2C1F2EEC-CF9F-4D8B-ACAC-79D8C1334D5E (Accessed 20 April 2023).

Lenz, K., Bomberg, C., Grundmann, R. A., Hönniger, S., Brauns, P., Feske, L., Früh, S., Schubert, F., Trott, T. and Zöll, J. (2018) *Strommarkt 2050: Analyse möglicher Szenarien der Entwicklung des deutschen und mitteleuropäischen Strommarktes bis zum Jahr 2050* [Online]. Available at https://docplayer.org/131349336-Strommarkt-analyse-moeglicher-szenarien-der-entwicklung-des-deutschen-und-mitteleuropaeischen-strommarktes-bis-zum-jahr-2050.html (Accessed 28 April 2023).

Li, H. and Nord, N. (2018) 'Transition to the 4th generation district heating - possibilities, bottlenecks, and challenges', *Energy Procedia*, vol. 149, pp. 483–498.

Low, M.-Y., Barton, L. V., Pini, R. and Petit, C. (2023) 'Analytical review of the current state of knowledge of adsorption materials and processes for direct air capture', *Chemical Engineering Research and Design*, vol. 189, pp. 745–767.

Lund, H., Østergaard, P. A., Nielsen, T. B., Werner, S., Thorsen, J. E., Gudmundsson, O., Arabkoohsar, A. and Mathiesen, B. V. (2021) 'Perspectives on fourth and fifth generation district heating', *Energy*, vol. 227, p. 120520.

Lund, H., Werner, S., Wiltshire, R., Svendsen, S., Thorsen, J. E., Hvelplund, F. and Mathiesen, B. V. (2014) '4th Generation District Heating (4GDH)', *Energy*, vol. 68, pp. 1–11.

McQueen, N., Gomes, K. V., McCormick, C., Blumanthal, K., Pisciotta, M. and Wilcox, J. (2021) 'A review of direct air capture (DAC): scaling up commercial technologies and innovating for the future', *Progress in Energy*, vol. 3, no. 3, p. 32001.

Mohammad, N. and Mishra, Y. (2019) 'Demand-Side Management and Demand Response for Smart Grid', in Kabalci, E. and Kabalci, Y. (eds) *Smart Grids and Their Communication Systems,* Singapore, Springer, pp. 197–231.

Ozkan, M., Nayak, S. P., Ruiz, A. D. and Jiang, W. (2022) 'Current status and pillars of direct air capture technologies', *iScience*, vol. 25, no. 4, p. 103990.

Palzer, A. and Henning, H.-M. (2014) 'A comprehensive model for the German electricity and heat sector in a future energy system with a dominant contribution from renewable energy technologies – Part II: Results', *Renewable and Sustainable Energy Reviews*, vol. 30, pp. 1019–1034.

Pereira, J. L. J., Oliver, G. A., Francisco, M. B., Cunha, S. S. and Gomes, G. F. (2022) 'A Review of Multi-objective Optimization: Methods and Algorithms in Mechanical Engineering Problems', *Archives of Computational Methods in Engineering*, vol. 29, no. 4, pp. 2285–2308.

Prognos, Öko-Institut and Wuppertal-Institut (2021) *Towards a Climate-Neutral Germany by 2045: How Germany can reach its climate targets before 2050* [Online]. Available at https://static.agora-

energiewende.de/fileadmin/Projekte/2021/2021_04_KNDE45/A-EW_213_KNDE2045_Summary_EN_WEB.pdf (Accessed 9 December 2023).

Ramsebner, J., Haas, R., Ajanovic, A. and Wietschel, M. (2021) 'The sector coupling concept: A critical review', *WIREs Energy and Environment*, vol. 10, no. 4.

Roestenberg, T. (2015) *Design study report ANTECY: ANTECY solar fuels development,* Antecy [Online]. Available at https://dokumen.tips/documents/ant-y-solar-fuels-development-home-study-report-finalpdf-in-a-thermocatalytic.html?page=1.

Sabatino, F., Grimm, A., Gallucci, F., van Sint Annaland, M., Kramer, G. J. and Gazzani, M. (2021) 'A comparative energy and costs assessment and optimization for direct air capture technologies', *Joule*, vol. 5, no. 8, pp. 2047–2076.

Sinha, A. and Realff, M. J. (2019) 'A parametric study of the techno-economics of direct CO 2 air capture systems using solid adsorbents', *AIChE Journal*, vol. 65, no. 7.

Snyman, J. A. and Wilke, D. N. (2018) *Practical Mathematical Optimization*, Cham, Springer International Publishing.

Stampi-Bombelli, V., van der Spek, M. and Mazzotti, M. (2020) 'Analysis of direct capture of CO2 from ambient air via steam-assisted temperature–vacuum swing adsorptiontemperature–vacuum swing adsorption', *Adsorption*, vol. 26, no. 7, pp. 1183–1197.

Sterchele, P., Brandes, J., Heilig, J., Wrede, D., Kost, C., Schlegl, T., Bett, A. and Henning, H.-M. (2020) *Study: Paths to a Climate-Neutral Energy System - The German Energy Transition in its Social Context,* Fraunhofer-Institut für Solare Energiesysteme ISE [Online]. Available at https://www.ise.fraunhofer.de/en/publications/studies/paths-to-a-climate-neutral-energy-system.html (Accessed 6 April 2023).

Sterchele, P., Brandes, J., Heilig, J., Wrede, D., Senkpiel, C., Haun, M., Jürgens, P., Kost, C., Schlegl, T., Bett, A. and Henning, H.-M. (2021) *Studie: Wege zu einem klimaneutralen Energiesystem – Update Klimaneutralität 2045,* Fraunhofer-Institut für Solare Energiesysteme ISE [Online]. Available at https://www.ise.fraunhofer.de/de/veroeffentlichungen/studien/wege-zu-einem-klimaneutralen-energiesystem.html (Accessed 6 April 2023).

Stötzer, M., Hauer, I., Richter, M. and Styczynski, Z. A. (2015) 'Potential of demand side integration to maximize use of renewable energy sources in Germany', *Applied Energy*, vol. 146, pp. 344–352.

Terlouw, T., Treyer, K., Bauer, C. and Mazzotti, M. (2021) 'Life Cycle Assessment of Direct Air Carbon Capture and Storage with Low-Carbon Energy Sources', *Environmental Science & Technology*, no. 55, pp. 11397–11411.

Triebs, M. S., Papadis, E., Cramer, H. and Tsatsaronis, G. (2021) 'Landscape of district heating systems in Germany – Status quo and categorization', *Energy Conversion and Management: X*, vol. 9, p. 100068.

Trosdorff, J. (2023) *Unpublished work for the analysis of buildings at CC4E* [Computer program].

UNFCCC (2015) *ADOPTION OF THE PARIS AGREEMENT - Paris Agreement text English*.

Verein Deutscher Ingenieure e.V. (2012): *Economic efficiency of building installations Fundamentals and economic calculation (VDI 2067)*, Berlin: Beuth Verlag GmbH.

Viebahn, P., Scholz, A. and Zelt, O. (2019) 'The Potential Role of Direct Air Capture in the German Energy Research Program—Results of a Multi-Dimensional Analysis', *Energies*, vol. 12, no. 18, p. 3443.

Vögele, S., Rübbelke, D., Mayer, P. and Kuckshinrichs, W. (2018) 'Germany's "No" to carbon capture and storage: Just a question of lacking acceptance?', *Applied Energy*, vol. 214, pp. 205–218.

Wietschel, M. (2019) *Integration erneuerbarer Energien durch Sektorkopplung: Analyse zu technischen Sektorkopplungsoptionen,* Fraunhofer-Institut für System- und Innovationsforschung ISI [Online]. Available at https://www.umweltbundesamt.de/sites/default/files/medien/1410/publikationen/2019-03-12_cc_03-2019_sektrokopplung.pdf (Accessed 9 December 2022).

Yan, X., Ozturk, Y., Hu, Z. and Song, Y. (2018) 'A review on price-driven residential demand response', *Renewable and Sustainable Energy Reviews*, vol. 96, pp. 411–419.

Zachariassen, H. (2023) Call Moritz Rickert, 15 March.

Zhang, Z., Pan, S.-Y., Li, H., Cai, J., Olabi, A. G., Anthony, E. J. and Manovic, V. (2020) 'Recent advances in carbon dioxide utilization', *Renewable and Sustainable Energy Reviews*, no. 125.

A Appendix

Appendix 1: Flowchart of the 1-hour short-term TES capacity scenario of the DH system (own illustration) ..... B
Appendix 2: Flowchart of the 12-hour short-term TES capacity scenario without a seasonal TES of the DH system (own illustration) C
Appendix 3: Flowchart of the 12-hour short-term TES capacity scenario with a seasonal TES of the DH system (own illustration) ..... D
Appendix 4: Simplified workflow diagram of the potential analysis of the physical implementation of DAC plants on the flat rooftops using CityGML geodata sets of Hamburg (Own illustration) ..... E
Appendix 5: Time series output of the modeled scenario "OF-stTES1h-wo/SeasTES-elUpper" as an example of a 1-hour short-term TES capacity scenario (own illustration) ..... F
Appendix 6: Time series output of the modeled scenario "OF-stTES12h-wo/SeasTES-elOptimum" and "OF-stTES12h-wo/SeasTES-elUpper" as an example of a 12-hour short-term TES capacity scenario without a seasonal TES (own illustration) ..... G
Appendix 7: Time series output of the modeled scenario "OF-stTES12h-w/SeasTES-elUpper" as an example of a 12-hour short-term TES capacity with an integrated seasonal TES scenario (own illustration) ..... H
Appendix 8: Time series output of the modeled scenario "FR-stTES1h-wo/SeasTES-elOptimum" with negative electricity costs and thus a prioritization of heat pump utilization (own illustration) I
Appendix 9: Time series output of the modeled scenario "FR-stTES12h-wo/SeasTES-elOptimum" with negative electricity costs and thus prioritization of heat pump utilization (own illustration) ..... J
Appendix 10: Overview of scenario-specific in- and outputs of the 1-hour short-term TES capacity sub-scenarios (own illustration) ..... K
Appendix 11: Overview of scenario-specific in- and outputs of the 12-hour short-term TES capacity sub-scenarios without seasonal TES (own illustration) L
Appendix 12: Overview of scenario-specific in- and outputs of the 12-hour short-term TES capacity sub-scenarios with seasonal TES (own illustration) ..... M

A.1 1st TES Scenario with a 1-hour Short-Term TES Capacity of the DH System + Heat Pumps

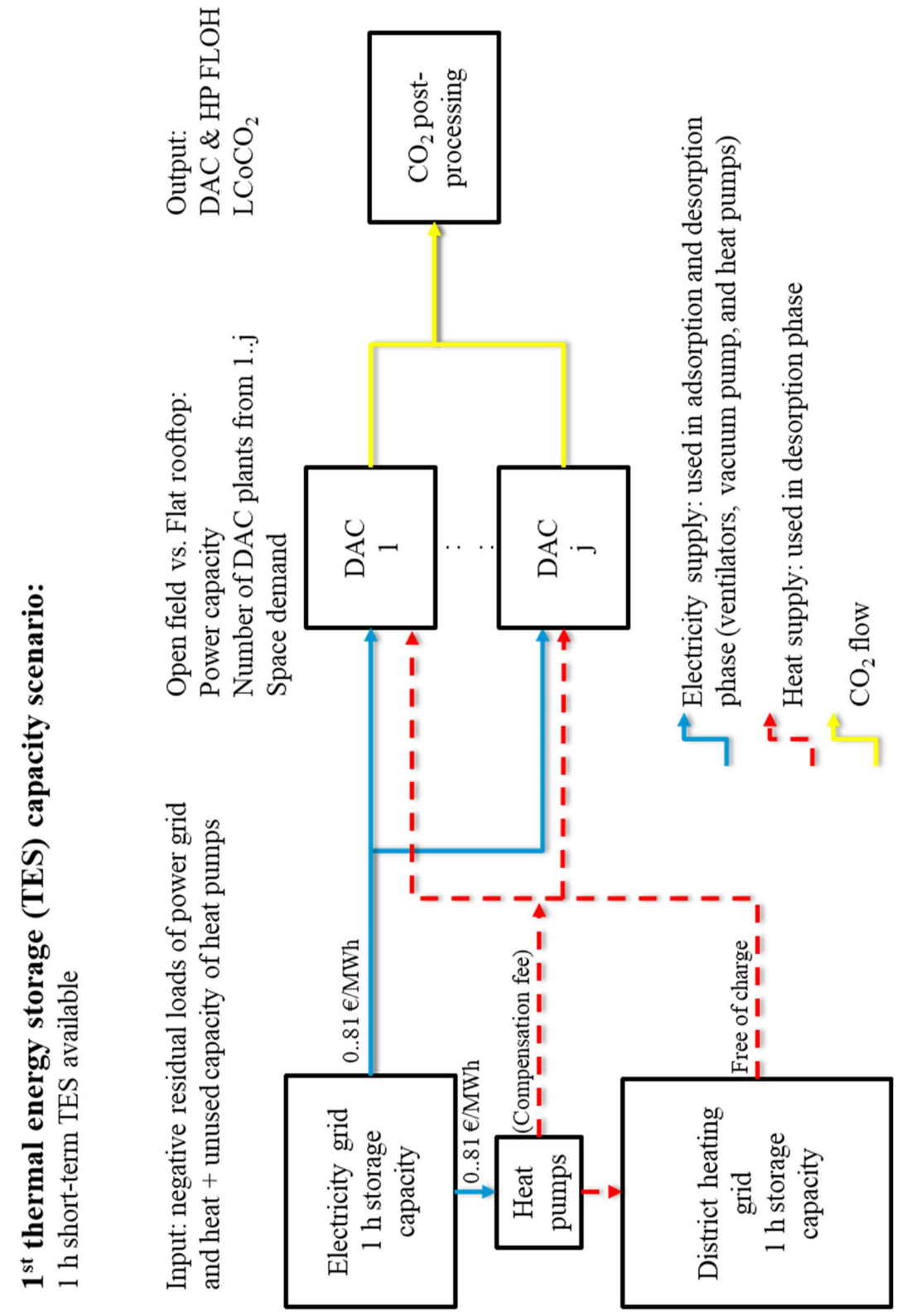

Appendix 1: Flowchart of the 1-hour short-term TES capacity scenario of the DH system (own illustration)

A.2 2nd TES scenario with a 12-hour short-term TES capacity of the DH system + heat pumps

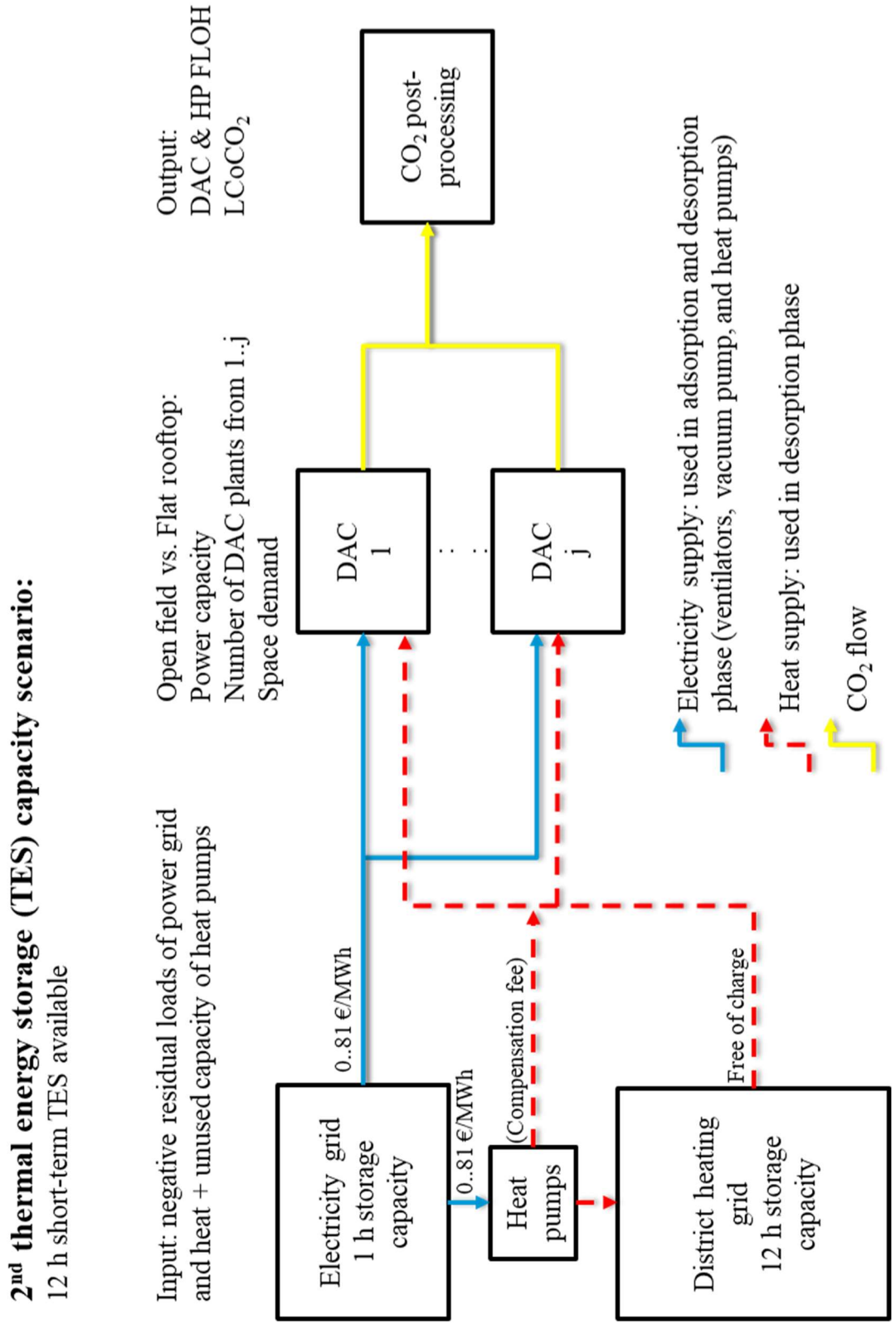

Appendix 2: Flowchart of the 12-hour short-term TES capacity scenario without a seasonal TES of the DH system (own illustration)

A.3 3rd TES scenario with a 12-hour short-term TES and seasonal TES + heat pumps

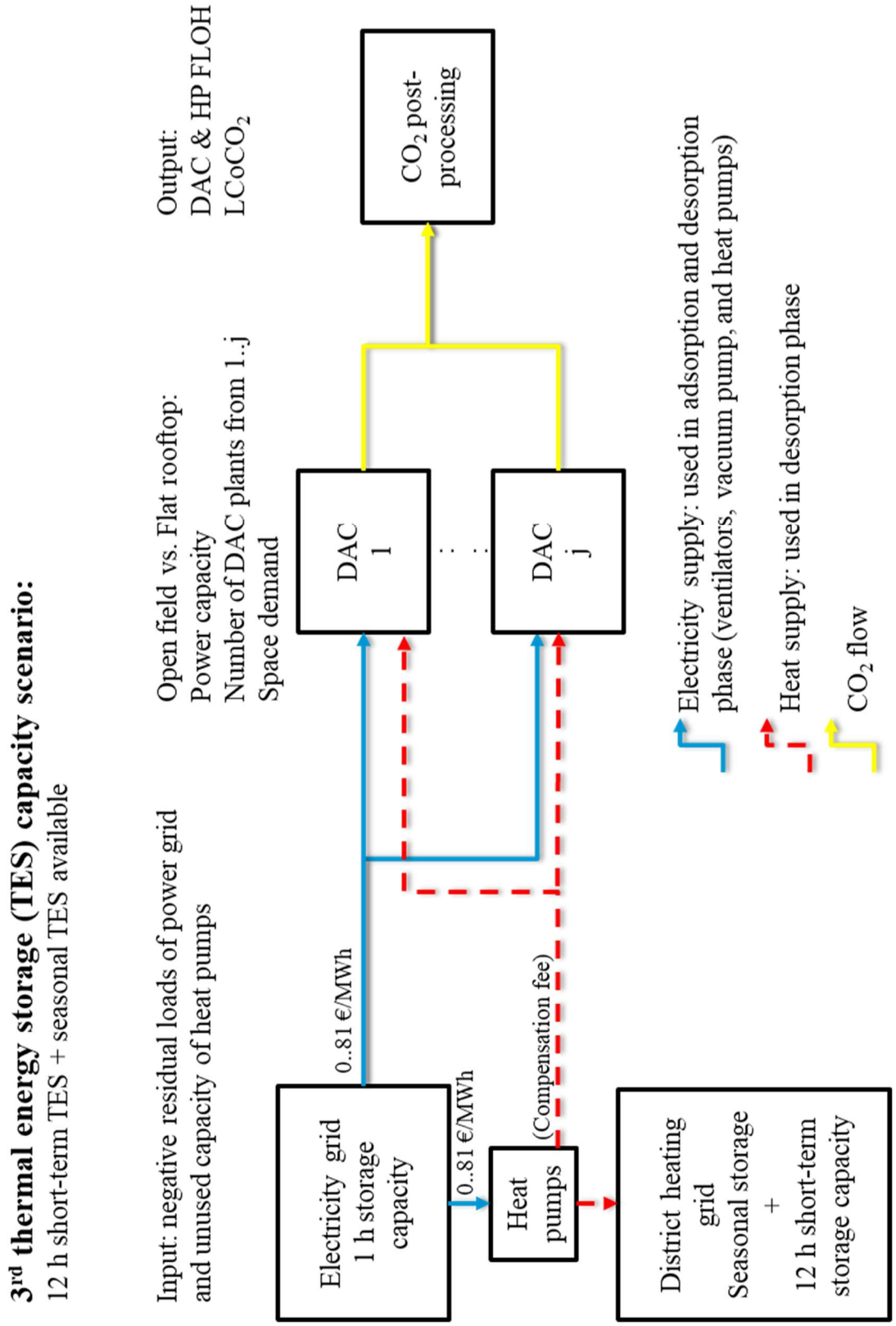

Appendix 3: Flowchart of the 12-hour short-term TES capacity scenario with a seasonal TES of the DH system (own illustration)

A.4 Workflow Diagram of Spatial Analysis

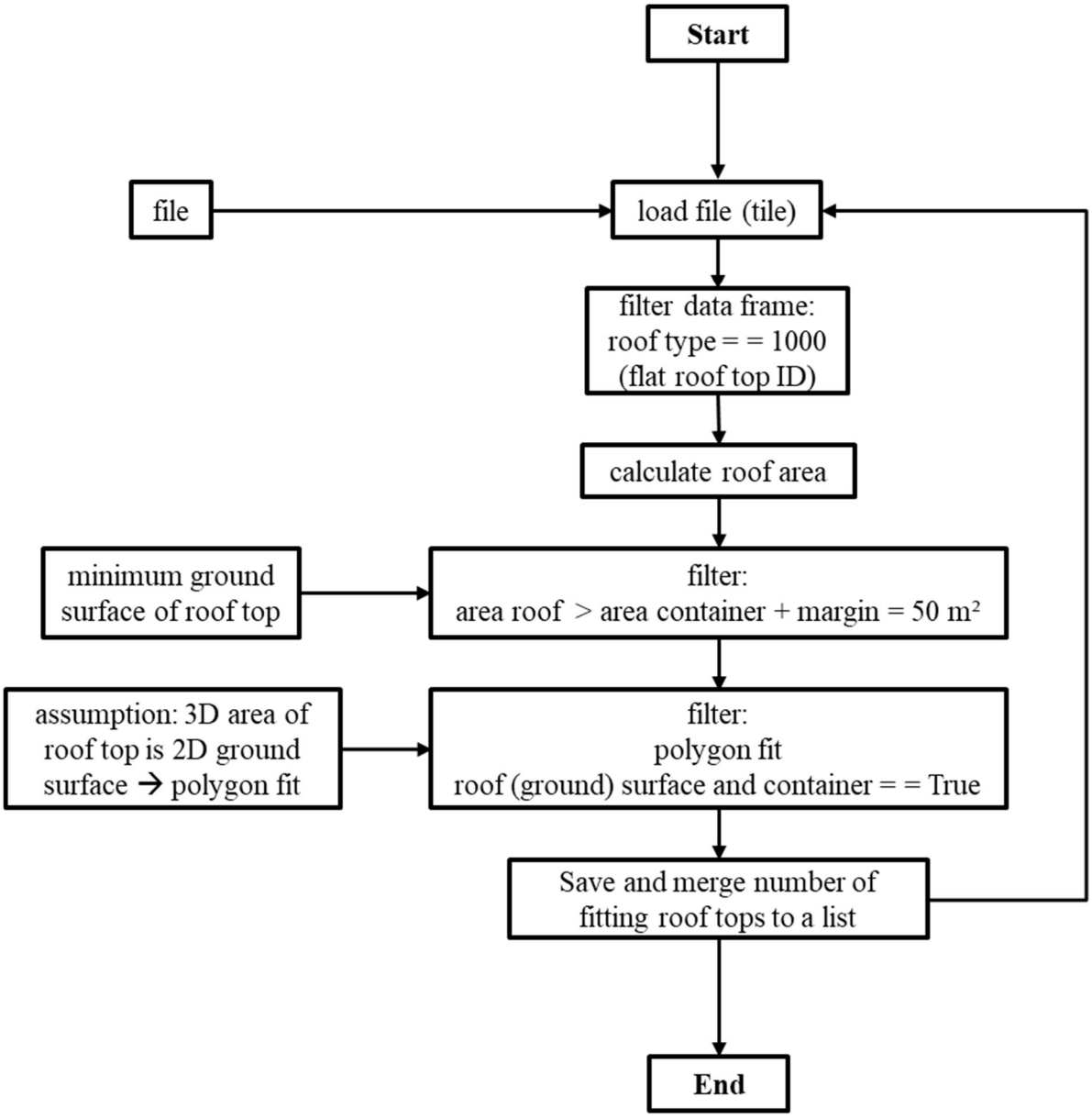

Appendix 4: Simplified workflow diagram of the potential analysis of the physical implementation of DAC plants on the flat rooftops using CityGML geodata sets of Hamburg (Own illustration)

A.5 Time Series of *OF-stTES1h-wo/SeasTES-elUpper*

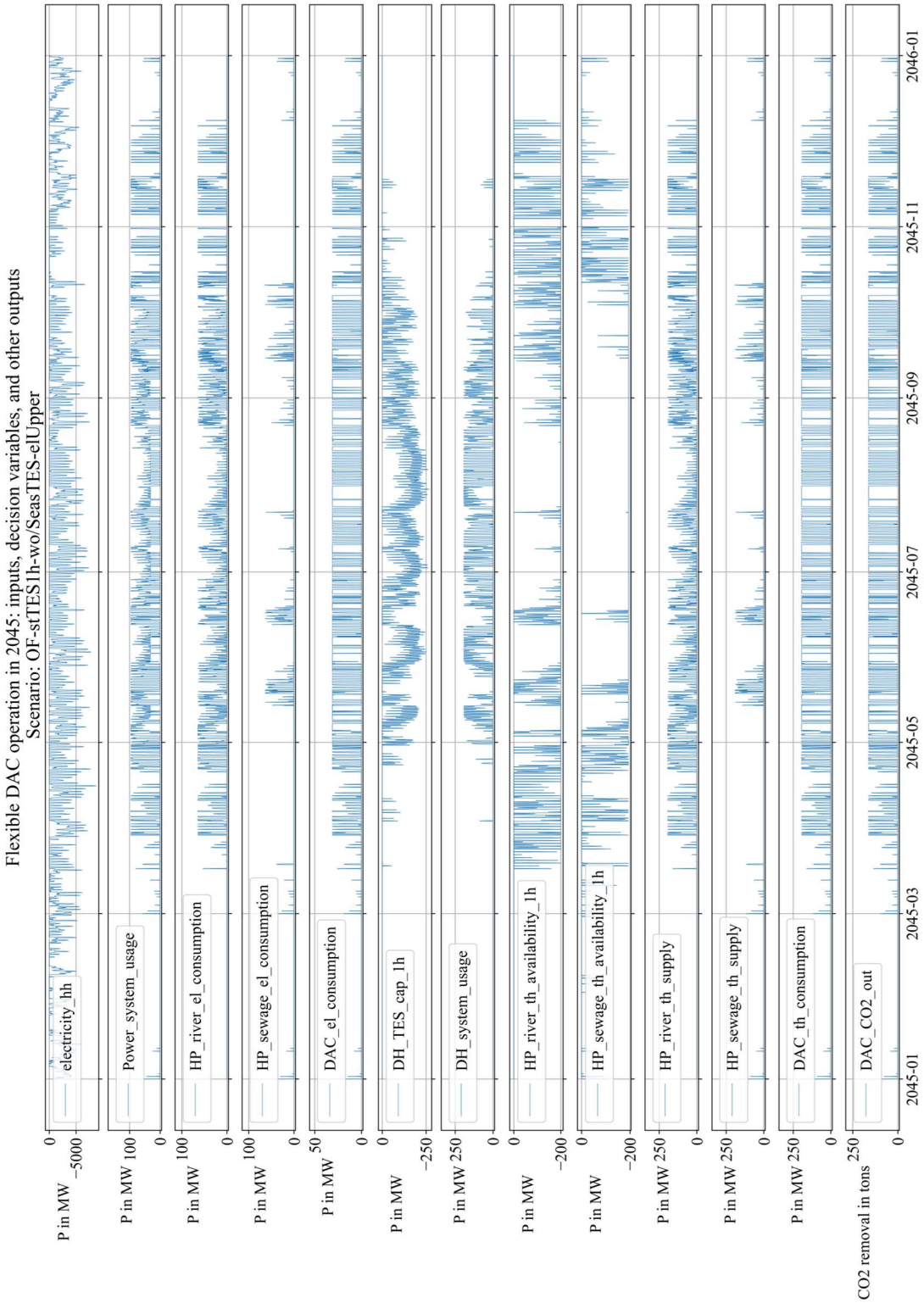

Appendix 5: Time series output of the modeled scenario "OF-stTES1h-wo/SeasTES-elUpper" as an example of a 1-hour short-term TES capacity scenario (own illustration)

A.6 Time Series of *OF-stTES12h-wo/SeasTES-elOptimum* and *OF-stTES12h-wo/SeasTES-elUpper*

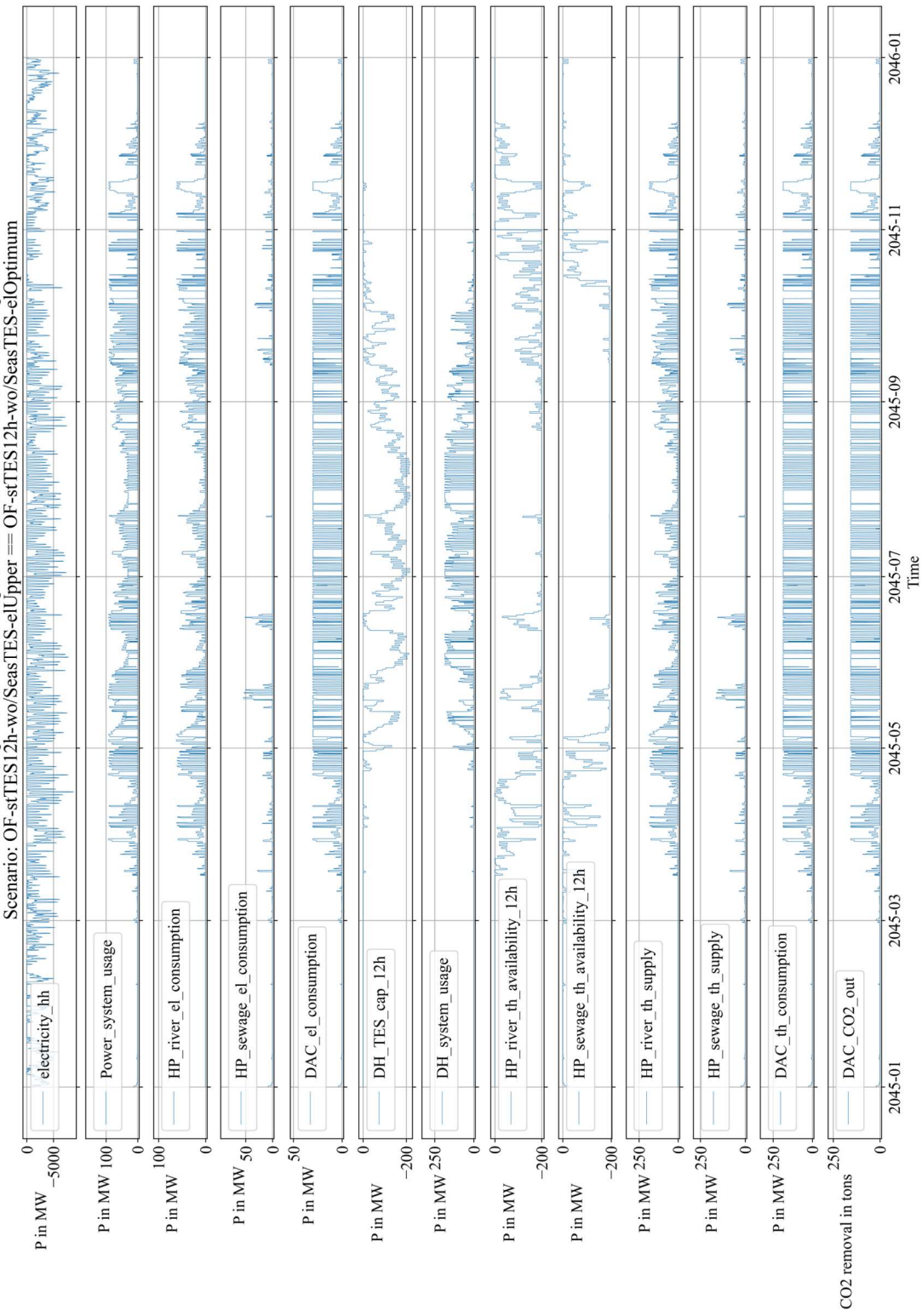

Appendix 6: Time series output of the modeled scenario "OF-stTES12h-wo/SeasTES-elOptimum" and "OF-stTES12h-wo/SeasTES-elUpper" as an example of a 12-hour short-term TES capacity scenario without a seasonal TES (own illustration)

A.7 Time Series of *OF-stTES12h-w/SeasTES-elUpper*

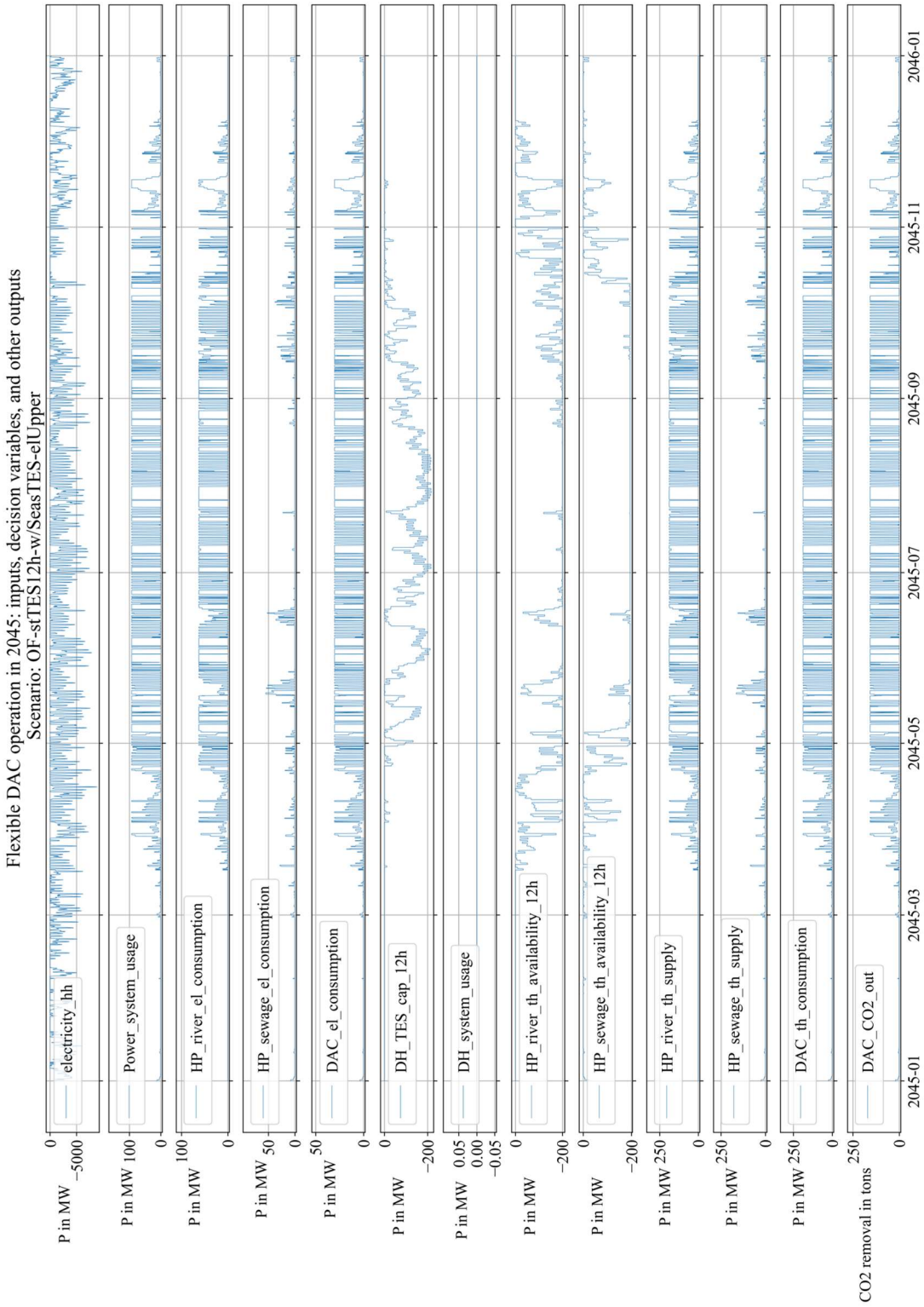

Appendix 7: Time series output of the modeled scenario "OF-stTES12h-w/SeasTES-elUpper" as an example of a 12-hour short-term TES capacity with an integrated seasonal TES scenario (own illustration)

A.8 Time Series of *FR-stTES1h-wo/SeasTES-elOptimum*

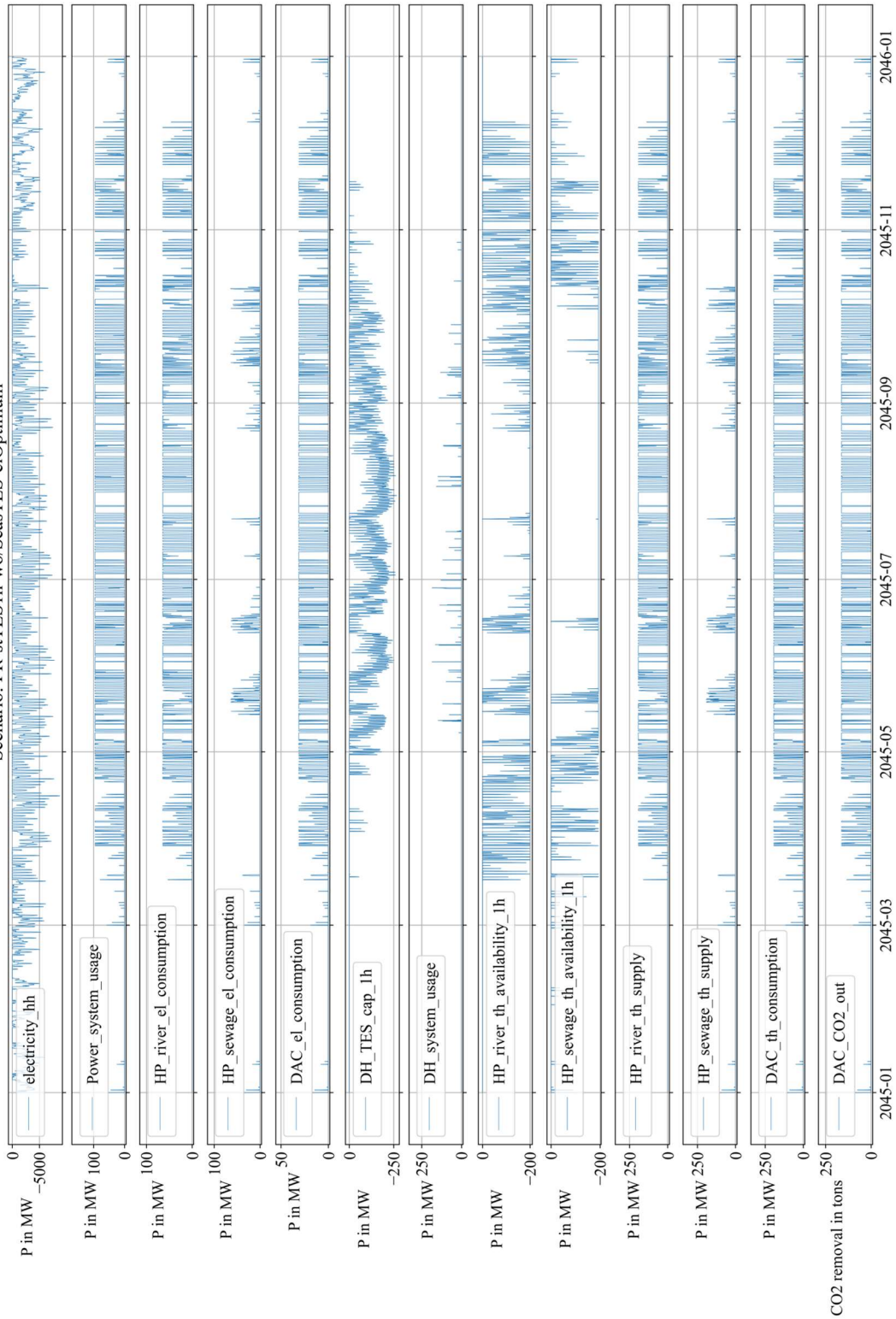

Appendix 8: Time series output of the modeled scenario "FR-stTES1h-wo/SeasTES-elOptimum" with negative electricity costs and thus a prioritization of heat pump utilization (own illustration)

A.9 Time Series of *FR-stTES12h-wo/SeasTES-elOptimum*

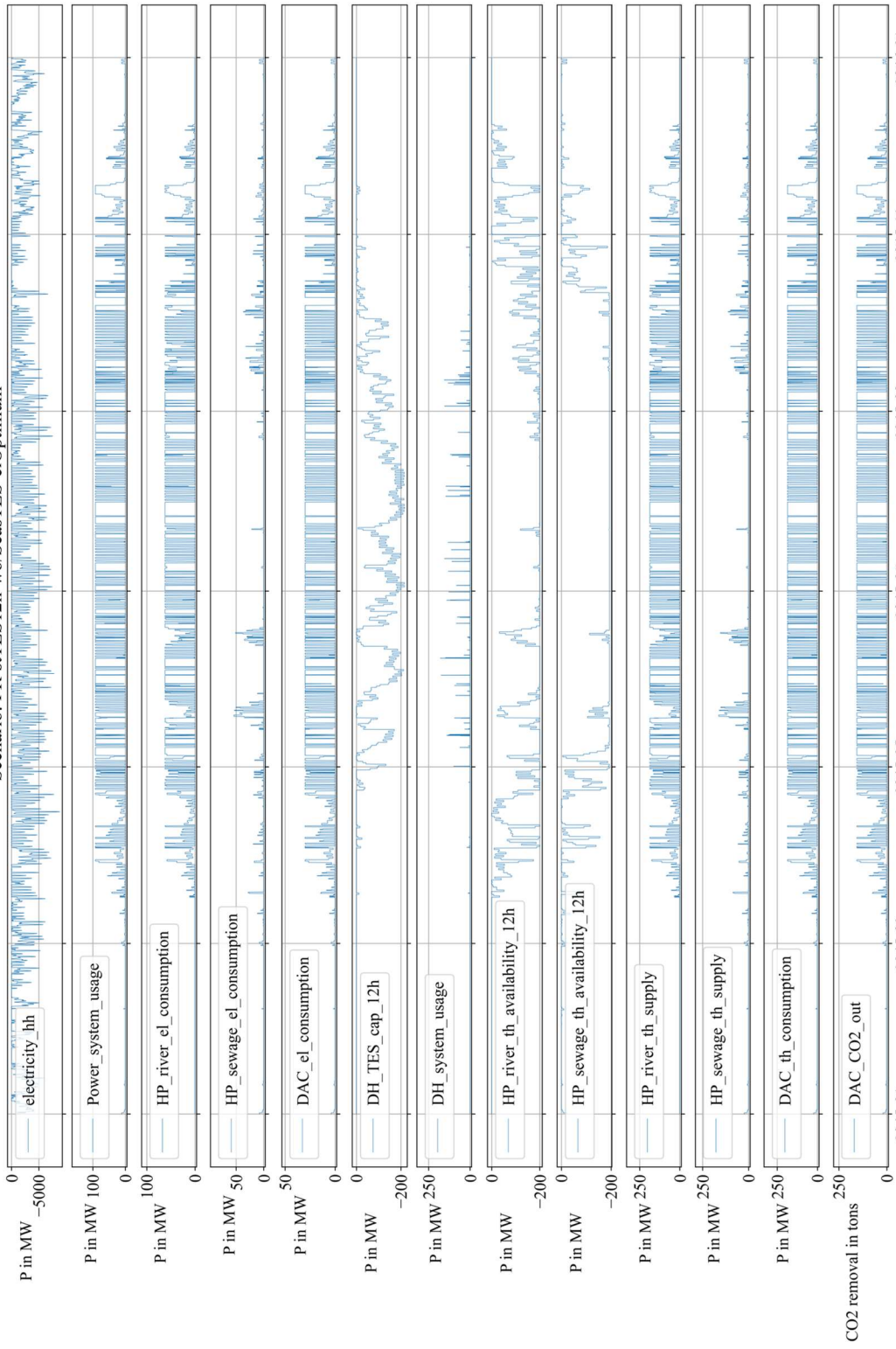

Appendix 9: Time series output of the modeled scenario "FR-stTES12h-wo/SeasTES-elOptimum" with negative electricity costs and thus prioritization of heat pump utilization (own illustration)

Appendix 10: Overview of scenario-specific in- and outputs of the 1-hour short-term TES capacity sub-scenarios (own illustra-

Inputs & results of scenarios	**OF-stTES1h-wo/SeasTES-elLower**	**OF-stTES1h-wo/SeasTES-elUpper**	**OF-stTES1h-wo/SeasTES-elOptimum**	**FR-stTES1h-wo/SeasTES-elLower**	**FR-stTES1h-wo/SeasTES-elUpper**	**FR-stTES1h-wo/SeasTES-thOptimum**	**FR-stTES1h-wo/SeasTES-elOptimum**
Short-term TES capacity of DH system	1 hour	1 hour	1 hour	1 hour	1 hour	1 hour	1 hour
DH system seasonal TES	No	No	No	No	No	No	No
River and sewage water HP time series	1 hour	1 hour	1 hour	1 hour	1 hour	1 hour	1 hour
Specific investment costs of DAC plant in €/(tCO_2/a)	189	189	189	482	482	482	482
Specific space demand of DAC plant in m²/(tCO_2/a)	0.078	0.078	0.078	0.100	0.100	0.100	0.100
LCoE (lower, optimum, upper) in €/MWh	1	81	<= 75	1	81	1 [81]	<= -124
LCoH of surplus heat in €/MWh	0	0	0	0	0	<= -133 [-192]	0
Compensation fee for sewage water HP in €/MWh	0.39	0.39	0.39	0.39	0.39	0.39	0.39
Electricity consumption by river HP in MWh/a (HP_river_el_consumption)	92,455.660	92,455.660	92,455.660	92,455.660	92,455.660	92,455.660	179,633.453
Electricity consumption by sewage water HP in MWh/a (HP_sewage_el_consumption)	11,520.173	11,520.173	11,520.173	11,520.173	11,520.173	11,520.173	11,520.173
Heat supply by river HP in MWh/a (HP_river_th_supply)	277,366.981	277,366.981	277,366.981	277,366.981	277,366.981	277,366.981	538,900.358
Heat supply by sewage water HP in MWh/a (HP_sewage_th_supply)	34,560.518	34,560.518	34,560.518	34,560.518	34,560.518	34,560.518	34,560.518
Full-load operation hours of river HP in h/a	1,386.8	1,386.8	1,386.8	1,386.8	1,386.8	1,386.8	2,694.5
Full-load operation hours of sewage water HP in h/a	178.1	178.1	178.1	178.1	178.1	178.1	178.1
DAC electricity consumption in MWh/a (DAC_el_consumption)	93,408.509	93,408.509	93,408.509	93,408.509	93,408.509	93,408.509	93,408.509
DAC thermal energy consumption in MWh/a (DAC_th_consumption)	579,375.378	579,375.378	579,375.378	579,375.378	579,375.378	579,375.378	579,375.378
In total consumed electricity in MWh/a	197,384.342	197,384.342	197,384.342	197,384.342	197,384.342	197,384.342	284,562.135
Neg. residual load share from power system of Hamburg in %	1.587	1.587	1.587	1.587	1.587	1.587	2.287
Consumed surplus heat of the DH system in MWh/a	267,447.879	267,447.879	267,447.879	267,447.879	267,447.879	267,447.879	5,914.502
Surplus heat share from DH system of Hamburg in %	64.303	64.303	64.303	64.303	64.303	64.303	1.422
DAC plant capacity in tCO_2/a (DAC_CO2_cap)	1,415,100.0	1,415,100.0	1,415,100.0	1,415,100.0	1,415,100.0	1,415,100.0	1,415,100.0
Full-load operation hours of DAC plant in h/a	3,003.8	3,003.8	3,003.8	3,003.8	3,003.8	3,003.8	3,003.8
Investment costs of DAC plant capacity in €	267,453,900.0	267,453,900.0	267,453,900.0	682,078,200.0	682,078,200.0	682,078,200.0	682,078,200.0
Space demand in m²	110,377.800	110,377.800	110,377.800	141,510.000	141,510.000	141,510.000	141,510.000
Space demand in km²	0.110	0.110	0.110	0.142	0.142	0.142	0.142
Number of DAC plant units (module size: 300 tCO_2/a) (DAC_number_of_plants)	4,717	4,717	4,717	4,717	4,717	4,717	4,717
LCoCO_2 in €/tCO_2	**68.88**	**102.39**	**99.88**	**174.99**	**208.51**	**99.50 [99.52]**	**99.68**

Appendix 11: Overview of scenario-specific in- and outputs of the 12-hour short-term TES capacity sub-scenarios without seasonal TES (own illustration)

Inputs & results of scenarios	**OF-stTES12h-wo/SeasTES-elLower**	**OF-stTES12h-wo/SeasTES-elUpper**	**OF-stTES12h-wo/SeasTES-elOptimum**	**FR-stTES12h-wo/SeasTES-elLower**	**FR-stTES12h-wo/SeasTES-elUpper**	**FR-stTES12h-wo/SeasTES-thOptimum**	**FR-stTES12h-wo/SeasTES-elOptimum**
Short-term TES capacity of DH system	12 hours	12 hours	12 hours	12 hours	12 hours	12 hours	12 hours
DH system seasonal TES	No	No	No	No	No	No	No
River and sewage water HP time series	12 hours	12 hours	12 hours	12 hours	12 hours	12 hours	12 hours
Specific investment costs of DAC plant in €/(tCO_2/a)	189	189	189	482	482	482	482
Specific space demand of DAC plant in m²/(tCO_2/a)	0.078	0.078	0.078	0.100	0.100	0.100	0.100
LCoE (lower, optimum, upper) in €/MWh	1	81	<= 81	1	81	1 [81]	<= -113
LCoH of surplus heat in €/MWh	0	0	0	0	0	<= -119 [-177]	0
Compensation fee for sewage water HP in €/MWh	0.39	0.39	0.39	0.39	0.39	0.39	0.33
Electricity consumption by river HP in MWh/a (HP_river_el_consumption)	91,605.618	91,605.618	91,605.618	91,605.618	91,605.618	91,605.618	177,099.342
Electricity consumption by sewage water HP in MWh/a (HP_sewage_el_consumption)	11,125.326	11,125.326	11,125.326	11,125.326	11,125.326	11,125.326	13,816.360
Heat supply by river HP in MWh/a (HP_river_th_supply)	274,816.854	274,816.854	274,816.854	274,816.854	274,816.854	274,816.854	531,298.027
Heat supply by sewage water HP in MWh/a (HP_sewage_th_supply)	33,375.979	33,375.979	33,375.979	33,375.979	33,375.979	33,375.979	41,449.079
Full-load operation hours of river HP in h/a	1,374.1	1,374.1	1,374.1	1,374.1	1,374.1	1,374.1	2,656.5
Full-load operation hours of sewage water HP in h/a	172.0	172.0	172.0	172.0	172.0	172.0	213.6
DAC electricity consumption in MWh/a (DAC_el_consumption)	93,408.509	93,408.509	93,408.509	93,408.509	93,408.509	93,408.509	93,408.509
DAC thermal energy consumption in MWh/a (DAC_th_consumption)	579,375.378	579,375.378	579,375.378	579,375.378	579,375.378	579,375.378	579,375.378
In total consumed electricity in MWh/a	196,139.454	196,139.454	196,139.454	196,139.454	196,139.454	196,139.454	284,324.212
Neg. residual load share from power system of Hamburg in %	1.577	1.577	1.577	1.577	1.577	1.577	2.285
Consumed surplus heat of the DH system in MWh/a	271,182.545	271,182.545	271,182.545	271,182.545	271,182.545	271,182.545	6,628.271
Surplus heat share from DH system of Hamburg in %	65.201	65.201	65.201	65.201	65.201	65.201	1.594
DAC plant capacity in tCO_2/a (DAC_CO2_cap)	1,362,300.0	1,362,300.0	1,362,300.0	1,362,300.0	1,362,300.0	1,362,300.0	1,362,300.0
Full-load operation hours of DAC plant in h/a	3,120.2	3,120.2	3,120.2	3,120.2	3,120.2	3,120.2	3,120.2
Investment costs of DAC plant capacity in €	257,474,700.0	257,474,700.0	257,474,700.0	656,628,600.0	656,628,600.0	656,628,600.0	656,628,600.0
Space demand in m²	106,259.400	106,259.400	106,259.400	136,230.000	136,230.000	136,230.000	136,230.000
Space demand in km²	0.106	0.106	0.106	0.136	0.136	0.136	0.136
Number of DAC plant units (module size: 300 tCO_2/a) (DAC_number_of_plants)	4,541	4,541	4,541	4,541	4,541	4,541	4,541
LCoCO_2 in €/tCO_2	**66.32**	**99.62**	**99.62**	**168.48**	**201.78**	**99.99 [99.91]**	**99.87**

A.12 Scenario-Specific In- and Outputs of All 12-Hour Short-Term + Seasonal TES Capacity Scenarios

Appendix 12: Overview of scenario-specific in- and outputs of the 12-hour short-term TES capacity sub-scenarios with seasonal TES (own illustration)

Inputs & results of scenarios	**OF-stTES12h-w/SeasTES-elLower**	**OF-stTES12h-w/SeasTES-elUpper**	**OF-stTES12h-w/SeasTES-elOptimum**	**FR-stTES12h-w/SeasTES-elLower**	**FR-stTES12h-w/SeasTES-elUpper**	**FR-stTES12h-w/SeasTES-elOptimum**
Short-term TES capacity of DH system	None	None	None	None	None	None
DH system seasonal TES	Yes	Yes	Yes	Yes	Yes	Yes
River and sewage water HP time series	12 hours	12 hours	12 hours	12 hours	12 hours	12 hours
Specific investment costs of DAC plant in €/(tCO_2/a)	189	189	189	482	482	482
Specific space demand of DAC plant in m^2/(tCO_2/a)	0.078	0.078	0.078	0.100	0.100	0.100
LCoE (lower, optimum, upper) in €/MWh	1	81	<= 55	1	81	<= -115
LCoH of surplus heat in €/MWh	0	0	0	0	0	0
Compensation fee for sewage water HP in €/MWh	0.33	0.33	0.33	0.33	0.33	0.33
Electricity consumption by river HP in MWh/a (HP river el consumption)	178,902.762	178,902.762	178,902.762	178,902.762	178,902.762	178,902.762
Electricity consumption by sewage water HP in MWh/a (HP sewage el consumption)	14,222.364	14,222.364	14,222.364	14,222.364	14,222.364	14,222.364
Heat supply by river HP in MWh/a (HP river th supply)	536,708.287	536,708.287	536,708.287	536,708.287	536,708.287	536,708.287
Heat supply by sewage water HP in MWh/a (HP sewage th supply)	42,667.091	42,667.091	42,667.091	42,667.091	42,667.091	42,667.091
Full-load operation hours of river HP in h/a	2,683.5	2,683.5	2,683.5	2,683.5	2,683.5	2,683.5
Full-load operation hours of sewage water HP in h/a	219.9	219.9	219.9	219.9	219.9	219.9
DAC electricity consumption in MWh/a (DAC el consumption)	93,408.509	93,408.509	93,408.509	93,408.509	93,408.509	93,408.509
DAC thermal energy consumption in MWh/a (DAC th consumption)	579,375.378	579,375.378	579,375.378	579,375.378	579,375.378	579,375.378
In total consumed electricity in MWh/a	286,533.635	286,533.635	286,533.635	286,533.635	286,533.635	286,533.635
Neg. residual load share from power system of Hamburg in %	2.303	2.303	2.303	2.303	2.303	2.303
Consumed surplus heat of the DH system in MWh/a	0.000	0.000	0.000	0.000	0.000	0.000
Surplus heat share from DH system of Hamburg in %	0	0	0	0	0	0
DAC plant capacity in tCO_2/a (DAC CO2 cap)	1,374,300.0	1,374,300.0	1,374,300.0	1,374,300.0	1,374,300.0	1,374,300.0
Full-load operation hours of DAC plant in h/a	3,093.0	3,093.0	3,093.0	3,093.0	3,093.0	3,093.0
Investment costs of DAC plant capacity in €	259,742,700.0	259,742,700.0	259,742,700.0	662,412,600.0	662,412,600.0	662,412,600.0
Space demand in m^2	107,195.400	107,195.400	107,195.400	137,430.000	137,430.000	137,430.000
Space demand in km^2	0.107	0.107	0.107	0.137	0.137	0.137
Number of DAC plant units (module size: 300 tCO_2/a) (DAC number of plants)	4,581	4,581	4,581	4,581	4,581	4,581
LCoCO₂ in €/tCO₂	**67.09**	**115.75**	**99.93**	**170.15**	**218.8**	**99.61**

B Digital Appendix

B.1 Flexible_DAC_plant_operation_optimization_model.py

Software script of the programmed optimization model.

B.2 Input_time_series_MILP - Parameter - Additional_calculations.xlsx

Excel file containing sheets with:

1. Table of input time series of the DH system, power system, and preliminary modifications of the heat pumps
2. Additional calculations for parameter setting (extrapolation/interpolation)
3. Overview of the scenarios
4. Overview of the scenarios' results
5. Illustration of the results

B.3 Collection of scenarios and their time series (inputs, variables, and other outputs).xlsx

Excel file containing sheets with an overview of the results + time series and results of each scenario.

B.4 Figures of the scenarios' time series

Folder containing time series plots of all scenarios.

Statutory Declaration

I herewith formally declare that I have written the submitted master's thesis independently. I did not use any outside support except for the quoted literature and other sources mentioned in the paper. I clearly marked and separately listed all literature and all other sources which I used when producing this academic work, either literally or in content. I am aware that the violation of this regulation will lead to the failure of the thesis.

21.07.2023 /_____

Date / Moritz Rickert